Université du Québec
INRS – ETE

DÉVELOPPEMENT ET OPTIMISATION D'UNE SOLUTION MICELLAIRE POUR L'AMÉLIORATION DU RENDEMENT DES TECHNIQUES CONVENTIONNELLES DE RÉHABILITATION D'AQUIFÈRES CONTAMINÉS AUX HYDROCARBURES LÉGERS

Par
Maxime Grenier

Mémoire présenté
pour l'obtention
du grade de Maître ès sciences (M.Sc.)

Jury d'évaluation

Examinateur externe	John Molson, Ph. D. Département de géologie et de génie géologique Université Laval
Examinateur interne	Miroslav Natsev, Ph. D. Commission géologique du Canada
Directeur de recherche	Richard Martel, Ph. D. INRS – ETE Université du Québec
Codirecteur de recherche	René Lefebvre, Ph. D. INRS – ETE Université du Québec

19 septembre 2011

RÉSUMÉ

Les travaux inclus dans ce mémoire s'inscrivent à l'intérieur d'un large projet de recherche sur l'élaboration d'un train de technologie, visant à améliorer le rendement des techniques conventionnelles de réhabilitation d'aquifères contaminés par des hydrocarbures en combinant les trois méthodes suivantes : l'extraction sous vide, le lavage de sol et l'oxydation chimique. Les travaux propres à ce mémoire sont axés uniquement sur le lavage de sol, plus spécifiquement sur le développement et l'optimisation d'une solution micellaire capable de récupérer les hydrocarbures à saturation résiduelle par mobilisation ou solubilisation. Suite à une caractérisation du contaminant (essence) et des matériaux géologiques provenant du site pilote associé au projet, des diagrammes de phases ont été développés pour sélectionner différentes solutions micellaires prometteuses. Des essais en petites colonnes de sol ont ensuite été réalisés pour identifier la meilleure solution micellaire parmi celles retenues grâce aux diagrammes de phases. La solution micellaire optimale obtenue est une solution à ratio égal entre le tensioactif Hostapur SAS et l'alcool n-butanol à 7,5% en poids de matière active, bonifiée avec 7,5 g/L de NaCl et 300 ppm de gomme de xanthane. Un essai à l'échelle pilote sur le terrain d'une station d'essence désaffectée a été réalisé pour tester la solution micellaire sélectionnée. L'essai a été effectué à l'aide d'un patron d'injection/pompage à 7 points, soit avec six puits de pompage formant un hexagone et un puits central d'injection. L'injection de la solution micellaire a été précédée d'un banc d'eau saline pour contrer l'effet de dilution de la salinité de la solution micellaire, et suivie d'un banc de solution de polymère pour pousser uniformément la solution micellaire vers les puits de pompage. Les résultats de l'essai ont démontré l'importance de l'évaluation de la porosité effective par l'entremise d'un essai de traçage avant d'effectuer le lavage de sol afin de mieux évaluer les quantités adéquates de produits chimiques à injecter pour réhabiliter le site. Les coûts des produits chimiques pour cet essai à l'échelle pilote ont été de 100$/m^3 de sol contaminé. Des mesures complémentaires ont été effectuées pour caractériser la solution micellaire optimale. Ces mesures ont montré que l'utilisation de très faibles concentrations de matière active (0,1%) permet de diminuer la tension interfaciale entre l'eau et l'essence de 96%, ce qui ouvre la porte pour une nouvelle avenue de recherche basée sur la mobilisation de l'essence pendant l'étape d'extraction sous vide.

REMERCIEMENTS

Tout d'abord, je me dois de remercier mon directeur de recherche, Richard Martel, pour l'opportunité qu'il m'a offert de travailler sur ce projet avec une équipe exceptionnelle, ainsi que pour tous les conseils et le support qu'il m'a offert durant ces trois dernières années. Merci également à mon codirecteur René Lefebvre pour le partage de ses connaissances, plus particulièrement dans le cadre du cours *Écoulement multiphase en milieu poreux*. Je dois remercier tout particulièrement Thomas Robert pour ses conseils judicieux, le partage de ses connaissances ainsi que ses réponses à mes nombreuses questions. Je remercie ensuite Uta Gabriel pour l'aide incroyable qu'elle m'a apporté tout au long du projet. Je souhaite remercier également Richard Lévesque pour son dur labeur à l'analyse des multiples échantillons du projet ainsi que les stagiaires en chimie qui ont mis la main à la pâte, soit Isabelle Durette, Véronyque Blanchet et Michaël Vachon. Un merci tout particulier à Luc Trépanier, Clarisse Deschênes-Rancourt, Nicolas Francoeur-Leblond, Martin Blouin et Jean-Philippe Drolet pour leur participation à l'essai de lavage de sol et toute l'énergie qu'ils y ont mis. Merci aussi à Samuel Roy, Guillaume Germain et Jean-Marc Ballard pour leur implication dans certaines portions du projet. Je tiens finalement à remercier les gens de TechnoRem qui ont bien voulu partager avec nous leur expertise dans le cadre de l'essai de lavage de sol : Jean-Marc Lauzon, David Morin, Olivier Pontlevoy, René Cournoyer et René Marcoux.

Plus personnellement, je remercie mes parents pour leur grand support et leurs encouragements, ma famille et mes amis, ainsi que ma tendre moitié, Sophie, pour sa présence ainsi que ses mots constants d'encouragement qui m'ont permis d'aller jusqu'au bout de ce projet.

TABLE DES MATIÈRES

LISTE DES TABLEAUX

LISTE DES FIGURES

LISTE DES ANNEXES

CHAPITRE 1

SYNTHÈSE

1.1 Introduction

1.1.1 Contamination des aquifères aux hydrocarbures pétroliers légers

La contamination des aquifères par des hydrocarbures pétroliers est un fléau répandu partout à travers le monde, particulièrement dans les pays industrialisés comme le Canada. Selon le Conseil Canadien des Ministres de l'Environnement (CCME), au Canada environ 60% des sites contaminés contiennent des hydrocarbures pétroliers (HP), ce qui en fait le groupe de contaminant le plus répandu au pays, soit sur plus de 10 000 sites contaminés (CCME, 2001). Dans le cas des hydrocarbures pétroliers légers comme l'essence et le diésel, les stations-service et les dépôts pétroliers sont grandement responsables de leur propagation dans le sol et l'eau souterraine. Ce sont les fuites au niveau des réservoirs souterrains de carburants et des conduites alimentant les pompes de service qui sont généralement responsables de la contamination que l'on retrouve au niveau de la nappe phréatique.

Les hydrocarbures pétroliers légers font partie de la grande catégorie des contaminants appelés liquides immiscibles légers (LIL) (ou *Light Non-Aqueous Phase Liquids - LNAPL*). En plus de leur toxicité et leur mobilité, les LIL comme l'essence sont des contaminants persistants dans les sols en raison de leur faible solubilité à l'eau et leurs tensions interfaciales (TIF) élevées avec l'eau. Lors d'une fuite ou d'un déversement de LIL, le contaminant plus léger que l'eau migre verticalement dans la zone non-saturée vers la surface de la nappe pour former une lentille sur la nappe phréatique qui se déplace horizontalement, préférentiellement dans le sens de l'écoulement de l'eau

souterraine. Lorsque les quantités déversées sont suffisamment importantes pour créer une pression en huile supérieure à la pression de déplacement de l'eau, le contaminant se propage dans la partie supérieure de la zone saturée. En raison des variations saisonnières du niveau de la nappe, la lentille se déplace aussi verticalement et crée des sols contaminés. Selon la position de la zone source, le contaminant léger se retrouve dans le milieu poreux avec des saturations variables, allant de saturation irréductible en eau à saturation résiduelle en essence. Selon le degré de saturation et les propriétés des aquifères, les différentes méthodes de réhabilitation conventionnelles d'aquifères ont des performances variables.

1.1.2 Les forces impliquées dans le piégeage des hydrocarbures pétroliers

Selon Bradner et Slotboom (1975), trois forces agissent sur le comportement des hydrocarbures pétroliers dans la zone saturée : (1) les forces capillaires, (2) les forces gravitationnelles et (3) les forces visqueuses. Les forces capillaires sont définies par l'équation de Young-Laplace :

$$Pc = \frac{2\sigma cos\theta}{R}$$

La force capillaire P_c dépend de la tension interfaciale (σ) entre l'eau et le HP, de l'angle de contact θ entre les gouttelettes de HP, l'eau et les particules de sol (mouillabilité), ainsi que du rayon (R) des pores du sol dans lesquels sont présentes les gouttelettes de HP. Une tension interfaciale eau – HP élevée combinée à de faibles valeurs d'angles de contact et une granulométrie fine engendrent des forces capillaires élevées. Dans le cas d'hydrocarbures légers comme l'essence, les tensions interfaciales créent des forces capillaires élevées. L'essence se retrouve piégée dans le milieu poreux par les forces capillaires qui empêchent la mobilisation dans l'aquifère. La diminution des forces capillaires par l'abaissement des tensions interfaciales ou un changement de mouillabilité peut permettre une amélioration de la récupération d'essence en favorisant sa mobilisation.

Les forces gravitationnelles sont quant à elles régies par l'équation suivante :

$$Fg = \Delta\rho gh$$

Les forces gravitationnelles dépendent donc de la différence de densité entre l'eau et le contaminant ($\Delta\rho$), de l'accélération gravitationnelle (g) et de la dimension des

gouttelettes de contaminants (h). Dans le cas de l'essence, sa faible densité par rapport à l'eau provoque des forces gravitationnelles orientées vers le haut.
Finalement, les forces visqueuses sont définies par l'équation suivante :

$$Fv = \frac{VL\mu}{k}$$

Les forces visqueuses sont donc gouvernées par la vitesse de Darcy (V) et la viscosité dynamique du fluide de déplacement (μ), la longueur de la gouttelette de contaminant entourée par le fluide déplaçant de déplacement (L) (dans le cas d'un déplacement horizontal) ou d'une épaisseur donnée (dans le cas d'un déplacement vertical) ainsi que la perméabilité du milieu poreux dans lequel circule le fluide (k). Les forces visqueuses peuvent être modifiées en modifiant la vitesse ou la viscosité. L'utilisation d'un polymère rhéofluidifiant améliore le balayage des zones contaminées en augmentant la viscosité dynamique du fluide de déplacement et en répartissant le fluide de déplacement dans les zones de grande comme de faible perméabilité.

1.1.3 Méthodes conventionnelles de réhabilitation d'aquifères contaminés aux hydrocarbures pétroliers légers

Au cours des dernières décennies, plusieurs techniques de réhabilitation de sols et d'aquifères contaminés aux hydrocarbures pétroliers (HP) ont vu le jour dans le domaine de l'environnement. Les méthodes de récupération assistée d'hydrocarbures ont vu le jour dans le domaine pétrolier au début des années 1950, dans le but d'améliorer les taux de récupération de pétrole à des fins économiques (Lake, 1989). La technique d'ennoyage ou «water flooding», la plus utilisée par les pétroliers, consiste à injecter de l'eau dans la formation pour augmenter les forces visqueuses. Cette technique n'est pas transférable pour des applications environnementales puisque les tensions interfaciales ne sont pas abaissées et laissent des saturations résiduelles en hydrocarbures sous formes de ganglions de dimensions variés (Chatzis et al., 1983; Larson et al., 1980; Wardlaw & McKellar, 1985) trop importantes pour satisfaire aux critères environnementaux, tant au niveau de la qualité de l'eau souterraine que des sols. Dans les années 1990, de nouvelles méthodes de récupération des HP ont du être développées pour le domaine de l'environnement afin de réduire au minimum les concentrations résiduelles en HP dans les sols et aquifères. Les diverses techniques développées permettent de récupérer les HP via plusieurs mécanismes : volatilisation, oxydation, solubilisation, mobilisation, pompage ou biodégradation. Les différentes

méthodes ont évidemment chacune leurs forces et faiblesses, des contraintes d'utilisation et des limitations de rendement. Parmi ces méthodes, trois seulement sont retenues pour une description détaillée, soit l'extraction sous vide (connue aussi sous le nom de «slurping») (Miller, 1996), l'oxydation chimique (ITRC, 2005) et le lavage de sol (Roote, 1997). Toutes trois sont des méthodes applicables *in situ*.

L'extraction sous vide consiste en un pompage à vide relativement important permettant de récupérer les LIL libres en phase flottante au-dessus de la nappe phréatique et dans la frange capillaire. Le vacuum exercé doit être suffisamment élevé pour aspirer le contaminant en phase libre jusqu'à la surface et à l'unité de traitement, mais pas trop grand non plus pour éviter de colmater la crépine du puits d'aspiration. Une succion bien ajustée crée donc un gradient de pression et permet de mobiliser les HP vers le puits (dans le rayon d'influence) sans créer de rabattement trop important de la nappe, minimisant ainsi le volume d'eau à traiter. Les fluides récupérés par extraction sous vide contiennent donc un mélange d'eau, de LIL et de gaz dont la densité globale est plus faible que l'eau, ce qui permet d'appliquer cette technique à des profondeurs dépassant les 8 mètres. L'extraction sous vide atteint sa limite d'efficacité à l'approche de la saturation résiduelle en HP. L'extraction sous vide permet de récupérer la phase flottante des HP tout aussi longtemps que la phase reste mobile. Lorsque la saturation en HP diminue en raison du pompage, il y a discontinuité de la phase huileuse et le HP devient immobile et irrécupérable à l'approche de la saturation résiduelle.

L'oxydation chimique utilisée comme méthode de restauration d'aquifères contaminés consiste à injecter dans le sol une solution contenant un oxydant, détruisant le contaminant organique en le convertissant en composés inoffensifs pour l'environnement (CO_2, H_2O, acides carboxyliques, etc.). Les oxydants les plus utilisés sont le peroxyde d'hydrogène (H_2O_2), le permanganate de potassium ($KMnO_4$), le persulfate (S_2O_8) et l'ozone (O_3). Pour certaines réactions d'oxydation, un catalyseur, par exemple le fer, favorisant la formation de radicaux hydroxyles ($OH^{\bullet}$) beaucoup plus puissant que l'oxygène libre, est nécessaire afin de mettre en marche la réaction. L'ajout de certains additifs est parfois nécessaire dans le but de stabiliser ou retarder la réaction ou bien afin de changer les conditions de pH lors de la réaction. L'oxydant est généralement injecté dans l'aquifère sous pression par un puits d'injection. Le volume injecté ainsi que la pression d'injection sont fonction de la capacité de la formation à permettre l'écoulement de la solution. L'oxydation chimique performe bien lorsque le HP

est dissous dans la phase aqueuse et moins bien lorsqu'il est en phase libre ou adsorbé sur les surfaces des minéraux (ou solides).

Le lavage de sol fait partie des techniques qui sont inspirées de ce qui est fait dans le domaine pétrolier pour la récupération assistée du pétrole (Pope et al., 1995). En hydrogéologie, la méthode consiste à injecter par un puits d'injection une solution micellaire, qui balaye la zone contaminée et qui est ensuite pompée à la surface avec le contaminant par des puits d'extraction selon un patron d'injection/pompage particulier (Dwarakanath et al., 1999; Falta, 1998; Farley et al., 1993; Fountain et al., 1991; Fountain et al., 1996; Knox et al., 1997; Martel, 1996; Sabatini et al., 1997). Contrairement à l'extraction sous vide, le lavage de sol est performant même lorsque le contaminant est à saturation résiduelle. Sa limitation est toutefois au niveau de la phase post-réhabilitation, puisque cette technique implique la génération de grands volumes d'effluents liquides à traiter en surface. Ceux-ci doivent être recyclés, traités et disposés. De plus, si les débits d'injection/pompage ne sont pas ajustés correctement, il est possible de perdre de la solution micellaire à l'extérieur de la parcelle de traitement in situ. La modélisation numérique de l'écoulement dans la parcelle est donc un point clé de la réussite de cette méthode.

1.1.4 Solutions micellaires

Une solution micellaire est composée d'un mélange d'eau et de tensioactif et/ou d'alcool. Un tensioactif, par définition, est un composé qui modifie la tension interfaciale entre deux liquides immiscibles. Il s'agit de molécules amphiphiles, i.e. possédant deux parties de polarité différente, une hydrophile et une lipophile. Il existe quatre types de tensioactif; anionique avec la partie hydrophile chargée négativement; cationique avec la partie hydrophile chargée positivement; amphotère avec la partie hydrophile possédant les deux charges; puis finalement non ionique sans charge nette. La partie lipophile du tensioactif a une affinité avec l'huile alors que la partie hydrophile préfère l'eau. À l'interface entre la phase aqueuse et huileuse, il y a accumulation de monomères de tensioactif avec leur groupe lipophile orienté vers la phase huileuse et leur groupe hydrophile orienté vers la phase aqueuse. Ce phénomène a pour effet de diminuer la tension interfaciale (Figure 1.1). Lorsque la concentration du tensioactif est augmentée, les parties lipophiles des monomères commencent à se regrouper en agrégats (micelles) contenant plusieurs monomères chacun. Lorsque la concentration micellaire critique (CMC) est atteinte, toute augmentation de la concentration du tensioactif ne fait

qu'augmenter le nombre de micelles et non pas la concentration des monomères (Figure 1.2). Étant donné que les CMC sont généralement petites (environ 10^{-5} à 10^{-4} kg-moles/m^3), le tensioactif est pratiquement toujours sous forme de micelles (Lake, 1989). Pour un tensioactif soluble dans l'eau, les micelles ont la capacité d'emprisonner des composés organiques en leur centre tout en restant soluble dans la phase aqueuse. L'inverse est également possible alors qu'un tensioactif soluble dans un composé organique peut emprisonner dans ces micelles (appelées micelles inverses) des molécules d'eau, faisant ainsi gonfler la phase organique.

La portion de la solution micellaire composée d'alcool et de tensioactif uniquement porte le nom de «matière active» en raison de sa capacité à récupérer activement les liquides organiques immiscibles comme les HP. Dépendamment du type de matière active choisie, de sa concentration ou des conditions de salinités, la récupération de HP dans la zone contaminée peut se faire selon quatre différents mécanismes. Premièrement, si la solution de lavage a pour effet de réduire grandement la tension interfaciale entre la phase aqueuse (l'eau de l'aquifère) et la phase huileuse (HP), cette dernière sera mobilisée dans une phase organique à l'avant du front de la solution de lavage, sous la forme d'un banc de HP. Deuxièmement, la matière active peut transférer dans les HP et ainsi faire gonfler la phase huileuse (formation de micelles inverses). Ce mécanisme diminue la tension interfaciale et les HP sont mobilisés à l'intérieur de la phase organique vers les puits de pompage. Troisièmement, les HP peuvent être solubilisés par la solution micellaire, i.e. que la matière active se partitionne préférentiellement vers la phase aqueuse et les micelles dans la phase aqueuse emprisonnent les HP. Quatrièmement, sous des conditions spécifiques de salinité optimale et de tensions interfaciales ultra-faibles, une troisième phase peut se former entre la phase organique pure et la phase aqueuse pure. Cette zone intermédiaire est généralement appelée phase de microémulsion centrale. Les HP sont donc récupérés dans cette microémulsion centrale par les puits de pompage (St-Pierre, et al., 2004).

L'ajout à la solution micellaire d'un polymère rhéofluidifiant comme la gomme de xanthane améliore la récupération des HP en diminuant les instabilités de viscosité au front du banc de solution de lavage, améliorant ainsi le balayage de la zone contaminée (Martel, 1995; Martel et al., 1998). En effet, un fluide rhéofluidifiant a pour propriété de changer de viscosité en fonction du taux de cisaillement, ce qui permet à la solution contenant le polymère de balayer plus également les zones de plus faibles perméabilités

(taux de cisaillement élevé et faible viscosité de la solution) par rapport aux zones de grandes perméabilités (taux de cisaillement plus faible et forte viscosité de la solution).

1.2 Travaux antérieurs

1.2.1 Développement de solutions tensioactives

Des travaux ont été faits par le passé sur le développement et l'étude de solutions tensioactives dans le but de les utiliser pour le lavage de sol et récupérer des liquides immiscibles (denses ou légers) dans les aquifères. Les diagrammes de phases indiquent les concentrations en matière active qui peuvent être injectées dans un aquifère (Falta, 1998). Les travaux de Martel et al. (1996) sur l'optimisation des solutions tensioactives par les diagrammes de phases ont permis d'évaluer les différents facteurs qui jouent un rôle sur la performance d'une solution de lavage pour un contaminant donné. Entres autres, la nature des composantes du système (tensioactif, alcool et liquide immiscible), le ratio alcool/tensioactif, la température de l'eau et la salinité jouent tous un rôle à un certain degré. L'étude révèle également que l'utilisation d'un alcool combiné avec un tensioactif est plus efficace que l'utilisation séparée d'alcools ou de tensioactifs. Lors de cette même étude, plusieurs contaminants ont été utilisés et testés en diagrammes de phases avec différentes solutions tensioactives : des LIL comme l'essence et le diesel, des solvents chlorés comme le PCE et le TCE ainsi que des huiles lourdes diverses (créosote, huile à moteur, huile synthétique à transmission et les liquides immiscibles denses (LID) de terrains contaminés de Ville Mercier et L'Assomption).

Une autre étude de Martel et Gélinas (1996) démontre que l'abaissement des tensions interfaciales (TIF) est en accord avec les prédictions faites par les diagrammes de phases. Pour une concentration en matière active donnée, les TIF sont plus basses pour un système qui dissout mieux le LIL. Les nombreux essais en colonnes effectués dans le cadre de cette étude ont révelé qu'il y a une bonne corrélation entre le taux de dissolution de LIL dans les diagrammes de phases et les essais en colonnes, mais que la baisse de température de 25 °C à 8 °C affecte négativement la performance de la solution tensioactive, contrairement aux diagrammes de phases qui ne permettaient pas de déceler une différence à ce niveau. Pour les essais d'extraction de diesel en petites colonnes de sable, certains facteurs autres que la nature de la solution tensioactive ont

influencé la performance de l'extraction : la direction d'écoulement (haut/bas), le volume de solution injecté et, à un niveau moindre, la salinité de l'eau.

Selon Martel et Gélinas (1998), la formulation d'une solution tensioactive est spécifique à un lieu contaminé et doit être modifiée si les propriétés de surface des solides (minéralogie, rugosité) changent localement ou si le comportement interfacial des liquides (type d'huile) change. Un essai en large colonne de sable a aussi permis de réaliser que plusieurs volumes des pores de solution de polymère (5 VP dans le cas présent) étaient nécessaire suite au passage de la solution de lavage afin d'abaisser suffisamment les concentrations en alcool et en tensioactif pour permettre leur biodégradation (Martel et al., 1998). L'ensemble des résultats, réalisations et conclusions énumérés précedemment se retrouvent dans la thèse de doctorat de Martel, 1996.

Les travaux de St-Pierre et al. (2004) sur la récupération de TCE par des solutions micellaires ont également permis d'évaluer la performance de certaines solutions de lavage pour le TCE ainsi que leurs mécanismes de récupération. Ces travaux montrent que le diagramme de phase d'un système donné permet de prédire le ou les mécanismes de récupération de la solution par l'inclinaison de ses *tie lines*. De plus, les travaux dévoilent l'importance capitale de tracer la *tie line* critique pour connaître le mécanisme de récupération associé à la concentration d'injection.

1.2.2 Contrôle de la mobilité des solutions de lavage

Pour que la solution de lavage employée soit efficace à son plein potentiel, il faut que la totalité de la zone contaminée soit balayée. Il y a deux types de balayage : en plan et en coupe (Lake, 1989). Le balayage en plan est contrôlé par le patron d'injection/pompage alors que le balayage en coupe dépend de l'hétérogénéité des couches et de la stabilité du front d'injection. Dans un milieu hétérogène, le patron de circulation de la solution de lavage est fortement contrôlé par les différences de perméabilité entre les différentes couches de matériaux géologiques. Le fluide circulant dans l'aquifère passera préférentiellement dans un horizon plus perméable (sable, gravier) plutôt qu'un horizon moins perméable (argile, silt), ce qui entraîne un mauvais balayage des zones moins perméables. Les travaux de Martel (1995) et Martel et al. (1998), ont permis d'optimiser le balayage en coupe d'une solution tensioactive avec l'aide d'une solution de polymère visqueuse comme agent mobilisateur. La gomme de xanthane a été selectionnée parmi plusieurs polymères en raison de sa solubilité et de ses propriétés rhéologiques. Pour

améliorer le balayage, la solution de xanthane peut être soit : (1) introduite directement dans la solution de lavage; (2) dans un banc à part devançant celui de la solution de lavage pour obtenir un front plus uniforme; (3) dans un banc à part suivant la solution de lavage pour pousser uniformément la solution de lavage et éviter les instabilités de viscosités; (4) ou bien une combinaison entre ces trois possibilités.

1.3 Objectifs et contributions

Cette étude s'inscrit dans le cadre d'un large projet de recherche dont le but est d'élaborer un train de technologies combinant le lavage de sol à l'extraction sous vide et l'oxydation chimique en polissage afin d'atteindre les objectifs de décontamination fixés par les organismes réglementaires. Pour la réalisation de ce projet, une station-service aux prises avec une contamination en essence sert de terrain pilote. L'objectif général de ce mémoire est de développer une solution de lavage efficace pour ce terrain pilote. Les objectifs spécifiques de cette étude sont donc concentrés sur la partie lavage de sol du projet. Dans un premier temps, au chapitre 2 du mémoire, le but est d'identifier une solution de lavage performante en fonction du contaminant retrouvé sur le site par le biais de diagrammes de phases. Dans ce même chapitre, il s'agit ensuite d'évaluer la performance de certaines solutions de lavage prometteuses identifiées par les diagrammes de phases et d'identifier leurs mécanismes de récupération par des essais en petites colonnes de sol (110 cm^3), dans le but d'arrêter le choix sur une seule solution optimale. Le troisième objectif consigné au chapitre 2 consiste à caractériser la relation entre le contaminant et la solution de lavage optimale par des mesures de tensions interfaciales et d'angles de contact. Pour cette première partie, j'ai réalisé seul la totalité des travaux. Finalement, abordé au chapitre 3 du mémoire, le dernier objectif de cette étude est de tester la solution de lavage sur le terrain à l'échelle pilote (45 m^3). Pour cette partie, j'ai participé à la conception de la stratégie d'injection et à la réalisation des travaux de terrain en collaboration avec d'autres membres de l'équipe de Richard Martel, et j'ai effectué seul la collecte et l'interprétation des résultats.

Même si des études semblables ont été réalisées par le passé par Martel et al., (1993; 1996; 1998), des recherches approfondies doivent être faites pour chaque projet différent nécessitant l'utilisation de solutions tensioactives, puisque l'optimisation d'une telle solution varie selon les types de contaminant et de sol. Les résultats obtenus dans le cadre des travaux de ce mémoire serviront de référence pour les phases ultérieures

du projet. Ce projet se distingue cependant des précédents par l'intégration du lavage de sols avec d'autres technologies de réhabilitation. Une grande partie des travaux a été présentée lors de deux conférences, soit RemTech 2010, Banff, Alberta (Grenier et al., 2010) et AIH/SGC 2009, Halifax, Nouvelle-Écosse (Grenier et al., 2009). L'article soumis dans le cadre de la présentation à l'AIH/SGC 2009 est présenté à l'Annexe A, alors que le résumé soumis pour la présentation à RemTech 2010 est présenté à l'Annexe B.

1.4 Méthodologie et approche de l'étude

La première étape de l'étude est de caractériser le contaminant, l'essence usée dans le cas présent, ainsi que les matériaux géologiques en place. Premièrement, une analyse granulométrique sur le sol provenant du site a été effectuée afin de connaître sa distribution granulométrique et son contenu en particules fines. Une analyse minéralogique a été réalisée afin d'identifier les principaux minéraux composant le sol. Une analyse chimique de l'essence a été faite pour identifier les différents composés de l'essence usée. Des mesures de densité, viscosité, tensions interfaciales entre l'essence et l'eau ainsi que des mesures d'angles de contact entre l'essence, l'eau et les minéraux majeurs présents dans le sol ont été effectuées.

L'étape suivante consistait à tester différentes combinaisons entre une série de tensioactifs et d'alcools par des diagrammes de phases, afin d'identifier les mélanges prometteurs pouvant dissoudre l'essence usée. Les courbes de miscibilité dans les diagrammes de phases ont été tracées selon la méthode décrite par Martel et al. (1993) et les courbes les plus basses ont été considérées comme étant les plus prometteuses. La construction des diagrammes de phases s'est faite à 8°C, soit la température de l'eau souterraine du terrain. Au total, 7 alcools et 18 tensioactifs différents ont été testés. Une stratégie basée sur l'indépendance des variables en jeu est élaborée afin de diminuer le nombre de possibilités de mélanges entre les alcools et les tensioactifs.

Les meilleures solutions ainsi trouvées ont ensuite été testées en petites colonnes de sol du site dans des essais de récupération d'essence pour vérifier leur performance. Les colonnes de sol sont des cylindres de verre de 10 cm de long et d'un diamètre de 3,7 cm avec, à chaque bout, des bouchons perforés en téflon pour uniformiser l'écoulement des fluides à l'entrée et à la sortie des colonnes. Les colonnes sont remplies de sol tamisé provenant du site et compacté selon une méthode élaborée par Martel (1996). Avant d'y faire circuler les solutions de lavage, les colonnes sont d'abord

saturées en CO_2 pour éliminer l'air, saturées en eau désaérée pour simuler les conditions d'un aquifère et ensuite pré-contaminées avec une masse connue d'essence. Suite au passage de la solution micellaire, une solution de xanthane est injectée pour pousser uniformément les ingrédients de la solution de lavage à l'extérieur de la colonne. Les effluents sont récupérés dans des vials et le sol est analysé à la fin de l'essai pour connaître le taux de récupération d'essence de chacune des solutions ainsi que leurs mécanismes de récupération.

En fonction des résultats des essais en colonnes, une solution optimale est choisie et des mesures complémentaires sont effectuées pour mieux caractériser la relation entre l'essence et la solution micellaire. Des mesures de tensions interfaciales entre les phases aqueuses et huileuses avec l'ajout de la matière active à différentes concentrations sont donc réalisées, ainsi que des mesures d'angles de contact entre ces mêmes phases aqueuses et huileuses en fonction de la concentration en matière active afin d'évaluer l'impact de la solution de lavage sur ces deux paramètres physiques importants. L'ensemble des travaux décrits précédemment sont décrits en détail dans le chapitre 2 du mémoire.

La dernière étape consiste à réaliser un essai de terrain à une échelle pilote afin de tester la solution de lavage dans des conditions réelles d'application de la technologie. L'essai a été effectué avec un patron d'injection/pompage hexagonal comprenant un puits d'injection central et six puits de récupération positionnés sous forme d'un hexagone en périphérie du puits d'injection. Une modélisation numérique de l'écoulement de l'eau souterraine a été faite à priori pour ajuster les débits d'injection et de pompage afin que la solution injectée soit totalement récupérée par les six puits de pompage. Cette étape permet aussi d'estimer le balayage en plan du patron d'injection/pompage choisi. Cette étape a été réalisée par Olivier Pontlevoy de la firme partenaire de l'étude, Technorem. L'injection de la solution micellaire est précédée d'un banc d'eau saline contenant un traceur pour mieux évaluer les temps d'arrivée de la solution dans les différents puits ainsi que pour diminuer la dilution de salinité au front de la solution de lavage. En effet, le sel fait partie des ingrédients de la solution de lavage et joue un rôle important dans la solubilisation de l'essence. La solution micellaire est ensuite injectée en deux bancs : un premier sans polymère suivant le banc d'eau saline; le deuxième avec polymère pour effectuer une gradation de viscosité et mieux balayer en coupe la zone contaminée. La séquence d'injection se termine avec une solution de xanthane pour pousser complètement la solution de lavage vers les puits de

récupération. Les effluents de chacun des puits de pompage sont recueillis ensemble dans un réservoir pour évaluer la quantité d'essence récupérée. Les travaux effectués lors de cet essai de terrain sont décrits dans le chapitre 3 du mémoire.

1.5 Résultats et discussion

Les mesures des propriétés physiques et chimiques de l'essence usée et des matériaux géologiques retrouvés sur le site pilote sont présentées dans le Tableau 2.3 du Chapitre 2. Les propriétés principales de l'essence usée sont une faible densité (0,788 g/cm^3), une faible viscosité (689 µPa•s) et une tension interfaciale élevée avec l'eau (64 mN/m). Une diminution de la tension interfaciale par la solution micellaire est souhaitable pour espérer une bonne récupération. Les analyses des matériaux géologiques montrent pour leur part un sol composé de quartz, feldspath et calcite avec une granulométrie passant principalement du sable fin au gravier fin.

Les diagrammes de phases réalisés pour sélectionner des solutions micellaires prometteuses sont présentés aux Figures 2.3 à 2.7 du Chapitre 2. Les diagrammes montrent que la performance d'un alcool utilisé seul n'est pas un bon indicateur de sa performance en tandem avec un tensioactif. En effet, les meilleurs alcools seuls, le n-propanol et l'iso-propanol, sont largement dépassés en terme de potentiel de dissolution d'essence par quatre alcools : le sec-butanol, l'iso-butanol, le n-propanol et le n-amyl (n-pentanol). Le meilleur ratio alcool/tensioactif identifié est de 1,0. L'alcool le plus performant en combinaison avec un tensioactif est le n-butanol. À un ratio alcool/tensioactif de 1,0 le n-butanol et trois tensioactifs ont été sélectionnés pour former les trois types de solutions prometteurs pour la dissolution de l'essence usée. Certaines de ces solutions ont ensuite été optimisées par augmentation de salinité ou par ajout d'un second alcool. De cette façon, quatre solutions micellaires prometteuses ont été sélectionnées pour être testées par le biais d'essais en colonnes de sol :

- n-BuOH/Arkopal N90 = 1,0;
- n-BuOH/Nansa HS90 =1,0;
- (n-BuOH/n-AmOH = 1,0)/SAS = 1,0;
- n-BuOH/SAS = 1,0 + 7,5 g/L NaCl.

Le Tableau 2.4 du Chapitre 2 présente la totalité des séquences d'injection testées lors des essais en colonnes ainsi que les résultats de récupération. Les solutions testées en concentration de matière active de 7,5% sont beaucoup plus performantes qu'à 5,0%.

La solution micellaire la plus performante suite aux essais en colonnes est : n-BuOH/SAS = 1,0 à 7,5% de matière active + 7,5 g/L de NaCl + 300 ppm de xanthane. Basé sur les effluents des colonnes, le ratio des mécanismes de récupération mobilisation/récupération est de 95/5 pour cette solution.

L'utilisation d'un banc d'eau salée avant l'injection de la solution micellaire (dans le cas d'une solution micellaire salée) permet d'améliorer la récupération d'essence en diminuant la dilution de la salinité au front de la solution micellaire. Comme l'eau salée diminue légèrement les tensions interfaciales, le banc d'eau salée permet même de récupérer une petite fraction d'essence. L'ajout de xanthane directement dans la solution micellaire permet également d'augmenter la performance de récupération de la solution. En plus de pousser uniformément la solution micellaire, le banc de solution de xanthane injecté après la solution micellaire permet de récupérer une portion supplémentaire d'essence grâce à l'augmentation des forces visqueuses. Un nombre de volume de pores de solution de xanthane de 1,6 semble suffisant comme le montre la Figure 2.10 du Chapitre 2 puisque la récupération stagne à ce nombre. Par contre, l'analyse des effluents des colonnes montre clairement que le nombre de volume des pores de solution de xanthane injecté a été insuffisant et que l'optimal d'injection serait plutôt entre 1,5 et 2,0 volumes des pores.

La solution micellaire optimale a une densité légèrement supérieure à celle de l'eau (1005 kg/m^3 versus 1000 kg/m^3 pour l'eau à 8°C) et une viscosité 1,5 fois supérieure à celle de l'eau (2217 µPa•s à 8°C). Les mesures de tensions interfaciales sont présentées à la Figure 2.11 du Chapitre 2 et révèlent qu'à une concentration en matière active aussi faible que 0,1%, la tension interfaciale entre l'eau et l'essence chute de 96%. Les résultats des mesures d'angles de contact sont présentés à la Figure 2.12 du Chapitre 2, mais aucune conclusion intéressante ne peut en être tirée. La technique utilisée pour les mesures pourrait être la cause de ces résultats. Une autre technique plus appropriée pourrait être employée et est décrite à la section du Chapitre 2 – *Results and discussion – Characterization of the optimal micellar solution.*

Tous les résultats relatifs à l'essai terrain à l'échelle pilote sont présentés au Chapitre 3. Pour l'essai pilote, les courbes d'arrivée des solutions saline et micellaire ont révélé que la porosité efficace dans la cellule d'essai était de 2,5%. La valeur de porosité utilisée pour les calculs des quantités de matière active nécessaires en fonction du volume des pores était plutôt de 20%. La quantité de matière active injectée a été huit fois plus élevée que ce qui était désiré. L'évaluation de la porosité efficace par l'entremise d'un

essai de traçage aurait donc été primordial avant d'effectuer un essai de lavage de sol afin d'éviter des coûts supplémentaires.

Une porosité efficace de cet ordre de grandeur est synonyme d'une proportion assez élevée d'eau immobile dans les pores de sol. Les résultats des mesures de conductivité électrique dans les effluents des différents puits d'observation de la cellule montrent que les concentrations en matière active et en sel des solutions injectées atteignent environ 70% seulement de leur valeur d'injection. L'eau immobile joue donc un rôle dans la dilution des solutions injectées et doit être considérée pour les projets futurs.

Au niveau de la récupération d'essence et des produits injectés obtenue par le suivi des concentrations en SAS dans l'effluent, les résultats globaux indiquent qu'un volume de 7,5 litres d'essence a été récupéré ainsi que 72% de la masse initiale en matière active. Ainsi 28% de la masse injectée en SAS est dans la cellule disponible pour l'étape d'oxydation chimique ultérieure. Selon les concentrations de SAS dans les puits à l'intérieur de la cellule après l'essai, seulement 8% de la masse initiale de SAS serait en solution. L'hypothèse de l'adsorption du SAS dans les pores de sol et à la surface des solides est très probable et des essais d'adsorption devraient être effectués pour valider cette hypothèse. L'hypothèse de la perte de matière active à l'extérieur de la cellule est écartée puisque la modélisation numérique confirme que le ratio d'injection/pompage de 1 /2 est suffisant (voir la Figure 3.15 du Chapitre 3). L'analyse de la performance de chaque puits de récupération est discutée en détail dans la section du Chapitre 3 – *Results and discussion – Product recovery.*

Les résultats d'analyse des échantillons prélevés dans les puits d'observation et de pompage de la cellule après l'essai montrent qu'en plus des concentrations résiduelles en SAS, des concentrations en essence élevées sont observées. Comme le montre le Tableau 3.6 du Chapitre 3, ces concentrations en essence plus élevées qu'avant le début de l'essai sont directement reliées aux concentrations résiduelles en SAS. En effet, l'essence étant dissoute par la solution micellaire, elle est donc en plus grande concentration dans la phase aqueuse restante dans la cellule. Ces concentrations en essence élevées dans la phase aqueuse sont donc de bonne augure pour l'étape suivante d'oxydation chimique du train de technologies, puisqu'une plus grande proportion d'essence sera disponible en solution pour être oxydée. Les travaux d'oxydation chimique sur le terrain ont été effectués par Technorem.

1.6 Conclusions et recommandations générales

Ces travaux s'inscrivent à l'intérieur d'un large projet de recherche visant à améliorer la récupération d'hydrocarbures en utilisant un train de technologies, combinant l'extraction sous vide, le lavage de sol et l'oxydation chimique. Ce mémoire est en lien avec l'étape de lavage de sol uniquement. Le but du lavage de sol étant d'utiliser une solution micellaire capable de solubiliser ou mobiliser l'essence, l'objectif principal de ce mémoire a été de développer, optimiser et tester une solution micellaire pour l'essence et les matériaux géologiques d'une station-service.

Le développement d'une solution micellaire optimale est passé par la construction de diagrammes de phases afin de sélectionner les solutions prometteuses à tester en colonnes de sol. La réalisation des diagrammes de phases a permis de faire les observations suivantes :

- la combinaison d'un alcool et d'un tensioactif permet une meilleure dissolution qu'en les utilisant séparément;
- le rendement d'un alcool seul n'est pas un bon indicateur de sa performance en combinaison avec un tensioactif;
- la combinaison de deux alcools avec un tensioactif peut améliorer la dissolution dans certains cas;
- la salinité d'une solution micellaire peut affecter significativement son rendement.

Les essais en colonnes ont permis d'identifier la meilleure solution micellaire : n-BuOH/SAS = 1,0 + 7,5 g/L de NaCl + 300 ppm de xanthane; et des observations ont pu être tirées de ces essais:

- l'injection d'un banc d'eau salée avant l'injection de la solution micellaire permet de diminuer la dilution de la salinité de la solution micellaire à son front d'avancement;
- l'ajout de polymère directement dans la solution micellaire augmente la performance de la solution;
- l'utilisation d'un banc de solution de polymère permet de récupérer une fraction supplémentaire d'essence en plus de sa fonction première de pousser uniformément la solution micellaire devant elle.

Un nombre de volumes des pores optimal de solution micellaire doit être établi pour son application sur le terrain. Une telle optimisation passe par la réalisation d'un essai en colonne supplémentaire avec l'utilisation d'une quantité de solution micellaire largement

nécessaire pour récupérer la totalité de l'essence ou jusqu'à ce qu'une récupération supplémentaire ne puisse plus être observée. Le nombre de volumes des pores optimal devrait être fixé juste avant le plafonnement de la récupération. Le même type d'exercice devrait également être réalisé pour optimiser le nombre de volumes des pores de la solution de polymère en fonction de la récupération de la matière active résiduelle.

La caractérisation de la solution micellaire a permis, entre autre, de réaliser qu'une très faible concentration de matière active (0,1%) était nécessaire afin de réduire la tension interfaciale entre l'eau et l'essence de 96%. Il serait intéressant de se pencher plus en détail sur cette propriété afin d'évaluer les différentes avenues possibles quant à la stratégie de réhabilitation adoptée. L'injection, sans pompage, d'une solution micellaire à une très faible concentration en matière active pourrait réduire suffisamment les tensions interfaciales pour permettre à l'extraction sous vide de récupérer davantage d'essence à faible coût.

La solution micellaire optimale a été testée sur le terrain à l'échelle pilote à l'aide d'un patron d'injection/pompage hexagonal à 7 points, dont un puits de pompage. L'essai pilote a été précédé d'une phase intensive d'extraction sous vide et a été suivie d'une phase d'oxydation chimique. Le lavage de sol a permis de récupérer une fraction supplémentaire d'essence non récupérable par extraction sous vide et a laissé derrière lui des concentrations en essence dans la phase aqueuse plus élevées qu'avant l'essai, rendant disponible en solution l'essence résiduelle pour la phase d'oxydation chimique.

Le coût unitaire des produits chimiques pour l'essai a été de 100$/$m^3$ de sol contaminé. Les résultats de l'essai ayant montré une porosité efficace beaucoup plus faible que préalablement estimée, les coûts des produits chimiques auraient pu être eux aussi beaucoup plus faibles si un essai de traçage préalable avait permis de déceler cet aspect important, puisque les résultats montrent qu'une grande portion de solution micellaire a été injectée en trop et n'a pas récupéré d'essence. Il est donc primordial qu'un essai de traçage soit réalisé quelques semaines avant l'essai de lavage de sol afin d'évaluer adéquatement la porosité efficace et ainsi commander les quantités appropriées de produits chimiques.

Lors d'un futur essai de lavage de sol à l'échelle pilote, il serait également très utile de prélever des échantillons de sol par carottage avant et après l'essai, comme il a déjà été fait par le passé (Martel, 1996), afin d'établir un bilan de masse sur l'essence et mieux évaluer l'impact de la réhabilitation.

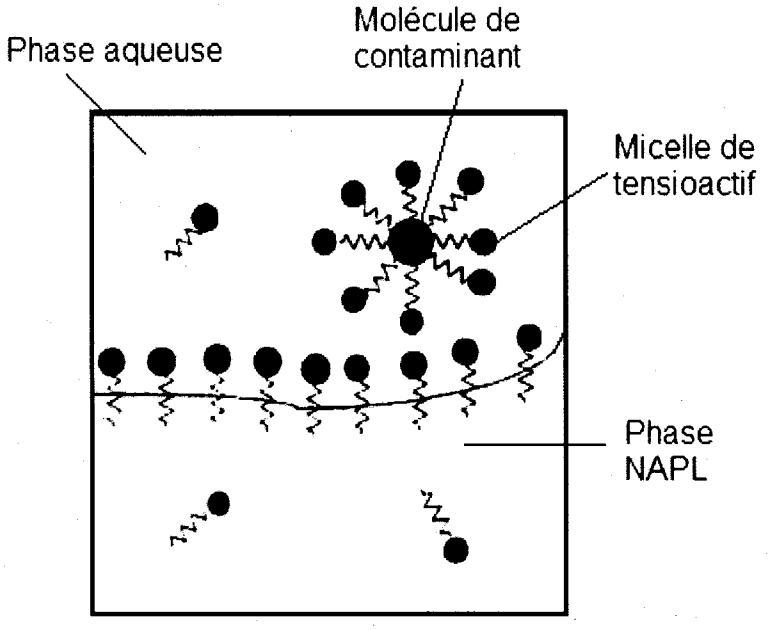

Figure 1.1. Tensioactif en contact avec les phases aqueuse et huileuse (Adapté de Lake, 1989)

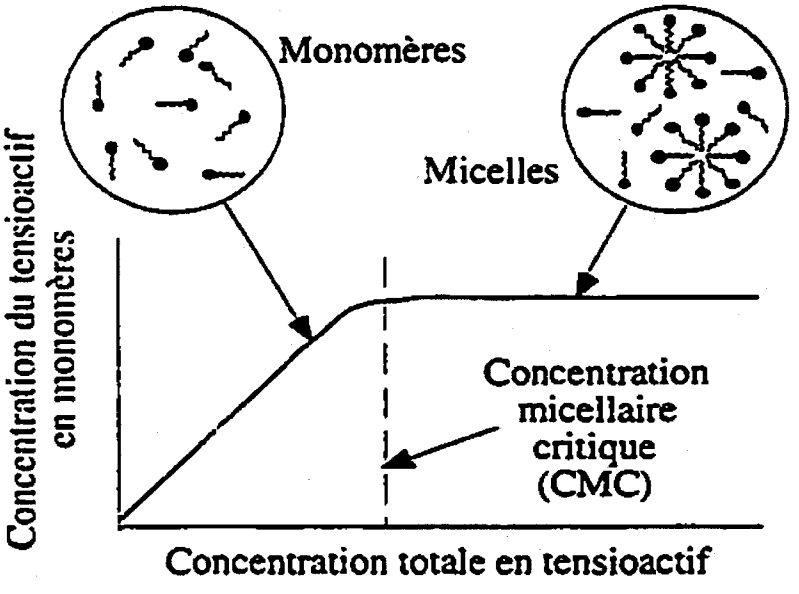

Figure 1.2. Concentration du tensioactif en monomère en fonction de la concentration totale en tensioactif (Adapté de Lake, 1989)

CHAPITRE 2

DEVELOPMENT OF AN OPTIMAL MICELLAR SOLUTION FOR A GASOLINE-CONTAMINATED AQUIFER

2.1 Résumé

Le développement d'une solution micellaire pour la réhabilitation d'un aquifère contaminé à l'essence a été effectué. L'optimisation de la solution micellaire en fonction de l'essence usée et des matériaux géologiques provenant du site contaminée a été faite en quatre étapes : 1) la caractérisation de l'essence et des matériaux géologiques provenant du site contaminé par des mesures de leurs propriétés physiques et chimiques; 2) la sélection de solutions micellaires prometteuses via des diagrammes de phases; 3) l'identification de la solution micellaire optimale par l'entremise d'essais en petites colonnes de sable; et 4) la caractérisation de la solution micellaire optimale via les mesures de ses propriétés physiques. L'essence usée a une densité et une viscosité plus faibles que celles de l'eau, ainsi qu'une tension interfaciale élevée avec l'eau. Les analyses minéralogiques et granulométriques sur les matériaux géologiques ont montré qu'ils se composent de quartz (51%), de feldspath (26%) et de calcite (22)% et sont en majorité constitués de sable fin à du gravier fin. Les diagrammes de phases ont été utilisés comme méthode pour sélectionner les quatre solutions micellaires les plus prometteuses à tester en colonnes de sable. La meilleure solution micellaire obtenue par diagrammes de phases a été optimisée par ajout de sel (NaCl) et de polymère (xanthane) et possède la composition suivante : n-BuOH/SAS = 1,0 + 7,5 g/L de NaCl + 300 ppm de xanthane. Les essais en colonnes de sable ont permis de confirmer l'amélioration de la récupération d'essence sous les conditions suivantes : un pré-conditionnement par l'injection d'un banc d'eau salée (en raison de l'utilisation d'une solution micellaire salée); 2) l'ajout de xanthane dans la solution micellaire; 3) un nombre de volume des pores (VP) injecté important de solution micellaire; et 4) un rinçage avec une solution de polymère. Le nombre optimal de volumes des pores de solution micellaire et de solution de polymère est respectivement de 1,6 et 1,5-2,0. À partir des diagrammes de phases et des essais en colonnes, il est proposé de suivre la séquence d'injection suivante : 1) 0,5 VP d'eau salée à 7,5 g/L de NaCl (pré-conditionnement); 2) 1,6 VP de n-BuOH/SAS = 1,0 à 7,5% de matière active + 7,5 g/L

de NaCl + 300 ppm de xanthane (solution micellaire-polymère de lavage); 3) 2,0 VP de solution de xanthane à 500 ppm (solution de polymère de rinçage). Les mesures de tension interfaciale (TIF) entre la solution micellaire optimale et l'essence usée ont révélé qu'une concentration de 0,1% en matière active permet d'abaisser la TIF de 96%. Une diminution maximale de 99,2% de la TIF est obtenue avec une concentration en matière active de 7,0%. Ces résultats procurent de nouvelles pistes pour l'optimisation de la récupération d'essence avec des solutions de lavage.

2.2 Abstract

The development of an optimal micellar solution for a gasoline-contaminated aquifer was carried out. The optimization of the micellar solution adapted to the weathered gasoline and geological materials from the contaminated site was completed through four main steps: 1) characterization of the gasoline and geological materials from the contaminated site through measurements of their physical and chemical properties; 2) selection of promising micellar solutions via phase diagrams; 3) identification of the optimal micellar solution through sand column experiments; and 4) characterization of the optimal micellar solution via measurements of its physical properties. The weathered gasoline has a density and a viscosity lower than water, as well as a high interfacial tension with water. Grain size and mineralogical analyses have sown that the geological materials present at the contaminated site were mainly made up of quartz (51%), feldspars (26%) and calcite (21%) with a grain size ranging mainly from fine sand to fine gravel. Phase diagrams were used as a screening tool to select the four most promising micellar solutions to be tested in the sand column experiments. The optimal micellar solution obtained from phase diagrams was optimized by adding salt (NaCl) and polymer (xanthan), to obtain the following composition: n-BuOH/SAS = 1.0 + 7.5 g/L of NaCl + 300 ppm of xanthan. The sand column experiments confirmed that the following conditions improve gasoline recovery: 1) injection of a salted water preflush prior to the micellar solution (for a salted micellar solution); 2) addition of xanthan in the micellar solution; 3) high injected pore volume (PV) of micellar solution; and 4) high injected rinsing PV of polymer solution. Optimal injected PV of micellar solution and polymer solution were of 1.6 and 1.5 to 2.0 respectively. From phase diagrams and sand column experiments, the following injection sequence is suggested: 1) 0.5 PV of salted water at 7.5 g/L of NaCl (preflush); 2) 1.6 PV of n-BuOH/SAS = 1.0 at 7.5% of active matter + 7.5

g/L of NaCl + 300 ppm of xanthan (washing micellar-polymer solution); 3) 2.0 PV of xanthan solution at 500 ppm (rinsing polymer solution). Interfacial tension measurements (IFT) between the optimal solution and the weathered gasoline revealed that a concentration of 0.1% of active matter allowed an IFT decrease of 96%. A maximum IFT drop of 99.2% occurred with a concentration of 7.0% of active matter. These results provide new approaches for the optimization of gasoline recovery using washing solutions.

2.3 Introduction

Aquifer contamination by petroleum hydrocarbons (PHC's) is a plague that is spread all over the world, and especially in industrialized countries such as Canada. In Canada, PHC's such as gasoline are the most widespread contaminants found in tens of thousands of contaminated sites (CCME, 2001). Besides their toxicity and mobility, PHC's are persistent contaminants in soil because of their low water solubility and their high interfacial tensions (IFT) with water. Because of these characteristics, existing remediation technologies are not always efficient enough to reach environmental standards for groundwater and soil quality.

According to Bradner and Slotboom (1975), three forces control PHC's behavior in the saturated zone: capillary forces, gravity forces and viscous forces. Capillary forces are defined by the Young-Laplace equation: $P_c = 2\sigma\cos\theta / R$ and depend on PHC-water IFT (σ), soil particle-PH-water contact angle (θ) and soil pore radius (R). Gravity forces are defined as: $F_g = \Delta\rho gh$, and depend on the density difference between water and gasoline ($\Delta\rho$), gravitational acceleration (g) and on gasoline droplet size (h). Viscous forces are a function of the displacing fluid velocity (v), dynamic viscosity (μ), porous media permeability (k) and pressure gradient in the displacing fluid for horizontal flow (dp/dx) as follows: $F_v = v\mu = k(dp/dx)$. To improve gasoline recovery in aquifers, among other actions, capillary forces should be decreased through wettability changes and by decreasing the IFT.

In the last decades, in situ recovery technologies were developed to improve aquifer remediation such as vacuum extraction (slurping), in situ chemical oxidation (ISCO) and soil washing. These technologies, when used alone, have limited effects. In vacuum extraction, when gasoline reaches residual saturation, the remaining gasoline exists as a discontinuous oil phase, which is immobile and unrecoverable. Gasoline adsorbed on

soil particles or trapped into pore spaces usually resists to chemical oxidation. Finally, the soil washing technology generates large amounts of washing solutions that have to be treated/disposed of and the high initial active matter cost make this technology non-economic.

Micellar solutions are aqueous solutions made of water, surfactant and alcohol. A surfactant is an amphiphilic molecule, i.e. having two different polarity parts, one hydrophilic and one lipophilic. Four types of surfactant exist: anionic (having the hydrophilic part negatively charged), cationic (having the hydrophilic part positively charged), amphoteric (having both charges) and non ionic (having no charge). Surfactant solutions can recover gasoline by two main mechanisms: dissolution and mobilization. Dissolution happens when the active matter (surfactant and alcohol) partitions preferentially in the aqueous phase and dissolves gasoline. Mobilization happens when the active matter partitions preferentially in the oil phase (gasoline), this way the gasoline volume is swelled and can be mobilized via an oil bank.

To overcome these limitations, a technology train is proposed. By coupling vacuum extraction (VE) and in-situ chemical oxidation (ISCO) with the soil washing technology, it may be possible to improve global aquifer remediation efficiency in order to reach environmental standards. This technology train starts with vacuum extraction to recover the mobile part of the gasoline, found as floating free phase, until it reaches residual saturation. The injection of a micellar solution follows VE to dissolve and/or mobilize the remaining adsorbed gasoline on soil particles and trapped in the porous medium. Most of the produced effluent is pumped and residual micellar solution makes gasoline available in the aqueous phase and to be oxidized with the ISCO technology afterwards. The injection of an acclimated bacteria population to polish the cleaning process completes the technology train.

To accomplish such a remediation technology sequence, laboratory experiments and a characterization of the porous medium and the contaminant (gasoline) have to be done. The plan is to first characterize the gasoline and its relationship with the porous media, followed by pseudo-ternary phase diagrams to identify promising micellar solutions. The best washing solutions will be tested using small sand column experiments (110 cm^3), in a 4 m^3 triangular sand tank experiment and in the field with a pilot test. This paper presents the initial phase of this project: 1) characterization of contaminant physical and chemical properties and soil grain size and mineralogy; 2) identification of promising washing solutions via pseudo-ternary phase diagrams; and 3) selection of the optimal

micellar solution through small sand column experiments. The 4 m^3 triangular sand tank experiment and the field test at pilot scale each are the object of another paper.

2.4 Experimental methods

2.4.1 Characterization of gasoline and geological materials from the contaminated site

A composite sample of weathered gasoline was obtained from observation wells located in the zone of interest at the site. Physical and chemical properties of gasoline such as density, viscosity, water content and chemical composition were respectively measured with a DMA 35N density meter (Anton Paar, Austria), an uncalibrated viscometer size 50 (Cannon Instrument Company, USA), an Aquastar V-200 titrator for Karl Fisher titration method (EM science, USA) and a Clarus 500 GCMS (Perkin Elmer, USA). Grain size analyses were done with conventional sieves and an Analysette 22 laser particle sizer (Fritsch, Germany). For mineralogy, x-ray diffraction analyses were conducted on the fine fraction with a D5000 x-ray diffractometer (Siemens, Germany). Pending drop method was used with a FTA200 apparatus (First Ten Angstrom, USA) to measure water-gasoline interfacial tension, mineral-water-gasoline contact angle (with quartz, calcite and feldspar) and gasoline surface tension at the aquifer temperature (8 °C). Since these measurements were repeated with the selected optimal micellar solution, they are discussed in a distinct section of the paper (2.4.4 Characterization of the best micellar solution).

2.4.2 Phase diagrams

Phase diagrams were carried out to evaluate the potential efficiency of different surfactant and alcohol mixtures for the gasoline dissolution/mobilization (Falta, 1998; Martel, et al., 1993). Pseudo-ternary diagrams have three poles: water at the lower left, gasoline at the lower right and active matter at the center top. The phase diagram shows, for different concentrations of each element, if the mixture consists of only one phase or is separated in two or even three phases. The initial aqueous micellar solution has to show only one phase before its injection in aquifers.

The boundaries of the single/multiple phase zones are determined with the cloud point method (Martel et al., 1993), consisting of adding one of the three elements with a gas

tight syringe to bring the resulting solution from clear (one phase) to cloudy (two or three phases) or vice versa. A miscibility curve is obtained by connecting all the cloud points. The lower the position of the curve in the diagram, the more efficient is the active matter of the solution because it dissolves the same quantity of gasoline at a lower concentration level (Falta, 1998; Martel et al., 1993). However, other considerations such as adsorption on soil particles, overall viscosity or density, or even cost and availability of the chemicals also have to be considered also. The construction of diagrams is done at 8 °C, the groundwater temperature at the site. To maintain this temperature, a refrigerated circulator (VWR International, USA), is used to cool down the 40 ml vial wherein the liquids are added to make the phase diagrams.

To find promising solutions, 7 alcohols (Table 2.1) and 18 surfactants were tested (Table 2.2). Previous studies showed that using a combination of alcohol and surfactant was more efficient than using a single component (Martel et al., 1993; Saint-Pierre et al. 2004). In order to simplify the number of possible combinations of alcohol and surfactant, all variables are considered independent, i.e. alcohol, surfactant and their ratio. The optimal ratio between the alcohol and the surfactant is first found by choosing one surfactant and one alcohol that are combined at various ratios (0.5, 1.0, 2.0, and 3.0) to make phase diagrams. When the alcohol/surfactant ratio was fixed by the lower miscibility curve, the alcohol type was changed to find the best alcohol. Seven alcohols were tested. With a fixed ratio and a fixed alcohol, 18 other curves were traced to find to best surfactant. Different optimizations were tried on best solutions such as adding a salt or a second alcohol. Also, alcohols were tested alone, to check which one is the most performing when used alone.

In anticipation of the 4 m^3 triangular sand tank experiment, a model oil had to be selected. This model oil would have to be: 1) available commercially in large volume; 2) less toxic and volatile than the weathered gasoline; and 3) as similar as possible to the weathered gasoline chemical composition and behavior toward one of the best micellar solutions. Three different oils were compared to the weathered gasoline: heptane, ethylbenzene and m-xylene.

2.4.3 Sand column experiments

Once the most promising micellar solutions are identified via phase diagrams, their recovery efficiency is evaluated through sand column experiments. This step is necessary before larger lab scale or pilot scale application of the technology.

All column experiments were done with geological materials from the contaminated site. Grain size diameter varies from 0.125 to 2 mm with a mean grain diameter (d_{50}) of 0.7 mm. The following sand column procedure is almost integrally taken from Martel (1996). The column itself is a glass cylinder with an internal diameter of 3.7 cm. Column lengths of 10 and 15 cm were used for the first and second series of column experiments, respectively. Both ends of columns are sealed with a perforated Teflon® cap. A ratio greater than 50 between the column diameter and the mean sand grain diameter (d_{50}) insures statistical uniformity of porosity (> 50, Rose, 1945) and flow rate (> 30, Schwartz et al., 1953). To minimize wall effects, the column length has to be at least twice its diameter. The seal between the glass cylinder and the Teflon® caps is provided by a Viton® O-Ring. A 125 µm stainless steel screen on each Teflon® cap prevents the loss of fines. To uniformly distribute the liquid at the inlet and outlet of the column, a small reservoir is built inside the Teflon® caps. The compaction of the dry sand in 5 mm layers was standardized by hitting the side of the column 25 times and then by dropping a weight (180 g) from a controlled height (7 cm) 12 times for each layer. For the first and second series of experiments, respectively, a constant dry density of 1.78 ± 0.07 g/cm^3 and 1.76 ± 0.05 g/cm^3 and a porosity of 0.303 ± 0.008 and 0.349 ± 0.012 were obtained. This degree of compaction prevents preferential liquid channeling (Ripple et al., 1973).

Interstitial air was eliminated from the sand column by circulating at least 30 pore volumes of carbon dioxide (CO_2). The water-soluble CO_2 was then eliminated when the column was saturated with water. To prevent air inflow, the column was saturated from the base with deaerated water, distilled and demineralized water. Before measuring hydraulic conductivity (K) with a constant-head permeability test, 10 pore volumes of water were circulated through the sand column (average value of K is 2.1 ± 1.5 x 10^{-5} m/s). Residual oil saturation was obtained by the injection of a known mass of gasoline. For the first and second series, respectively, between 9 to 10 and 10 to 11 grams of gasoline were placed in a Teflon® tubing that was connected to a peristaltic pump. The slug of oil was pushed at high velocity (8.43 cm/s), from top to bottom in the sand column, by 100 ml of water. The water and gasoline discharged by the column were collected in a Teflon® funnel and the immiscible fluids were separated. The residual

gasoline was calculated by subtracting the mass of gasoline recovered from the mass injected. The residual gasoline saturation (proportion of the pore volume) obtained during the experiments was 21.3 ± 3.0% and 17.4 ± 3.0% for first and second series, respectively.

The goal of the sand column experiments in series #1 was to eliminate three out of the four promising micellar solutions provided from the phase diagrams. For experiments in series #1, the residual oil was washed with 1.65 ± 0.15 pore volumes of micellar solution, representing a volume of 52 ± 3 ml. This injected volume was however, not enough to recover 100% of the gasoline. This incomplete recovery was necessary to evaluate the relative efficiency of different washing solutions. A small peristaltic pump was used to inject solutions at a velocity of 22 ± 3 cm/d. All washing solutions were followed by 1.7 ± 0.3 PV of polymer solution at the same velocity to recover most of the micellar solution in the column. For all experiments, columns were placed horizontally for a better representation of the horizontal sweep in the field (Figure 2.1). For experiments in series #2, the injection of various pore volumes of micellar and polymer solutions was tested and the injection velocity was raised to 49 ± 3 cm/d. All injected solutions in series #1 and #2 are shown in Table 2.4.

The selected solution will next be tested in the 4 m^3 triangular sand tank and at the pilot scale. Due to constraints from the industrial partner of the project, the pilot scale test had to be preempted, before the end of sand column experiments. Because of that, the micellar solution for the pilot test was chosen simply from visual interpretation of the liquid effluents from each column test in series #1 combined to the phase diagrams results.

Since injected solutions in the field were slightly modified from the original optimal micellar solution chosen with phase diagrams and visual interpretation of series #1 of sand column experiments, a second series of sand column experiments had to be done to reproduce what was effectively injected during the pilot test and to evaluate the effect of parameters such as: 1) a salted water preflush prior to the micellar solution (for a salted micellar solution); 2) the addition of xanthan in the micellar solution; 3) the micellar solution injected pore volumes; 4) the polymer solution injected pore volumes; and 5) the use of a model oil contamination instead of the weathered gasoline.

The gasoline recovery efficiency was evaluated from these column tests by gasoline mass difference in soils before and after the injection sequence. This evaluation technique gives the recovered mass for the complete injection sequence (preflush +

micellar solution + polymer solution). Recovered gasoline mass in column effluent was evaluated also to identify the proportion of gasoline recovered by the micellar solution only, to identify the recovery mechanism and to make the mass balance of the tests. Gasoline concentrations in soils and liquid effluents were evaluated from the BTEX analyses on a Clarus 500 GCMS (Perkin Elmer, USA). The GCMS was equipped with a DB-5 MS UI column (30 m long, 0.250 mm ID and a 0.25 microns filter). To limit the number of analyses, recovered gasoline in the effluent was measured only for micellar solutions having 7.5% of active matter.

2.4.4 Characterization of the best micellar solution

In order to obtain a global portrait of the chosen micellar solution, physical properties like density and viscosity were measured with a DMA 35N density meter (Anton Paar, Austria) and an uncalibrated viscometer size 50 (Cannon Instrument Company, USA), respectively.

The pending drop method was used with a FTA200 apparatus (First Ten Angstrom, USA) to measure the impact of the active matter concentration on the water-gasoline IFT and mineral-water-gasoline contact angle (with quartz, calcite and feldspar) at the aquifer temperature (8 °C). IFTs between the aqueous and oil phases at equilibrium were obtained by adding different concentrations of active matter (0.1%, 1.5%, 3.0% and 7.0%) to an equal mass ratio of gasoline and water in a 10 ml vial. These same aqueous and oil phases (with same active matter concentrations) were used for the mineral-aqueous phase-oil phase contact angle evaluation.

2.5 Results and discussion

2.5.1 Characterization of gasoline and geological materials

Mineralogical analyses of soil particles by x-ray diffraction show that the main minerals in the fine fraction (< 63 microns) are in the following order of importance: quartz (51%), feldspars (26%) (albite, orthoclase and microcline) and calcite (22%). Grain size of soil particles is distributed with coarse sand (33%), medium sand (19%), fine sand (18%), fine gravel (17%), coarse gravel (10%) and silt (3%) (see grain size curve on Figure 2.2). The mean gasoline surface tension (gasoline-air) was evaluated from 10 measurements at 22.7 ± 0.1 mN/m. The mean IFT (gasoline-water) was evaluated from 10 measurements at 13.7 ± 0.1 mN/m. Based on mineralogical analyses, the three major

minerals (quartz, feldspar and calcite) were chosen for the measurement of mineral-water-gasoline contact angle. The mean contact angle on quartz was evaluated from 20 measurements at 76.4 ± 14.8°. With feldspar, 10 measurements were done for a mean value of 78.9 ± 5.9°. With calcite, the mean value was 85.8 ± 5.6° evaluated from 10 measurements. Contact angle measurements showed that all tested mineral surfaces were oil wet with the weathered gasoline. Mean gasoline density was 0.788 g/cm^3 and viscosity was 689 µPa-S at 8 °C. The BTEX proportion in the weathered gasoline was 16.1%: 8.1% xylenes (m, p, o), 6.7% toluene, 1.2% ethylbenzene and 0.1% benzene. Table 2.3 summarizes all physical and chemical properties of gasoline and geological materials.

2.5.2 Phase diagrams

Used alone, alcohols n-PrOH and i-PrOH seem to give the best results (Figure 2.3). The alcohol i-PrOH and surfactant Aerosol OT were selected for determination of the optimal alcohol/surfactant mass ratio. Results show that the best alcohol/surfactant mass ratio is 1.0 (Figure 2.4), confirming previous experiments with gasoline (Martel et al., 1993). From the seven tested alcohols, n-BuOH showed the lowest miscibility curve in the water-rich zone with the surfactant Hostapur SAS (Figure 2.5). Therefore, n-BuOH was selected to evaluate the efficiency of 18 surfactants at a fixed mass ratio of 1.0. Three surfactants were selected based on the low position of their miscibility curve in the water-rich zone: Arkopal N90, Nansa HS90 and Hostapur SAS. The addition of NaCl at a concentration of 7.5 g/L yield a lower miscibility curve position in the phase diagram for the n-BuOH/SAS =1.0 solution. The addition of n-AmOH to n-BuOH in an equal proportion helped to obtain a lower miscibility curve position for the non salted n-BuOH/SAS =1.0 solution. From these tests, four micellar solutions were selected for the subsequent sand columns experiments: n-BuOH/Arkopal N90 = 1.0; n-BuOH/Nansa HS90 =1.0; (n-BuOH/n-AmOH = 1.0)/SAS = 1.0; n-BuOH/SAS = 1.0 with 7.5 g/L NaCl (Figure 2.6). For the determination of the model oil, miscibility curves show that the m-xylene has the closest behavior to the weathered gasoline with the (n-BuOH/n-AmOH = 1.0)/SAS = 1.0 solution (Figure 2.7).

Phase diagrams in Figures 2.3 and 2.5 show that the alcohol performance when used alone is not correlated with its performance when used in combination with a surfactant. Indeed, when used alone, n-PrOH and i-PrOH are the most promising, while they are poorly performing in combination with the Hostapur SAS surfactant compared to other

alcohols. The phase diagram of Figure 2.4 shows that adding surfactant to an alcohol solution increases the dissolution of gasoline until it reaches a critical alcohol/surfactant ratio of 1.0. Based on phase diagrams, the best micellar solution is the n-BuOH/SAS = 1.0 + 7.5 g/L NaCl since its miscibility curve is the lowest.

2.5.3 Sand column experiments

Visual interpretation was used at first to evaluate the most performing solution from series #1 of the sand column experiments. Figure 2.8 shows the recovered effluents from sand column experiments in series #1. Based on the coloration of the aqueous phase and the volume of the oil phase, the solution that seemed to recover the largest amount of gasoline was n-BuOH/SAS = 1.0 at 7.5% of active matter + 7.5 g/L NaCl. Since this solution was the most efficient in phase diagrams, this solution was chosen for the pilot test.

Following the pilot test, the performance of micellar solutions in soil was evaluated through chemical analyses of residual gasoline in soil of the sand columns and from recovered gasoline in the column effluent. The gasoline recovery in the sand column tests (recovered mass/initial mass) is presented in Table 2.4. A poor performance (low recovery) is observed with solutions at a low active matter concentration (5.0%).

Based on the soil analyses only, the most efficient solutions with a gasoline recovery of 94.2% and 95.4% respectively were n-BuOH/SAS = 1.0 + 7.5 g/L NaCl and (n-BuOH/n-AmOH = 1.0)/SAS = 1.0, both having 7.5% of active matter. However, gasoline is not recovered simply by the micellar solution (see Figure 2.9). In fact, a part of the gasoline is recovered prior to the arrival of the micellar solution front, by the salted water bank, and after the flow/circulation of the micellar solution, by the polymer solution flood. From this observation, it is believed that the evaluation of the optimal micellar solution should not be based on the gasoline recovery for the complete injection sequence, but only on the gasoline recovery associated with the flow/circulation of the micellar solution in the column (Table 2.4). Figure 2.10 presents the gasoline recovery associated with the micellar solution as a function of eluted pore volumes. With the objective of 80% gasoline recovery, it is possible to identify which micellar solution reaches this objective with the least injected pore volumes. For micellar solutions used with the weathered gasoline, the solution that crosses the 80% gasoline recovery line first is the micellar-polymer solution used in the field: n-BuOH/SAS = 1.0 at 7.5% active matter + 7.5 g/L NaCl + 300 ppm xanthan. Micellar solutions tested in series #1 without xanthan, (n-

BuOH/n-AmOH = 1.0)/SAS = 1.0 at 7.5% of active matter and n-BuOH/SAS = 1.0 at 7.5% active matter + 7.5 g/L NaCl arrive respectively in second and third places, very close to each other. When the best solution was used with the model oil, the recovery is easier, meaning that recovery in the 4 m^3 sand tank experiment is overestimated compared to the pilot test with the weathered gasoline.

The sand column experiments showed that the (n-BuOH/n-AmOH = 1.0)/SAS = 1.0 solution is slightly better than the n-BuOH/SAS = 1.0 at 7.5% of active matter + 7.5 g/L NaCl solution, whereas the phase diagrams showed the opposite. However, even if the addition of n-amyl alcohol increases the efficiency, the cost of n-AmOH is 2.4 higher expensive than n-BuOH (VWR). Also, n-amyl alcohol is 2.1 times more toxic than n-butanol, with a LD_{50} (oral, rat) of 390 mg/kg versus 790 mg/kg for the n-butanol (Fisher).

With the visual interpretation of the effluent, it was possible to estimate the recovery mechanism of each micellar solution. The gasoline is considered mobilized when it is recovered in the oil phase and solubilized when it is recovered in the aqueous phase. Except for n-BuOH/Nansa HS90 = 1.0, all solutions show mobilization as the main recovery mechanism (Table 2.4). The best micellar solution showed a mobilization / solubilization ratio of 95/5 in the sand column experiment, but showed a 0/100 ratio in the field. This was probably due to the low gasoline saturation in the field.

The impact of different parameters on gasoline recovery efficiency, such as the salted water preflush bank and the addition of xanthan directly in the micellar solution, could not be evaluated as anticipated. Due to a leak in one of the sand columns (column #2, series #2), a comparison with other column tests was not possible. However, even if not confirmed by the experiment, it is believed that the salted water preflush surely helped to avoid the dilution of salinity at the injection front of the micellar solution. Since the salt has a small impact on lowering the interfacial tension between water and gasoline, the salted water bank has a direct impact by recovering a certain amount of gasoline prior to the arrival of the micellar solution (see Figure 2.9). For the addition of xanthan directly in the micellar solution, assuming that the preflush of salted water bank has an effect only at the beginning of the recovery, it is clear that it improves the recovery of gasoline. In Figure 2.10, the micellar solution with xanthan (red curve) recovers gasoline using less pore volumes than the micellar solution without xanthan (purple curve).

Using greater volumes of micellar and polymer solutions allows a better gasoline recovery. When the pore volumes of micellar solution injected increase from 0.8 PV to 1.6 PV the gasoline recovery increases by 23.2% (increasing from 63.9% to 87.1%). It

could be interesting in future experiments to test in sand columns what number of pore volumes the best micellar solution can recover 100% of the gasoline initial saturation. Figure 2.10 shows that for the optimal micellar solution (red curve), the gasoline recovery seems to slow down and reach almost a plateau at 1.6 eluted pore volumes.
The same recommendations may be drawn for the effect of the injected pore volumes of xanthan solution. An increase of simply 0.3 eluted pore volumes (from 0.2 to 0.5) after the injection of the micellar solution resulted in a 13.7% increase in gasoline recovery (from 8.3% to 21.9%). According to the obtained results, a good range of injected pore volumes of xanthan solution could be between 1.5 and 2.0 PV.

2.5.4 Characterization of the best micellar solution

The best micellar solution obtained from phase diagrams and sand column experiments was n-BuOH/SAS = 1.0 at 7.5% of active matter + 7.5 g/L of NaCl + 300 ppm of xanthan. Its density and viscosity measured at 8 °C are respectively 1005 kg/m^3 (denser than water at 999 kg/m^3) and 2217 µPa•s (1.5 times more viscous than water). However, a graph of the viscosity as a function of the shear rate would have been preferable because of the shear thinning behavior of the polymer.
The IFT as a function of active matter concentration shows that for a small proportion of 0.1% of active matter, the IFT between the aqueous and oil phases drops by 96% (Figure 2.11). For higher concentrations of active matter, IFT drops slowly until it reaches a plateau at 7.0% of active matter. Because of the limit of detection of the apparatus, interfacial tensions associated with concentrations of active matter larger than 7.0% could not be obtained.
The measurements of contact angle as a function of the active matter concentration, with a confidence interval at 95% equivalent to ± 2σ (standard variation), show that no correlation or continuity can be observed (Figure 2.12). It can thus be concluded that the active matter concentration has no effect on the contact angle (and on wettability).
However, the large variability between values at the same active matter concentration are directly related with the surface heterogeneity of mineral thin sections (quartz, calcite and feldspar) and a modification in the measurement technique could help reducing the standard variation. The technique used for measurements was to put several drops of gasoline on the mineral thin section for the same active matter concentration, let them equilibrate for a fixed period of time, make all measurements, clean the set up and then new drops of gasoline were put on slates with a different active matter concentration.

Another technique was developed by Martel and Gélinas (1994) and consisted to keep the same spot on the thin section for measurements at different active matter concentrations to avoid the surface heterogeneity factor. The method is: 1) to put an oil droplet on a mineral thin section in a small glass reservoir; 2) to cover the thin section and the oil droplet with a known mass of water; 3) a parafilm sheet is added on top of the glass reservoir to limit losses of volatile organic compounds; 4) active matter is added and mixed with the water to obtain the desired active matter concentration; and 5) contact angle measurements are carried out after each addition of active matter. Further measurements should be done with this technique to maximize chances to yield reproducible results.

To characterize with more precision the main recovery mechanisms of the optimal micellar solution, the critical tie line could have been traced down on the phase diagram via additional chemical analyses. The critical tie line is a good tool to predict the evolution of the recovery mechanism as a function of proportion of active matter and gasoline (Falta, 1998).

2.6 Conclusions and recommendations

The development of an optimal micellar solution for a gasoline contaminated aquifer was carried out. To optimize the micellar solution as a function of a weathered gasoline and geological materials from a contaminated site, four main steps were followed:

1) Characterization of the weathered gasoline and geological materials from the contaminated site through measurements of their physical and chemical properties;
2) Selection of promising micellar solutions via phase diagrams;
3) Identification of the best micellar solution through sand column experiments;
4) Characterization of the best micellar solution via measurements of its physical properties.

The characterization of the weathered gasoline revealed a density lighter than water and a viscosity lower than water (respectively 0.788 g/cm^3 and 689 µPa•s), as well as a high interfacial tension with water (64 mN/m). Grain size and mineralogical analyses have shown that the geological materials of the contaminated site were mainly made of quartz, feldspar and calcite with a grain size varying from fine sand to fine gravel.

Phase diagrams were used as a screening tool to select promising micellar solutions. Different mixtures of surfactant and alcohol were tested at different alcohol/surfactant ratios. Parameters like the variation of the salinity and the combination of two different alcohols mixed with a surfactant were tested. From this step, the four most promising alcohol/surfactant solutions were retained to be tested in the sand column experiments. From the four promising solutions, the solution that showed the best performance from phase diagrams is n-BuOH/SAS = 1.0 + 7.5 g/L of NaCl.

The four best alcohol/surfactant mixtures were tested in sand column experiments at different active matter concentrations. An upgraded version of the optimal micellar solution obtained from phase diagrams was chosen as the best overall solution: n-BuOH/SAS = 1.0 + 7.5 g/L of NaCl + 300 ppm of xanthan. These experiments allowed confirming that the following parameters improve gasoline recovery: 1) a salted water preflush prior to the micellar solution (for a salted micellar solution); 2) the addition of xanthan in the micellar solution; 3) a high injected pore volume of micellar solution; and 4) a high injected pore volume of polymer solution. The optimal injected pore volumes of micellar and polymer solutions are 1.6 and 1.5-2.0 respectively. It could be interesting in future experiments to optimize with more precision the pore volumes of micellar and polymer solutions. From the overall results, including phase diagrams and sand column experiments, the following injection sequence is suggested:

1) 0.5 PV of salted water at 7.5 g/L of NaCl (preflush);
2) 1.6 PV of n-BuOH/SAS = 1.0 at 7.5% of active matter + 7.5 g/L of NaCl + 300 ppm of xanthan (micellar-polymer solution);
3) 2.0 PV of xanthan solution at 500 ppm (polymer solution).

The density and viscosity of the best micellar-polymer solution, measured at 8 °C, are respectively 1005 kg/m^3 (denser than water at 999 kg/m^3) and 2217 µPa•s (1.5 times more viscous than water). However, a graph of viscosity as a function of the shear rate would have been better because of the shear thinning behavior of the polymer.

Interfacial tension measurements on the best solution revealed that a concentration of 0.1% of active matter allowed an interfacial tension decrease of 96%. A maximum measurable interfacial tension drop of 99.2% occurred with a concentration of 7.0% of active matter. In future experiments, it could be interesting to test the recovery of gasoline with a micellar solution at a concentration of active matter as low as 0.1%. Used in combination with the vacuum extraction technology, it could be an interesting research avenue to enhance gasoline recovery.

The measurements of the effect of the best micellar solution on the contact angle between minerals and the aqueous and oil phases were not conclusive. The heterogeneity of the mineral surface is at the origin of the problem and could be resolved by using another technique that keeps the same droplets of gasoline on the minerals thin section when the active matter concentration is increased.

These results provide guidelines for the optimization of washing solutions for gasoline recovery. However, this optimization is only valid for a specific contaminant and geological materials from a contaminated site.

2.7 Acknowledgments

This project was funded through grants from the Natural Sciences and Engineering Research Council of Canada (NSERC) CRD program, TechnoRem as the industrial partner and through NSERC discovery grants of Richard Martel.

Table 2.1. List of alcohols tested in phase diagrams

Trade Name	Abbreviation	Molecular Structure
Ethanol	EtOH	CH_3CH_2OH
n-Propanol	n-PrOH	$CH_3CH_2CH_2OH$
iso-Propanol	i-PrOH	$(CH_3)_2CHOH$
n-Butanol	n-BuOH	$CH_3CH_2CH_2CH_2OH$
iso-Butanol	i-BuOH	$(CH_3)_2CHCH_2OH$
sec-Butanol	s-BuOH	$CH_3CH_2CH(OH)CH_3$
n-Amyl Alcohol	n-AmOH	$CH_3CH_2CH_2CH_2CH_2OH$

Table 2.2. List of surfactants tested in phase diagrams

Trade Name	Type	Chemical Name	H_2O %
CAHS	Amphoteric	Cocamidopropyl hydroxysultaine	50.0
Clariant® Hostapur SAS-60	Anionic	Secondary alkanesulfonate	27.2
CCC® Triton GR7M	Anionic	Sulfosuccinate	0.2
Clariant® Genapol LRO paste	Anionic	Alcoxy-diglycolsulfate sodium	29.0
Stepan® Steol CS-330	Anionic	Sodium laureth sulfate	69.0
Clariant® Hostapur OS liquid	Anionic	Alpha-olefinesulfonate-sodium salt	55.2
Clariant® Hostapal BV conc	Anionic	Alkylaryle sulfate polyglycolique	46.9
DowFax* 3B2-D	Anionic	Decyl benzenesulfonic	8.2
Cytec® Aerosol AY 100%	Anionic	Sodium diamyl sulfosuccinate	4.7
DowFax 8390 solution	Anionic	Hexadecyl diphenyl oxide disulfonate	56.4
Huntsman ® NANSA HS90/S	Anionic	Sodium dodecyl benzene sulphonate	2.2
Cytec® Aerosol OT	Anionic	Sodium dioctyl sulfosuccinate	3.3
Cavasol® W7 M	Cyclodextrin	methyl-beta-cyclodextrin	3.5
Cavasol® W7 HP	Cyclodextrin	hydroxypropyl-beta-cyclodextrin	3.7
Cavamax® W7	Cyclodextrin	beta-cyclodextrin	11.8
Croda® TWEEN 80	Non ionic	Polysorbate 80	2.3
Huntsman® Surfonic PE-2597	Non ionic	Phosphated polyglycol ether	1.0
Arkopal N-090	Non ionic	Ethoxylate nonylphenol	0.8

Table 2.3. Physical and chemical properties of weathered gasoline and geological materials

Properties	Values
[redacted]	
Surface tension - 8 °C (mN/m)	22.7
IFT with water - 8 °C(mN/m)	13.7
Contact angle - 8 °C (°)	
Quartz	76.4
Feldspar	78.9
Calcite	85.8
Density - 8 °C (g/cm3)	0.788
Viscosity - 8 °C (µPa-S)	689
BTEX proportion (%)	16.1
Xylene	8.1
Toluene	6.7
Ethylbenzene	1.2
Benzene	0.1
[redacted]	
Minerals (%)	
Quartz	51
Feldspar	26
Calcite	22
Grain size distribution (%)	
Fine gravel	17
Coarse sand	34
Medium sand	22
Fine sand	25
Silt	2

Table 2.4. Injected solutions in sand columns with their gasoline recovery % and recovery mechanism in series #1 and #2

Batch #	Pre Flush solution	Eluted PV	Micellar solution	Active Matter %	Eluted PV	Polymer solution	Eluted PV	Gasoline recovery % for the complete injection sequence	Gasoline recovery (%) for the micellar solution only	Recovery mechanism Mobilisation / Solubilisation
1	-	-	n-BuOH/SAS = 1.0 + 7.5 g/L NaCl	7.5	1.8	600 ppm xanthan	0.7	94.2	84.4	80/20
1	-	-	n-BuOH/SAS = 1.0 + 7.5 g/L NaCl	5.0	-	600 ppm xanthan	-	55.8	-	-
1	-	-	n-BuOH / Arkopal N90 = 1.0	5.0	-	600 ppm xanthan	-	16.1	-	-
1	-	-	(n-BuOH/n-AmOH = 1.0) / SAS =1.0	7.5	1.7	600 ppm xanthan	0.4	95.4	88.8	58/42
1	-	-	(n-BuOH/n-AmOH = 1.0) / SAS =1.0	5.0	-	600 ppm xanthan	-	53.3	-	-
1	-	-	n-BuOH / Nansa HS90 = 1.0	5.0	-	600 ppm xanthan	-	61.1	-	-
2	-	-	n-BuOH / Nansa HS90 = 1.0	7.5	1.7	600 ppm xanthan	0.8	79.6	47.6	0/100
2*	Salted water 7.5 g/L NaCl	0.4	n-BuOH/SAS = 1.0 + 7.5 g/L NaCl	7.5	1.3	600 ppm xanthan	0.0	56.9	56.6	58/42
2	Salted water 7.5 g/L NaCl	0.4	n-BuOH/SAS = 1.0 + 7.5 g/L NaCl + 300 ppm xanthan	7.5	1.6	600 ppm xanthan	0.0	87.6	87.1	89/11
2	Salted water 7.5 g/L NaCl	0.4	n-BuOH/SAS = 1.0 + 7.5 g/L NaCl + 300 ppm xanthan	7.5	0.8	600 ppm xanthan	0.5	86.7	63.9	100/0
2	Salted water 7.5 g/L NaCl	0.5	n-BuOH/SAS = 1.0 + 7.5 g/L NaCl + 300 ppm xanthan	7.5	0.8	500 ppm xanthan	0.2	76.4	54.8	95/5
2**	Salted water 7.5 g/L NaCl	0.4	n-BuOH/SAS = 1.0 + 7.5 g/L NaCl + 300 ppm xanthan	7.5	0.8	500 ppm xanthan	0.0	81.1	77.1	100/0

* An injected PV of 1,5 was planned but an unstoppable leak put an end to the experiment

** A model oil contamination was used instead of weathered gasoline

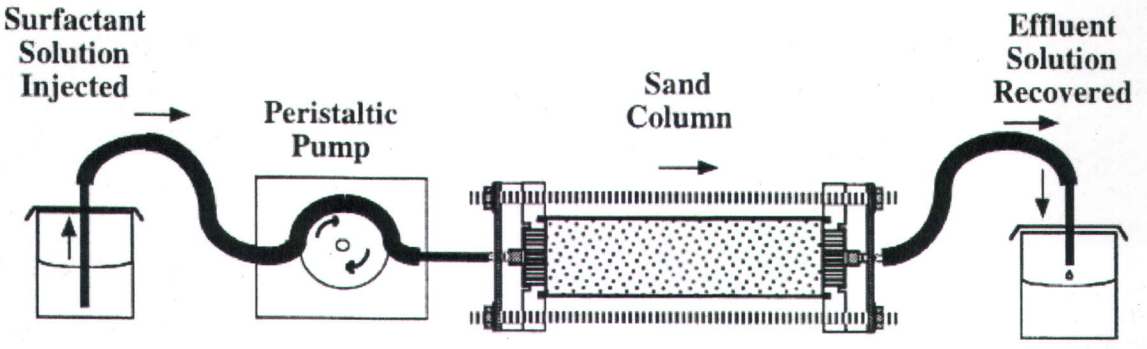

Figure 2.1. Horizontal sand column experiment set up (adapted from Martel (1996))

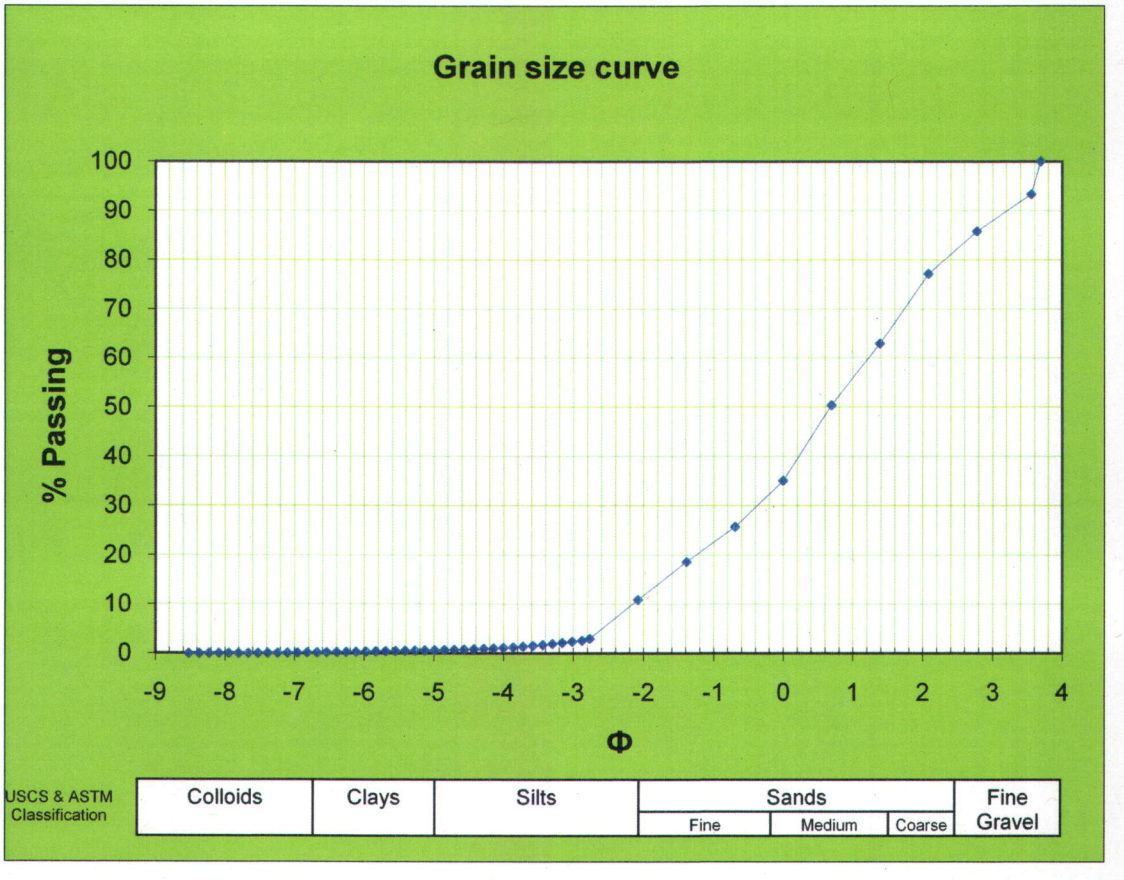

Figure 2.2. Grain size curve of the studied site soil particles

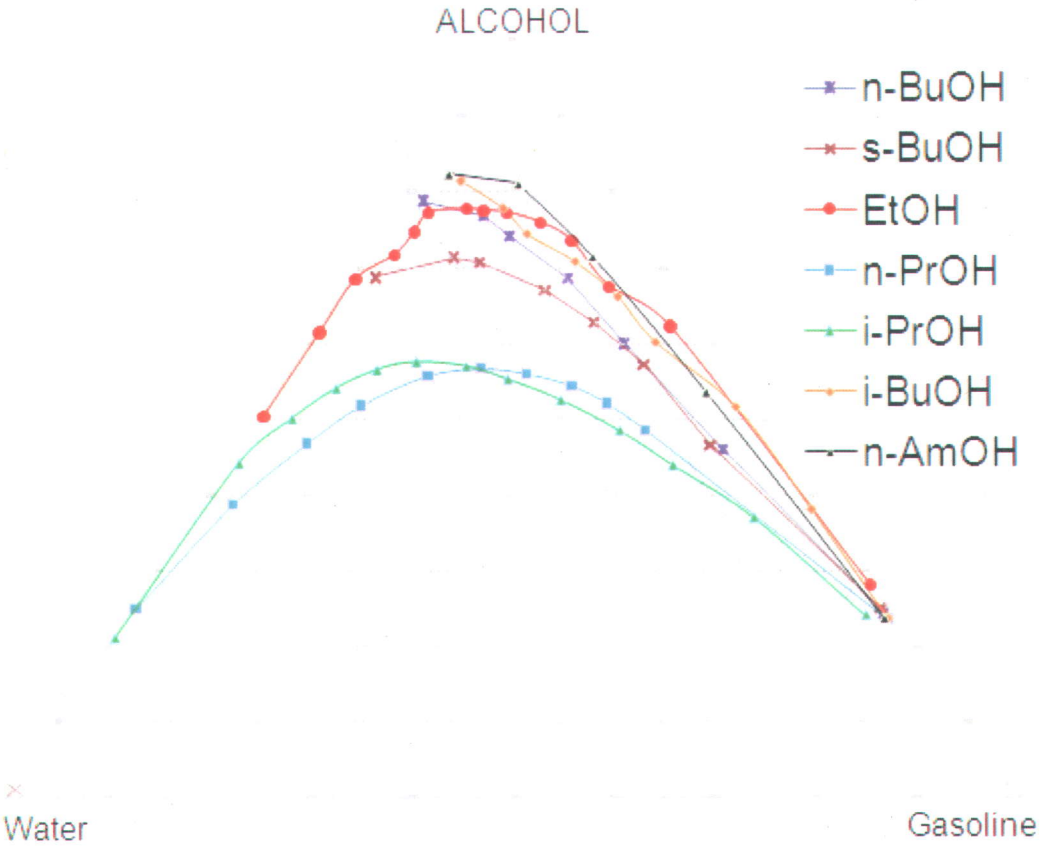

Figure 2.3. Phase diagram with miscibility curves for the tested alcohols

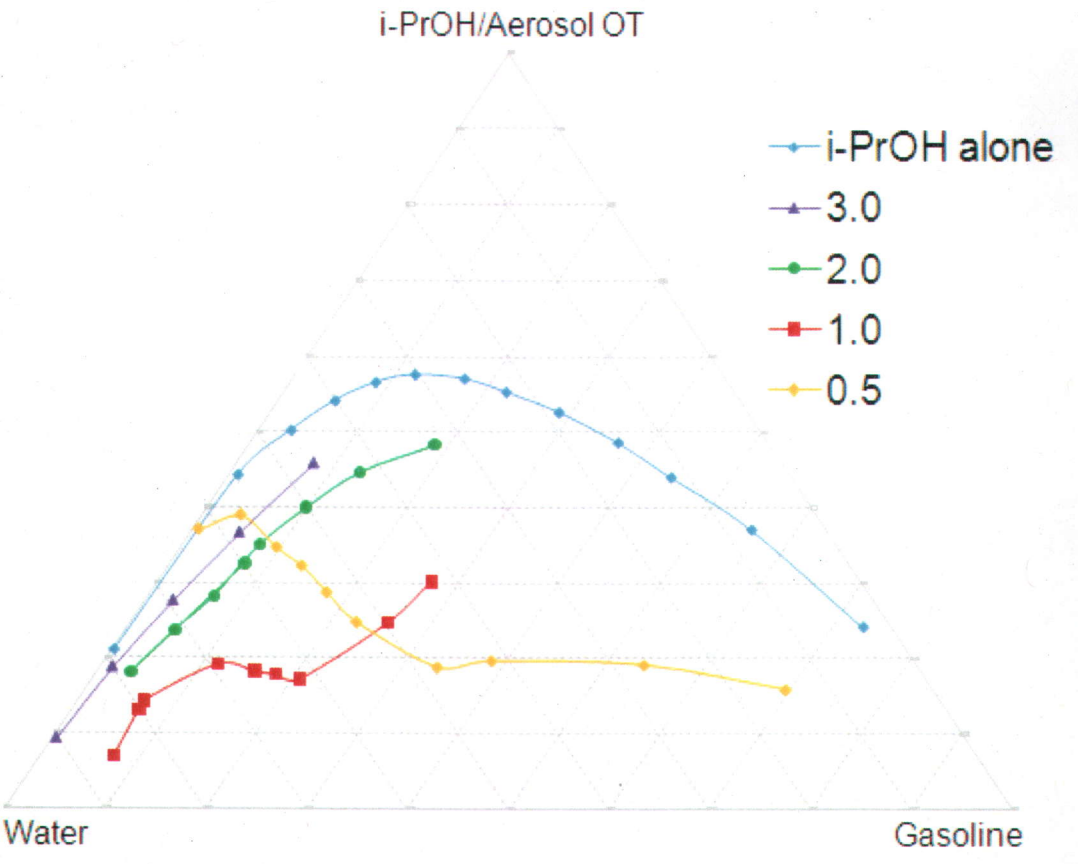

Figure 2.4. Phase diagrams with miscibility curves for different i-PrOH/Aerosol OT ratios

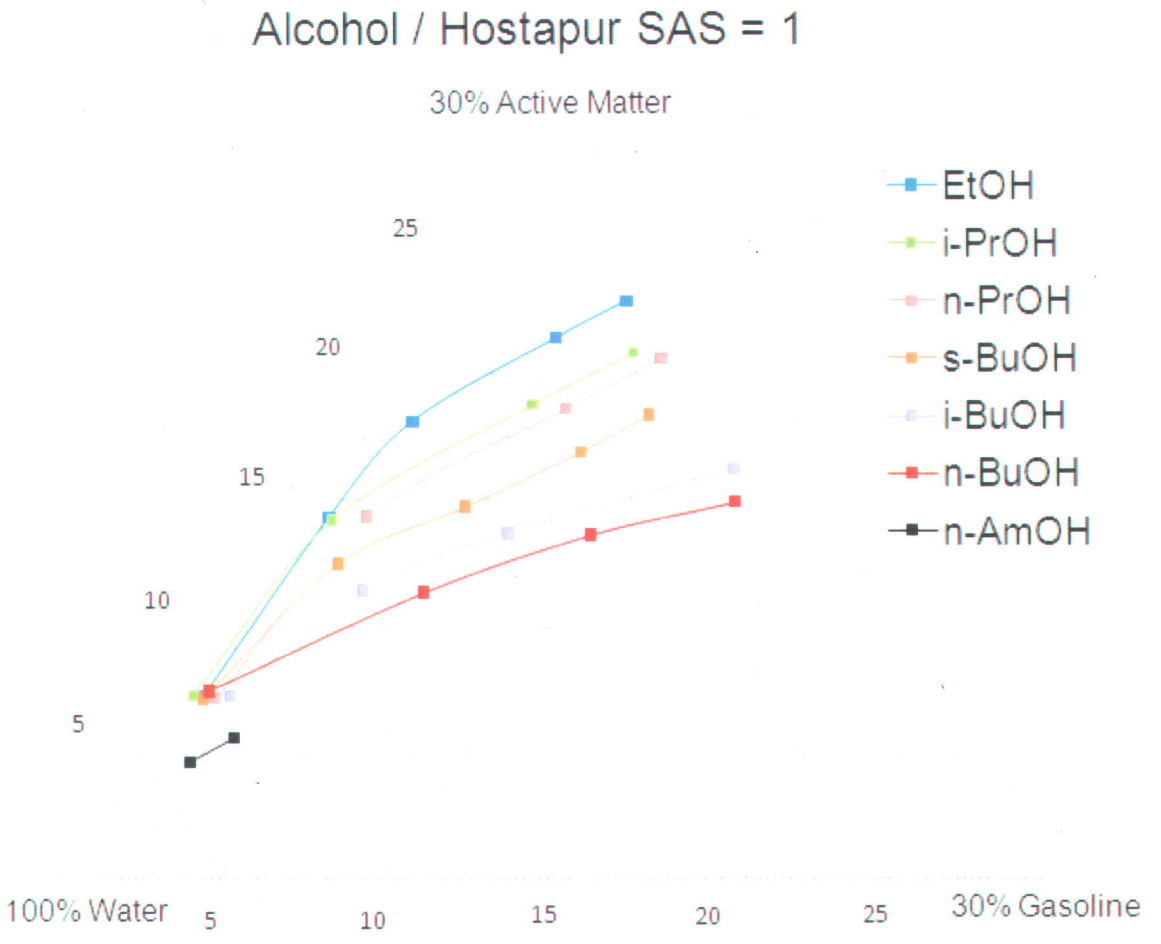

Figure 2.5. Phase diagram with miscibility curves for different alcohols with the surfactant Hostapur SAS at a ratio of 1.0

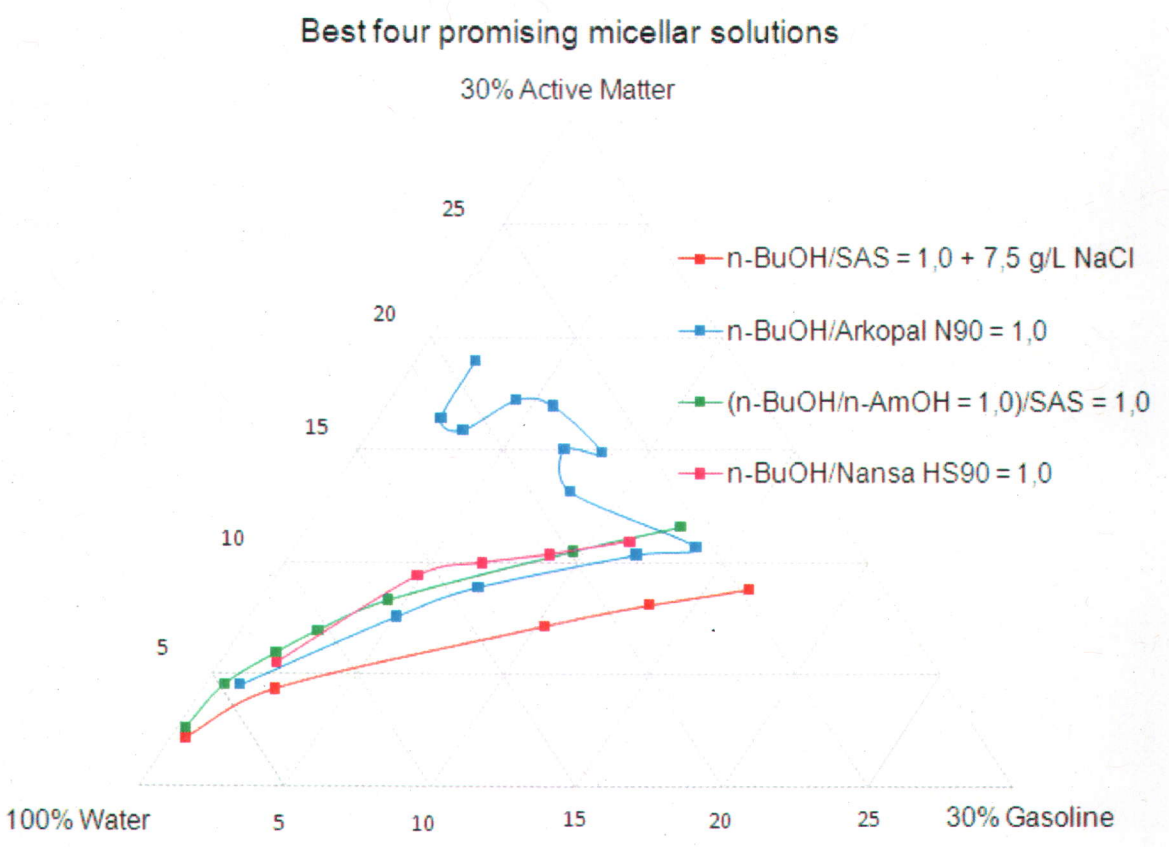

Figure 2.6. Phase diagram with miscibility curves for promising micellar solutions

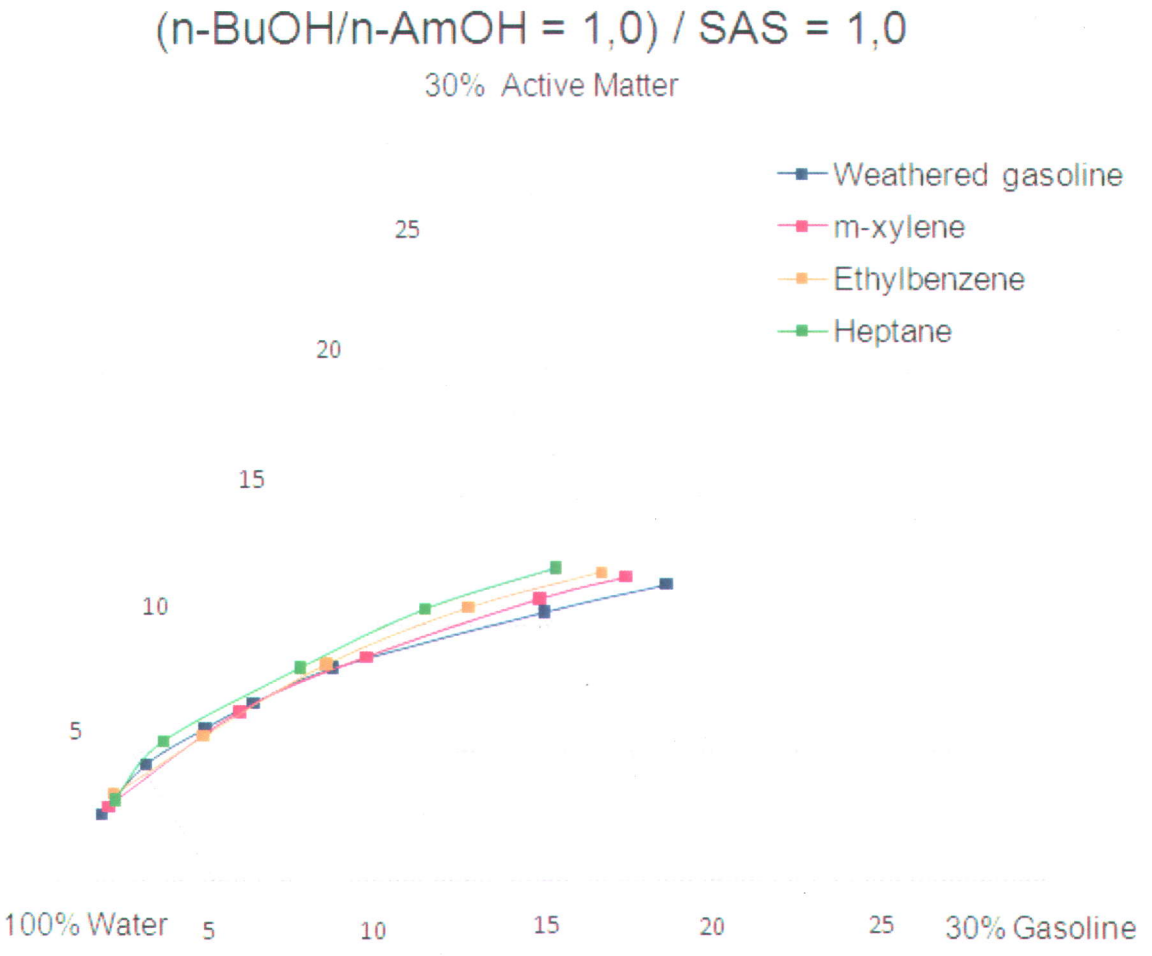

Figure 2.7. Phase diagram with miscibility curves for model oil to replace gasoline in sand tank experiments

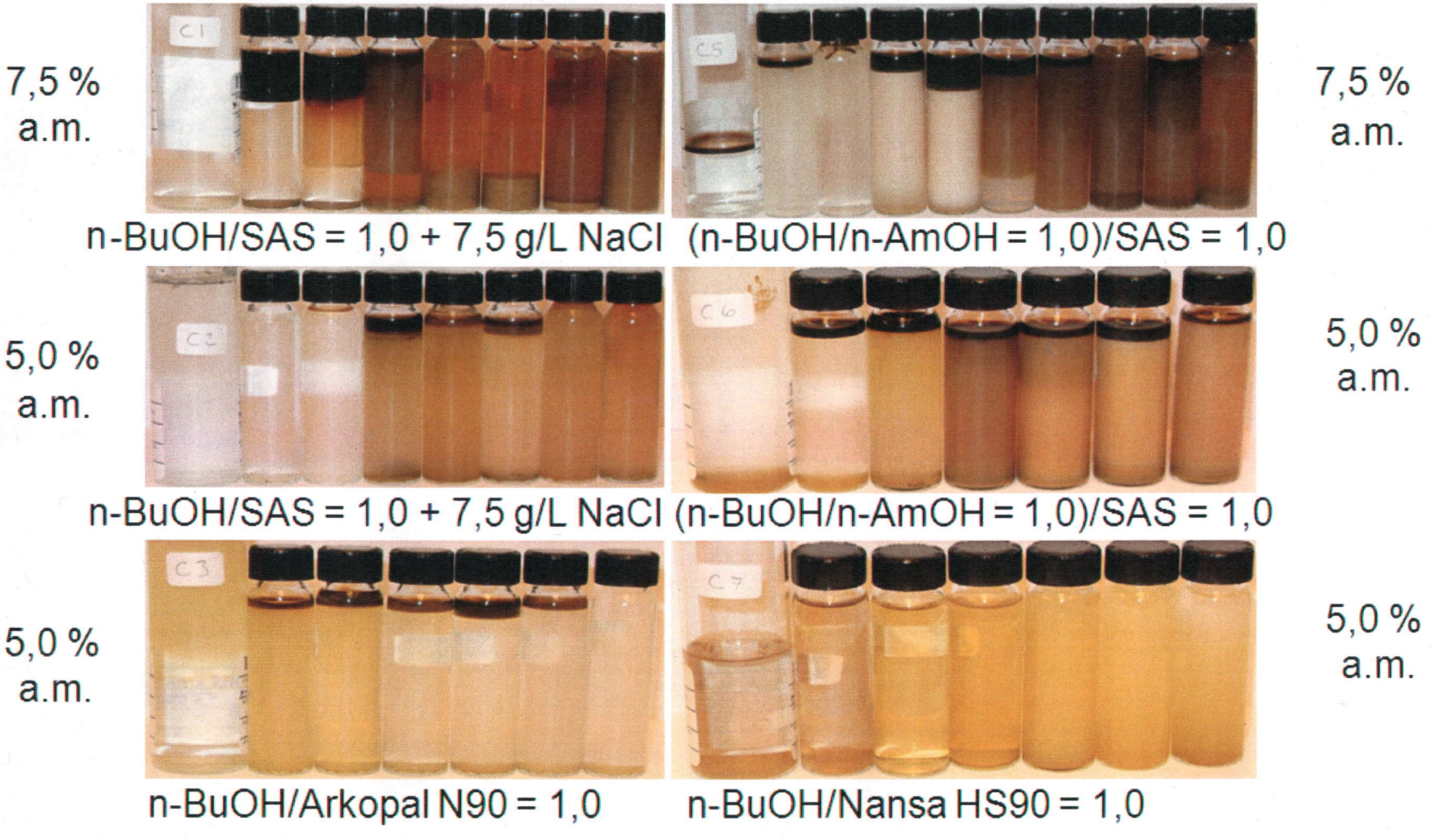

Figure 2.8. Recovered effluents from sand column experiments in series #1

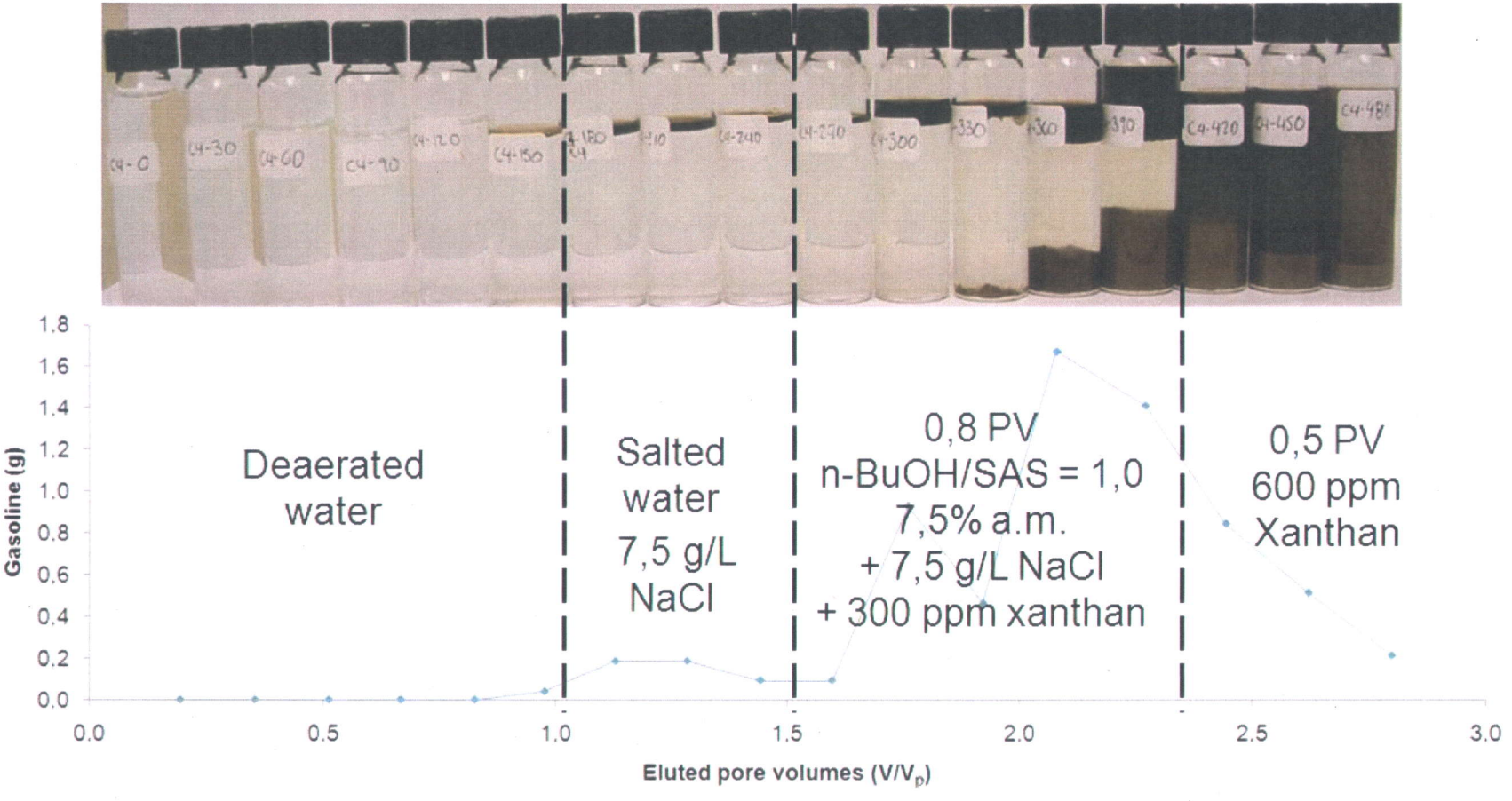

Figure 2.9. Gasoline mass recovered in the effluent of a sand column experiment with the injected solutions sequence

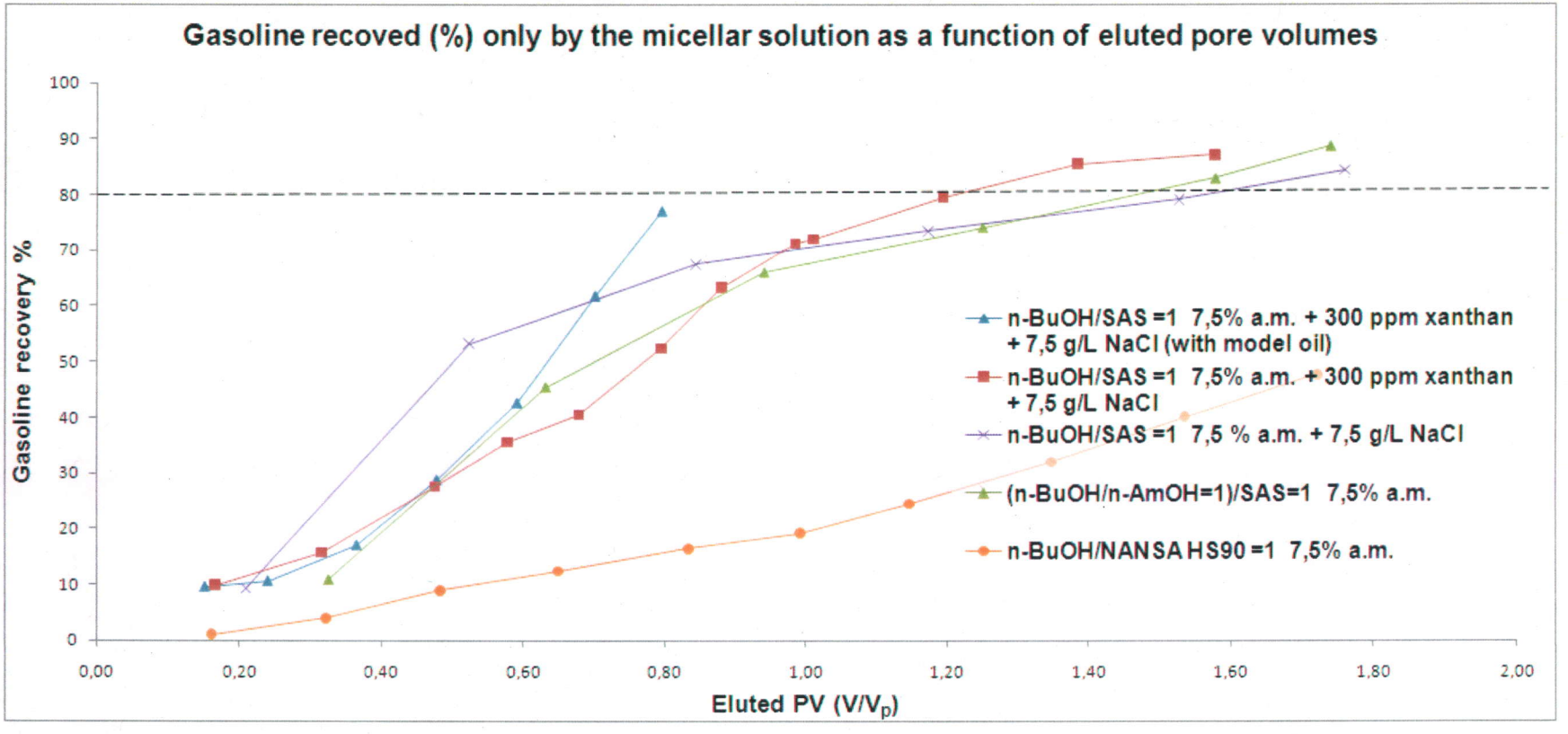

Figure 2.10. Gasoline recovered (%) only by the micellar solution as a function of eluted pore volumes for sand column experiments

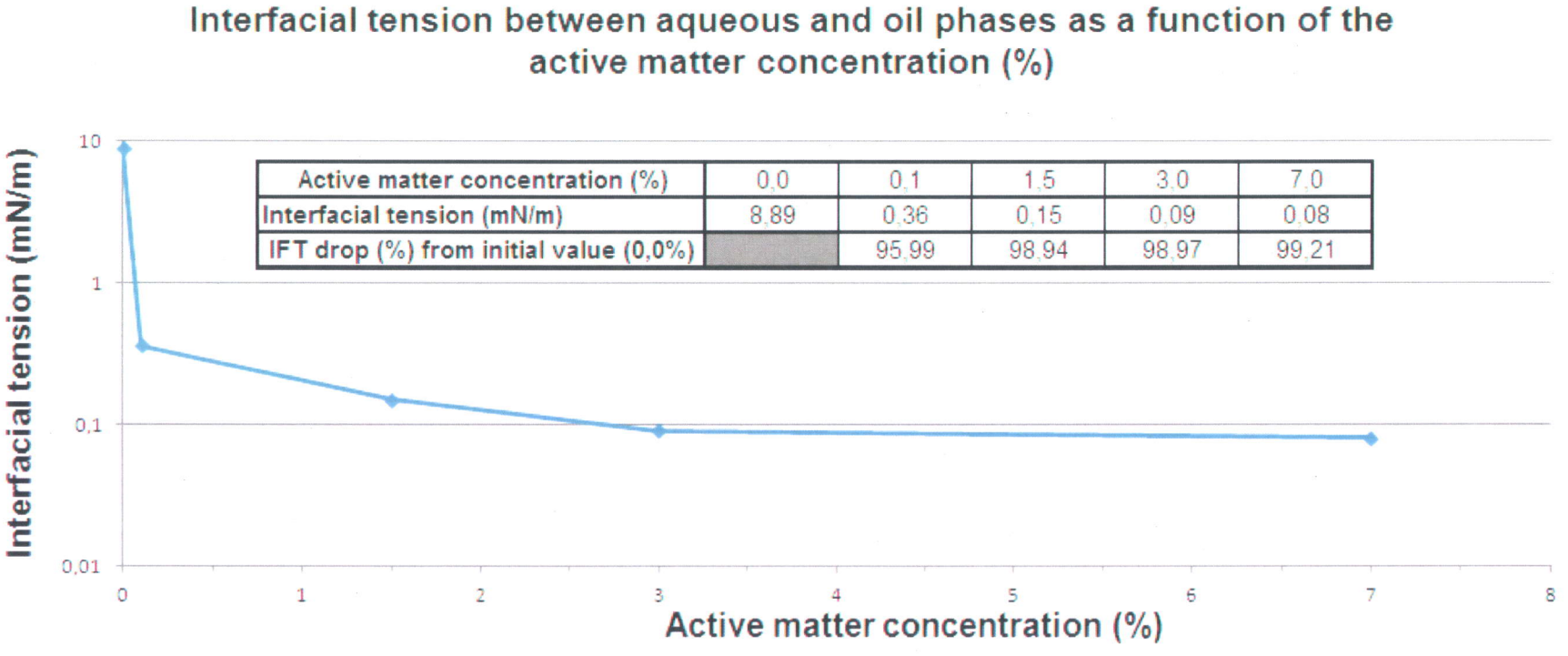

Figure 2.11. Interfacial tension between aqueous and oil phases as a function of the active matter concentration (%)

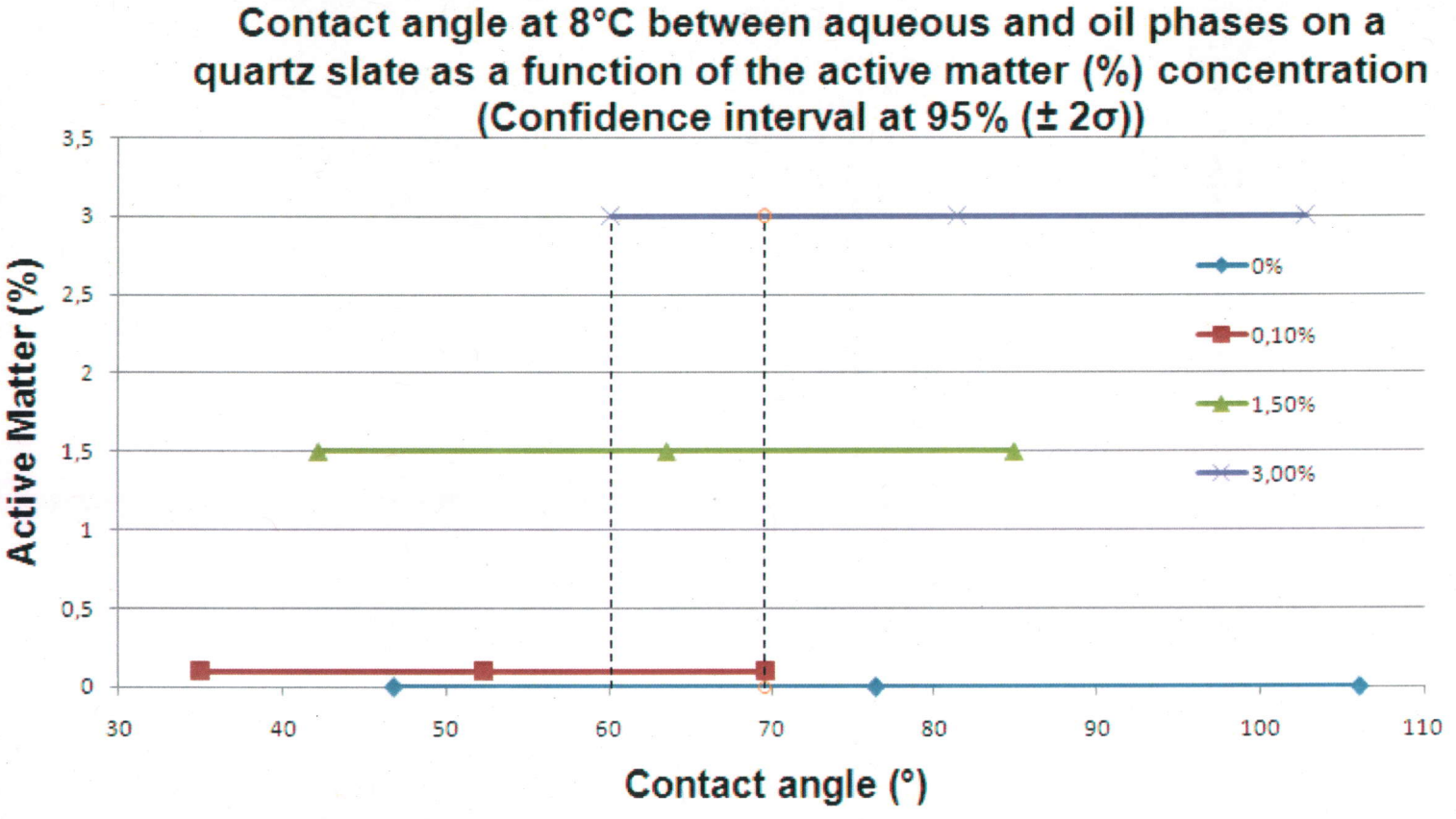

Figure 2.12 Contact angle at 8 °C between aqueous and oil phases on a quartz slate as a function of the active matter concentration (Confidence interval at 95% (± 2σ))

CHAPITRE 3

SOIL WASHING WITH A MICELLAR SOLUTION: FIELD TEST AT A GAS STATION (LAVAL, QUÉBEC, CANADA)

3.1 Résumé

En tant que technique de réhabilitation *in situ* d'aquifère, le lavage de sol avec une solution micellaire permet de récupérer des hydrocarbures pétroliers à saturation résiduelle. Un essai de terrain s'est déroulé sur le site d'une station service désaffectée (Laval, Québec, Canada), où le contaminant majeur était de l'essence. Le lavage de sol a été précédé d'une étape d'extraction sous vide permettant de récupérer la plus grande partie de la phase flottante afin d'amener l'essence à saturation résiduelle dans le sol. La solution micellaire a été injectée dans l'aquifère à partir d'un puits d'injection vertical situé au centre d'un patron à 7 points (avec 6 puits de pompage formant un patron hexagonal). La solution micellaire solubilise l'essence résiduelle présente soit sous forme adsorbée sur les particules de sol ou trappée au centre des pores ou dans des fractures. La solution micellaire comprenant aussi un polymère rhéofluidifiant a balayé 43,5 m^3 d'aquifère contaminé. Cette solution a été optimisée en laboratoire spécifiquement pour l'essence et les matériaux géologiques retrouvés sur le site par diagrammes de phases et essais en petites colonnes de sol (110 cm^3). Une modélisation de l'écoulement de l'eau souterraine a aussi été effectuée pour optimiser le ratio des débits d'injection/pompage. Les buts principaux de cet essai de terrain sont : 1) d'évaluer le rendement du lavage de sol à l'échelle pilote suite à une étape d'extraction sous vide dans un milieu hétérogène; et 2) vérifier si la concentration en essence dans la phase aqueuse en place a augmenté à la fin de l'essai en raison de la présence de la solution micellaire, afin d'améliorer le potentiel de destruction de l'essence par oxydation chimique. Le coût des produits chimiques pour l'essai pilote ont été de 100 $\$/m^3$. Pour cet essai, une récupération en essence de l'ordre de 7,5 L, équivalent à une réduction de concentration en HP dans le sol de 67 mg/kg a été observée. Cet article présente la méthodologie associée au procédé et les résultats obtenus en laboratoire et sur le terrain.

3.2 Abstract

Soil washing with a micellar solution as an *in situ* aquifer remediation technology allows the recovery of petroleum hydrocarbons at residual saturation. A pilot field test took place at a decommissioned gas station (Laval, Quebec, Canada) contaminated by gasoline. Soil washing was done after a preliminary step of vacuum extraction to remove most of the floating phase and bring gasoline to residual saturation. The micellar solution was injected in the aquifer through an injection well located in the middle of a 7-spot pattern (6 pumping wells arranged in a hexagonal pattern). The micellar solution solubilised the remaining gasoline adsorbed on soil particles or trapped into the porous medium. The polymer-micellar solution swept 43.5 m^3 of contaminated aquifer. The optimal micellar solution for this site-specific contaminant and geological material was previously optimised in the lab through phase diagrams and small sand column tests (110 cm^3). Groundwater flow modelling was also carried out to optimise the injection/pumping ratio. The main goals of this field test were: 1) to evaluate the efficiency of soil washing in a heterogeneous medium following a vacuum extraction step at the pilot scale; and 2) check if gasoline concentration in the aqueous phase has increased, due to residual micellar solution at the end of the test, which could help stimulate chemical oxidation. The unit cost of chemicals for the pilot test was 100 $\$/m^3$ of contaminated soil. A gasoline recovery of 7.5 L, equivalent to a removal of 67 mg/kg gasoline concentration in soil was observed. This paper presents the laboratory and field methodology developed for this technology as well as pilot test results.

3.3 Introduction

The field test was as part of a two-year research project designed to improve global aquifer remediation efficiency to reach environmental standards by coupling vacuum extraction and in situ chemical oxidation (ISCO) with soil washing into a technology train. Vacuum extraction reaches its efficiency limit when gasoline reaches residual saturation. For chemical oxidation, the adsorbed gasoline on soil particles or trapped in pore spaces resists oxidation. The technology train idea is to overcome these limitations by coupling the three technologies in a specific order: 1) an initial step of vacuum extraction to recover the mobile part of the gasoline free phase to bring the gasoline saturation to its residual state; 2) injection of a micellar solution to solubilize and/or mobilize gasoline at

residual saturation; and 3) oxidize the residual micellar solution and its gasoline content in the aqueous phase.

Previous work in the laboratory was carried out to optimize a washing solution for *in situ* NAPL recovery in contaminated aquifers, specifically for weathered gasoline present at a decommissioned gas station (Laval, Qc, Canada) (Grenier et al., 2011). Past studies (Desnoyers et al., 1983, Martel et al., 1993, Martel, 2007) showed that organic contaminant recovery by washing solutions was improved when alcohol and surfactant were combined, rather than used separately.

The objectives of this field test are: 1) to evaluate the efficiency of soil washing in a heterogeneous medium following a vacuum extraction step at the pilot scale; and 2) check if gasoline concentration in the aqueous phase had increased, due to residual micellar solution at the end of the test, in order to help the chemical oxidation of the remaining gasoline. This paper presents the lab and field methodology developed for this technology as well as pilot test results.

3.4 Experimental methods

3.4.1 Washing solution optimization

The first goal to achieve was to identify a washing solution able to solubilize and/or mobilize gasoline present at a decommissioned gas station. To select promising washing solutions, phase diagrams were defined by the titration technique of the cloud point (Desnoyers et al., 1983). This technique consists of injecting into a vial a small amount of NAPL into a surfactant solution until it becomes cloudy. The obtained cloudy mixture of water, NAPL and surfactant corresponds to a point on the miscibility curve of the phase diagram. By repeating that step at different active matter concentrations, other points may be added to trace the miscibility curve. Usually, 10 to 15 points are necessary to define the curve. The lower the curve is on the phase diagram, the better the washing solution is: it solubilizes the same amount of NAPL at a lower active matter concentration and reduces costs of chemicals (Falta, 1998; Martel et al., 1993). Phase diagrams identified the most efficient washing solution for a given contaminant. All phase diagrams were made at 8 °C, the groundwater temperature.

After most promising solutions were found, small sand column tests were carried out to evaluate the mineralogical and grain size effects, i.e. which solution is the most efficient when injected into the specific soil from the site. All sand columns were carried out using

the following procedure: 1) the glass cylinder is filled with compacted sand from the site; 2) carbon dioxide is injected to flush pores from its air content; 3) deaerated water is introduced to obtain a water saturated soil; 4) upward injection at high velocity (≈ 84 cm/h) of about 10.5 grams of weathered gasoline from the site pushed by 100 ml of deaerated water to reach residual gasoline saturation of 18 ± 3% (volume); and 4) horizontal injection of the washing solution with a peristaltic pump followed by polymer solution at a velocity of 2.10 ± 0.35 cm/h. Recovered gasoline in the effluent was analyzed with a GC-MS. Horizontal washing was selected since it represents the displacement type that occurs in the field. Viscosity and density of the washing solution are parameters than can affect the NAPL recovery. Solution density was measured with a density meter (Anton Paar, Austria) and the viscosity with a Cannon-Fenske viscometer (Cannon Instrument Company, USA).

3.4.2 Field test

The decommissioned gas station is located in Laval, 15 km northwest of Montreal. The gas station was operational from 1963 to 2005 and two episodes of spills/leaks from a gasoline pipe and reservoir were recorded in 1982 and 2005. A plume area of gasoline of about 2 500 m^2 was estimated from site characterization. The site is characterized by a silty sand with various proportions of gravel (0 to 2 m deep), underlain by a unit of blocks and/or boulders with some sand and traces of gravel. The water table is 7 m deep, located in the blocks and boulders unit. The measured field hydraulic conductivity from slug tests in observation wells is about 10^{-5} m/s and the total porosity is estimated at 20%. Groundwater flows east with a natural gradient of 0.013 and with a mean velocity of 80 m/y.

Before the beginning of the field test, vacuum extraction was carried out to recover the mobile part of the gasoline free phase to bring the gasoline saturation to its residual state before soil washing. No free phase was observed in wells before the soil washing step.

3.4.3 Chemicals and costs

The anionic surfactant Hostapur SAS-30® (Clariant, USA, distributed by Charles Tennant, Canada), a secondary alkanesulfonate, has an active matter content of 30% and 70% water. The normal butyl alcohol (n-butanol) was obtained from ChemCo Inc,

Quebec, Canada. Potassium bromide KBr was obtained from Laboratoire-Mat, Quebec, Canada and manufactured by Sigma-Aldrich. The xanthan gum (polymer) was provided by Jungbunzlauer, Switzerland. The cost of each chemical is provided in Table 3.1. For 43.5m^3 of contaminated soil, the unit cost of chemicals was 104$/$m^3$.

3.4.4 Pumping/injection pattern

The field test was carried out on a 43.5 m^2 cell, representing 1.7% of the contaminated area (2 500 m^2). The contaminated layer to be treated was a function of the water table level and injection well screen length. The injection well was screened from 6.5 m to 8.0 m deep and the water table was 7.0 m deep, to yield a 1.0 m thick treated zone (between 7.0 and 8.0 m deep) for a potential of 43.5 m^3 of contaminated soil. Figure 3.1 shows a vertical section of the cell showing the historic water table variation, the contaminated zone and the treated zone. With a total porosity of 20%, the corresponding pore volume is 8.7 m^3.

The test plot was equipped with a vertical central injection well and 6 surrounding extraction wells, forming a 7-point hexagonal pattern. The mean distance between the injection well and extraction wells is 4.26 m (3.27 to 5.71 m). Four observation wells inside the test plot and 11 outside complete the instrumentation of the experimental field set up (Figure 3.2).

The injection/pumping flow rate for the whole field test was fixed at 1:2 to insure that the injected solution was completely pumped by the extraction wells. A pre-test modeling of groundwater flow with the software *Feflow* was carried out to confirm that this 1:2 injection/pumping flow rate ratio was safe.

3.4.5 Process and equipment

The fluids to be injected were contained in a 1 m^3 reservoir, linked by a 1.5 " flexible tubing at its base to the injection well (Figure 3.3). The injection flow was controlled at 1.5 GPM (5.67 L/min) with a gate valve followed by a flowmeter 0-2 GPM, FL3702 (Omega, USA) (Figure 3.5). The first fluids to be injected have low viscosity and can be injected simply by gravity. The following injected fluids with high viscosity were injected using a diaphragm pump (Figure 3.4) on the line to be able to maintain the flow rate. Fluids enter into the aquifer by the 1.5 m PVC screen (with 0.15 mm slots), at the bottom of the well.

At each of the 6 pumping wells, effluent enters into the well by the PVC screen (with 0.25 mm slots) and is pumped via a bladder pump. A control panel for each pair of bladder pumps allows control of the flow rate (Figure 3.6). The pumping rate was maintained at twice the injection rate (3.0 GPM - 11.34 L/min) for the 6 pumping wells, with a mean pumping rate at each well of 1.89 L/min. The bladder pumps are 1.0 m long and their top were fixed flush to the level of the water table, so the effluent was pumped at 1.0 m below the water table. Two small ½" flexible tubes were attached to the top of the bladder pump, one for the air intake/exhaust and one for the effluent to the surface. The effluent was stored in a 1 m^3 tote tank for temporary storage (Figure 3.7).

Once the temporary storage 1 m^3 tote tank was full, the 6 effluent tubes were transferred into a second 1 m^3 tote tank, allowing time to sample and empty it with a Cyclone pool pump into an open-top container.

Before disposal of the effluent at the end of the field test, a salting out step was applied using 10 g/L of NaCl to separate the surfactant from the effluent. The goal of this step is to remove surfactant that causes foam formation before waste water treatment, consisting of an oil/water separation and an activated carbon filtration. The bottom layer made of the surfactant precipitate is finally pumped by a specialized firm who will dispose of it adequately.

3.4.6 Solutions preparation

Throughout the field test, solutions to be injected were prepared one by one directly in the field. Four different solutions had to be prepared: a salted water solution, a micellar solution, a micellar-polymer solution and a polymer solution. Solutions were prepared directly in the 1 m^3 reservoirs and/or in 200 L drums.

The first solution prepared was a salted water solution at a concentration of 7.5 g/L of NaCl. The salt was weighted on a small cooking balance (Starfrit, maximum weight: 5 kg, ± 1 g) and put into a small bucket that was used to dissolve the salt with hot water and then transferred into a 1 m^3 tote tank. This process was repeated until the mass of salt reached 7.5 kg. The reservoir was then filled with water to the 1000 litres line. The solution was thoroughly mixed with a paint drill mixer to completely dissolve the salt. The process was repeated five times for a total of 5000 L of brine.

A first micellar solution was prepared with a 300 ppm Br^- concentration, to serve as a tracer in the solution. A concentration of 447 ppm (0.447 g/L) of KBr was used as the Br^- tracer. To keep a 7.5 g/L salt concentration, only 7.053 g/L of NaCl had to be added

(7.053 g/L NaCl + 0.447 g/L KBr) into the solution. A mass of 37.5 kg of n-butanol and 37.5 kg of SAS had to be used to make a 1 m^3 solution. The n-butanol 200 L barrel was placed on a heavy weight balance (Weigh-Tronix, Wi-125, maximum weight: 907.2 kg, ± 0.1 kg) and its content was transferred with a bucket into the 1 m^3 reservoir. The exact amount of n-butanol was obtained once the balance had displayed a 37.5 kg loss in the barrel. The same process was used with SAS. Considering SAS-30 contains only 30% of active matter and 70% of water, a mass of 125 kg of SAS-30 was necessary to make the solution containing 37.5 kg of pure SAS. The 1 m^3 reservoir was then filled with water and then homogenized with the drill mixer. The process was repeated four times for a total of 4000 L of solution.

The micellar-polymer solution with 300 ppm of xanthan gum concentration was prepared with the same process as the micellar solution (37.5 kg of n-butanol, 125 kg of SAS-30 and 7.5 kg of NaCl). The three ingredients were mixed with 850 L of water with the drill mixer. Xanthan gum was added to this solution with 150 L of a concentrate at 2000 ppm to make a 300 ppm xanthan solution. To prepare this concentrate (0.4 kg of xanthan gum was poured into 200 L of water) the mixing operation had to be very gentle to not damage by shearing the xanthan molecules, thus keeping its rheological properties. A stirrer (Caframo, Canada) with Teflon® rods and palms was used to mix the xanthan solution at low speed. The solution was mixed into the 1 m^3 reservoir at low speed with the drill mixer before its injection. A total of 4000 L of solution was prepared.

The last injected solution is a polymer solution that was prepared at a 500 ppm xanthan gum concentration. A volume of 250 L of concentrate xanthan gum solution at 2000 ppm was added to 750 L of water into a 1 m^3 reservoir to make a 500 ppm xanthan solution. The process was repeated 10 times for a total of 10 000 L.

3.4.7 Injection steps

The first step is to achieve steady state groundwater flow in the pilot test cell by injecting water into the injection well and pumping it into the six extraction wells. Monitoring of the water level variation until it stabilized indicated that steady state had been reached. The different solutions are then injected following a specific order, starting with 5 m^3 (0.57 PV) of salted water at 7.5 g/L of NaCl followed by 4 m^3 (0.46 PV) of micellar solution. The salted water is injected first to avoid salinity dilution at the displacement front of the micellar solution. Then 4 m^3 (0.46PV) of micellar-polymer solution is injected followed by 10 m^3 (1.15 PV) of polymer solution to finish the injection sequence. Pore volume

equivalence of injected solution is based on the total porosity value of 20%, obtained from the site characterization.

3.4.8 Sampling

The objectives of the sampling (groundwater and effluent) were to know the initial conditions in the aquifer, to follow the evolution of the chemical composition of fluids in the contaminated zone and the amount of gasoline collected in each extraction well throughout the field test. To do so, samples were taken prior, during and after the field test, in observation, extraction and injection wells, as well as the effluent reservoir and injection reservoir. Overall, over 500 water samples were taken during the field test.

To sample the effluent reservoir, a mixer rod fixed to a drill is first used to homogenize the effluent (Figure 3.8). Two small 10 ml clear glass with Teflon® septum cap vials were filled (without air bubble) for VOC analysis and one 250 ml clear glass wide mouth jar for other analyses.

During the injection/extraction sequence, extraction wells were sampled every hour, by filling a 250 ml wide mouth jar at each effluent tube.

A peristaltic pump (MasterFlex® easy-load® L/S, Cole-Parmer, Canada) was used to collect samples from observation wells during the field test (Figure 3.9). A clear ¼" Teflon® tube connected to the peristaltic pump by a Swagelock® connector and a flexible Viton® tube complete the sampling set-up.

The sampling of groundwater prior to and after the pilot test from the observation, injection and extraction wells, was done with bailers (2") and samples were collected in 250 ml clear glass wide mouth jars.

3.4.9 Effective porosity estimation

The effective porosity estimation should normally be done several weeks prior to the soil washing via a tracer test, in order to be able to estimate the amount of chemicals needed. The first estimate was made with a porosity of 20%. However, a second estimate of effective porosity was made from data collected with the salted water bank and micellar solution breakthrough curves. The equation employed to evaluate the effective (or mobile) porosity, is the following:

$$\theta_{eff} = \frac{Vol_{inj50}}{\pi r^2 h}$$

where the Vol_{inj50} is the volume when the observed concentration reached 50 percent of its maximum value (Payne et al., 2008). The expression $\pi r^2 h$ represents the volume of the porous medium cylinder containing the injected solution, since the flow is radial from the injector.

For the salted water bank arrival, the breakthrough curve was plotted with the electric conductivity of water as a function of the injected volume. The electric conductivity was evaluated directly in the field with a YSI multiparameter probe. For the micellar solution bank, breakthrough curves were plotted with the surfactant concentration as a function of the injected volume. Surfactant concentrations were evaluated with a two phase volumetric titration method in the lab (Clariant, 2002).

3.5 Results and discussion

3.5.1 Washing solution optimization

After combining different proportions of surfactant and alcohol in phase diagrams, the most promising washing solutions were tested in sand columns. The optimal solution determination was based on the gasoline recovery, which was based on the amount of gasoline inside the column before and after the washing. The identified optimal solution was an equal ratio of SAS and n-butanol at 7.5% active matter and 7.5 g/L of NaCl. After a washing solution volume equivalent to 1.8 pore volumes injected, the optimal solution recovered 94.2% of initial gasoline (Table 3.2).

3.5.2 Effective porosity estimation

From the salted water bank arrival, only one well could be used to trace the breakthrough curve. For all other wells, the salted water arrived before the predicted arrival time estimated from the total porosity. The breakthrough curve of the salted water bank arrival at the observation well PO-125, installed at 1.23 m from the injection well, shows an effective porosity of 4.2% (Figure 3.10). With the micellar solution bank arrival, four breakthrough curves were traced from extraction wells PO-110, PO-127, PO-128 and PO-130. Effective porosity estimated from the surfactant concentration breakthrough curves for these wells are respectively 0.9%, 1.3%, 2.8% and 3.1% (Figures 3.11-3.14). The well PO-128 being the farthest from injector, the effective porosity estimated from its breakthrough curve (2.8%) should represent the entire cell more accurately than other

wells close to the injector. The 2.5% mean value of effective porosity from all five wells corroborates that hypothesis.

This effective porosity value of 2.5% is much smaller than the 20% value estimated when the characterization of the site was done. Based on Payne et al. (2008), the effective porosity of sand and gravel aquifers (silty sand in the present case) is often less than 10 %, mainly in a 2-10% range. Table 3.3 shows examples of effective porosity determined from tracer tests for different case studies (Payne et al., 2008). The value of 2.5% for the present case is similar to the 5% value of the silty sand case presented in that table (Savannah River Site, South Carolina).

From the 2.5% effective porosity data, accurate quantities of chemicals could be ordered as a function of desired pore volumes of solutions that needed to be injected. Since this 2.5% value was only known after the pilot test, a correction has to be made on the pore volumes of solutions injected originally based on the 20% porosity value. Since there is a factor 8 between 20% and 2,5%, real injected pore volume of each solution is 8 times higher than expected (Table 3.4), which has an impact on the cost. The effective porosity evaluation via a tracer test several weeks prior to the washing process is a critical step.

If the value of 20% is used as the total porosity instead of the effective porosity, it would mean that the mobile water represents 2.5% (effective porosity) and the immobile water represents 17.5%. Even if a large part of the water does not contribute to the flow, the mobile water properties are strongly affected by immobile water. When the performance of an injected solution depends on its salinity, the probable dilution effect of the immobile water should be taken into consideration. Electric conductivity measurements (used as a salinity indicator) from observation well PO-125 have shown that the maximum observed value represents 70% of the electric conductivity of the initial injected solution, representing a dilution of 30%. This means that the immobile water has an important salinity dilution power. The dilution effect seemed to affect the active matter concentration as well. Measurements of the SAS concentration from observation well PO-125 have shown that the maximum attained value represents also around 70% of the SAS concentration of the initial injected solution (dilution of 30%). The longer the solution pathway to the extraction well, the more important the dilution effect of the immobile water will likely be. To avoid or at least decrease the dilution effect of the immobile water on the mobile water (injected solution), an adjustment of the injected solution salinity and active matter concentration could be done as a function of the

dilution factor observed in a previous tracer test. The dilution of such an adjusted injected solution could bring it to its expected properties. Such an important factor as dilution by immobile water was not taken into consideration during the laboratory experiments since its effects were negligible in the small sand columns experiments.

3.5.3 Product recovery

The recovery of gasoline and ingredients of the injected solutions was made using 6 extraction wells. The only monitored ingredient of the injected solutions is the surfactant (SAS), since previous studies (Martel, 1996) showed that the evolution of alcohol and surfactant concentrations follow each other.

For different reasons, all extraction wells did not have the same recovery performance. Factors like their position from the injector, connectivity with the aquifer and differences in pumping rates between extraction wells were probably the most important. Table 3.5 presents the recovery performances for each extraction well. Even if extraction wells PO-111 and PO-124 respectively pumped 13 and 23% of the total pumped volume, they only registered recoveries of 1.2 and 4.1% of the total recovered gasoline mass and 0.7 and 1.4% of the recovered surfactant mass. The upstream position from the injector of well PO-124 and its poor connectivity with the aquifer could explain its poor performance. For PO-111, the low recovery could be explained by its upstream position, combined with the lowest pumping rate. Since their participation in the recovery process is so low, only the four other extraction wells will be considered for further analysis (PO-110, 127, 128 and 130). The most productive extraction well has been PO-127, registering recoveries of 53.8 and 45.3% of the total recovered masses of gasoline and surfactant respectively, which could be explained by different factors: 1) PO-127 is the most closely aligned downstream extraction well from the injector (see Figure 3.15); and 2) high gasoline concentrations from the injector to PO-127. Figure 3.15 illustrates the simulated flow from the injector to the six extractors. Figure 3.15 also illustrates the non-swept zones of the cell (for the horizontal sweep) that represent around 10% of the cell area. The high concentration of stream lines from the injector to PO-127 confirms that its straight downstream position is consistent with its high product recovery. The low concentration of stream lines in the direction of PO-111 reflects its low pumping rate.

For each of the four active extraction wells, it is of interest to know if the gasoline was recovered via mobilization or dissolution. The recovery mechanism could be different from one well to another and could change at any moment for the same extraction well,

depending on the amount of gasoline along the solution pathway. The breakthrough curves combination of relative concentrations of gasoline and surfactant in the extraction wells allows evaluating the recovery mechanism as a function of injected volume (Figures 3.16-3.19). For extraction wells PO-127, 128 and 130, breakthrough curves of gasoline and surfactant arrival (Figures 3.17-3.19) show that the surfactant arrives prior to the gasoline, or practically at the same time for PO-130. This means that the gasoline is solubilized in the micellar solution. Figure 3.16 shows that the gasoline at the extraction well PO-110 arrives slightly prior to the surfactant. Such a result would normally indicate that the first part of the extracted gasoline had been mobilized via an oil bank at the displacement front of the micellar solution. However, absolutely no gasoline floating phase was observed in the collected samples. From this observation, the recovery mechanism for well PO-110 has to be solubilization as well as at all three other extraction wells.

From the same breakthrough curves of gasoline and surfactant arrival for extraction wells (Figures 3.16-3.19), the sequence of injected solutions can be observed. All four extraction wells present the same pattern: 1) the first cubic meters of solution is represented by the salted water bank, showing no sign of gasoline and surfactant concentration; 2) the rise in gasoline and surfactant concentrations indicates the arrival of the micellar solution; 3) when the micellar-polymer solution arrives, gasoline concentrations have already dropped quite low while surfactant concentrations are leveling off at their maximum values; and 4) the polymer solution finally arrives and then surfactant concentrations start dropping to join gasoline concentrations at low values. Since the gasoline concentrations never reach a plateau and start dropping as fast as they rise, the volume of injected micellar and micellar-polymer solutions could have been reduced significantly. The 0.92 PV (0.46 + 0.46) of micellar and micellar-polymer solutions from original calculations would have been more appropriate than the 7.36 PV (3.68 + 3.68) actually injected. From these numbers, the cost of chemicals could have been around 8 times lower, i.e. 13 $/m^3$.

To evaluate the total gasoline recovery for the pilot test, samples from the effluent 1 m^3 tote tanks were used. A total of 38 m^3 of effluent was collected. Gasoline masses in each 1 m^3 effluent tote tank were cumulated to yield a total gasoline recovered mass of 5.9 kg (7.5 L). This mass represents a removal of gasoline concentration in soil of 67 mg/kg. The mass of recovered gasoline increases very quickly in the first 3 m^3 of effluent collected, increasing from 9 to 667 grams, due to the presence of micellar solution

(Figure 3.20). The recovery then decreases slowly with some fluctuation, to finish with the 38th 1 m^3 tote tank effluent containing 53 grams of gasoline.

Surfactant masses were cumulated as well to make a mass balance. For a 284.9 kg of injected surfactant mass, a total of 204.1 kg was collected in the effluent to yield a 72% recovery. A mass of 80.8 kg (28%) is still supposed to be in the cell. Figure 3.21 shows that surfactant recovery has reached a plateau and no more significant mass recovery could have been possible even by injecting more polymer solution. Two hypotheses can be drawn on the remaining surfactant: 1) it is trapped in the porous medium or adsorbed on soil particles; and 2) some micellar solution went out of the cell, not being caught by the extraction wells. The surfactant mass balance has to be completed with residual concentrations in wells inside the cell, to be sure no micellar solution was lost out of the cell. The surfactant concentrations in wells after the test were evaluated from ten wells inside the cell. The obtained mean value per well is 0.0185% (% m/V). Since the soil cell volume is 43.5 m^3, the effective porosity is 2.5% and the density of pure SAS is 1155 kg/m^3, the surfactant mass left in the effective porosity is 23.2 kg (8.1% of the injected mass). The surfactant mass balance not being completed at 100%, tests should be done to evaluate the surfactant adsorption by the specific soil from the site. Another possibility is that the missing surfactant mass could be in the immobile water because of the dilution effect. Since the numerical modeling with *Feflow* confirmed that the injection/pumping ratio of 1:2 was safe, the assumption of loss of solution out of the cell has to be rejected.

Since some surfactant is still in the cell (28% of initial mass), solubilized gasoline should be present in liquid samples taken after the test. Table 3.6 confirms this assumption, revealing that six out of 8 wells in the cell have a gasoline concentration increase from before to after the test. For these six wells showing gasoline concentration increases, five of them contain high residual surfactant concentrations. The two wells showing gasoline concentration decreases are associated with negligible surfactant concentrations. Because gasoline concentrations in the aqueous phase have increased after the soil washing, gasoline is now available in the aqueous phase to be oxidized in the following chemical oxidation. Since *in situ* chemical oxidation is more effective when the gasoline is in the aqueous phase instead of being adsorbed on soil particles, the chemical oxidation efficiency should be improved. The residual ingredients from the micellar solution in the cell could potentially be oxidized as well as the gasoline.

3.6 Conclusions and recommendations

A pilot test on gasoline recovery in a saturated heterogeneous silty sand aquifer was performed at a decommissioned gas station in Laval (Qc), using micellar and micellar-polymer solutions. The micellar solution was designed after several laboratory experiments using phase diagrams and sand column experiments to optimize the solution. A 7-point injection/pumping hexagonal well pattern was used. The soil washing was preceded by a vacuum extraction step and followed by chemical oxidation. The main objectives of this pilot scale field test were: 1) to evaluate the efficiency of the micellar solution for a heterogeneous silty sand aquifer; and 2) check if gasoline concentration in the aqueous phase had increased, due to residual micellar solution at the end of the test, to help in the chemical oxidation. The unit cost of chemicals for the pilot test was 100 $/m^3$ of contaminated soil.

The pilot test has shown the importance of performing a tracer test several weeks prior to the soil washing. Since the evaluation of effective porosity from the characterization step was overestimated, the quantities of chemicals injected may be overestimated. An effective porosity of 2.5% was evaluated from a salted water bank and micellar solution bank breakthrough curves at extraction the wells. This value is much lower than the 20% estimated from the site characterization. The injected solution volumes were therefore 8 times greater than expected. Gasoline recovery shows that an excessive volume of micellar and micellar-polymer solutions had been injected. The cost of chemicals could have been lower based on the real effective porosity of 2.5% and would be around 13 $/m^3$ of contaminated soil.

Gasoline recovery shows that after a sequence of injection composed of: 1) 4.6 PV of salted water; 2) 3.68 PV of micellar solution; 3) 3.68 PV of micellar-polymer solution; and 4) 9.2 PV of polymer solution, a total of 7.5 L of gasoline had been extracted from the cell. This volume is equivalent to the removal of 67 mg of gasoline/kg of soil. The surfactant recovered in the effluent represents 72% of the initial injected mass. Since the residual 28% of the micellar solution remaining in the cell still contains gasoline, gasoline concentrations in the aqueous phase were higher following the test compared to before the test. The gasoline in the aqueous phase was now available to be oxidized with the

following chemical oxidation step. Work on the compatibility between the micellar solution and the oxidant is in progress.

3.7 Acknowledgments

This project was funded through grants from the Natural Sciences and Engineering Research Council of Canada (NSERC) CRD program with TechnoRem as the industrial partner. Special thanks to Richard Levesque for his help with sample analysis and to everyone who participated during the field test: Richard Martel, Uta Gabriel, Luc Trépanier and Clarisse D.-Rancourt (co-authors), as well as Thomas Robert, Nicolas Francoeur-Leblond, Martin Blouin, Jean-Philippe Drolet and Jean-Marc Ballard.

Table 3.1. Costs of chemicals used for pilot test

Product	Unit Cost ($/kg)	Used Quantity (kg)	Total Cost ($)
Pure SAS (100%)	10.80	300	3240
n-Butanol	3.70	300	1110
Salt (NaCl)	0.55	180	100
Xanthan Gum	11.70	5	60
Total			4510

Table 3.2. Overall gasoline recovery % for sand columns experiments in series #1

Column	Solution	Gasoline Recovery %
1	n-BuOH/SAS = 1 + 7,5 g/L NaCl 7,5% a.m.	94,2
2	(n-BuOH/n-AmOH=1)/ SAS = 1 7,5% a.m.	92,5
3	n-BuOH/Nansa HS90 = 1 5,0% a.m.	61,1
4	n-BuOH/SAS = 1 + 7,5 g/L NaCl 5,0% a.m.	55,8
5	(n-BuOH/n-AmOH=1)/ SAS = 1 5,0% a.m.	53,3
6	n-BuOH/Arkopal N90 = 1 5,0% a.m.	16,1

Table 3.3. Examples of effective porosity evaluation from tracer tests for different case studies (Payne et al., 2008)

TABLE 3.2
Summary of mobile porosity estimates determined by tracer tests.

Location	Aquifer	Aquifer Material	Mobile Porosity	Notes
Quebec, Canada	--	Poorly Sorted Sand & Gravel	8.5%	6.4 m^3 injection in 7.25 hours
Central Valley, California	--	Poorly Sorted Sand & Gravel	4% to 7%	575 m^3 injection over 30 days; arrival monitored in 7 wells
Northern Texas	Ogallala	Poorly Sorted Sand & Gravel	9%	1460 m^3 injection over 28 days
New Jersey	Passaic Formation	Fractured Sandstone	0.1% to 0.7%	24.6 m^3 injection over 2 days
Los Angeles, California	Gaspur Aquifer	Alluvial Formation	10.2%	17 m^3 injection over 8 hours
Northern New Jersey	--	Glacial Outwash	14.5%	7.57 m^3 in 3 days
Northern Missouri	--	Weathered Mudstone Regolith	7% to 10%	4.54 m^3 in 9 days
Sao Paulo, Brazil	--	Alluvial Formation	7%	18.9 m^3 injection over 2.5 days
Phoenix Arizona	--	Alluvial Formation	7%	2.27 m^3 in 8 hours
Savannah River Site, South Carolina[1]	Atlantic Coastal Plain	Silty Sand	5%	Model Calibration
Kaiserslautern, Germany	Trifels Formation	Fractured Sandstone	0.08% to 0.1%	Multiple injections and volumes between 0.1 m^3 and 5 m^3
West Texas	Rio Grande River Valley	Alluvium, Sand & Gravel	1.7%	18.9 m^3
Northern Texas	Ogallala	Alluvium, Poorly Sorted Sand & Gravel	0.3 to 1.7%	Dipole test, 61.3 m^3 in 22.8 hrs
Central Colorado	Cherry Creek	Alluvium, Sand & Gravel	11% to 18%	Two Injection tests, 4.9 m^3 and 7.6 m^3
Central Colorado	Denver Formation	Siltstone, Sandstone, Mudstone	1% to 5%	Monipole - Tracer Injected in monitoring well / Pumping well

[1]Hamm et al

Table 3.4. Adjustment of injected pore volumes with the 2,5% effective porosity value

Injected solutions	Injected volume (m^3)	Pore volume equivalent based on θ_{eff} = 20% (m^3)	Pore volume equivalent based on θ_{eff} = 2,5% (m^3)
Salted Pre Flush	5	0,57	4,6
Micellar Solution	4	0,46	3,68
Micellar + Polymer solution	4	0,46	3,68
Polymer solution	10	1,15	9,2

Table 3.5. Recovery performances for extraction wells

Extraction wells	% from total pumped volume	% from total collected gasoline mass	% from total collected surfactant mass
PO-110	14,26	21,13	28,99
PO-111	13,01	1,20	0,67
PO-124	22,58	4,08	1,39
PO-127	21,03	53,78	45,28
PO-128	17,22	14,53	8,66
PO-130	11,89	5,28	15,02
Total	100,00	100,00	100,00

Table 3.6. Gasoline concentrations in wells of the cell before and after the pilot test

Well #	Before Test (mg/L)	After Test (mg/L)	↑ or ↓ In concentrations	Surfactant % After Test (% m/V)
PO-NEW	37,3	9,0	↓	< 0,01
PO-111	20,2	20,9	↓	< 0,01
PO-124	30,4	39,1	↑	0,02
PO-125	9,4	40,6	↑	0,02
PO-127	23,2	254,3	↑	0,03
PO-128	93,8	211,2	↑	0,03
PO-129	111,5	343,2	↑	0,02
PO-130	49,9	121,4	↑	< 0,01

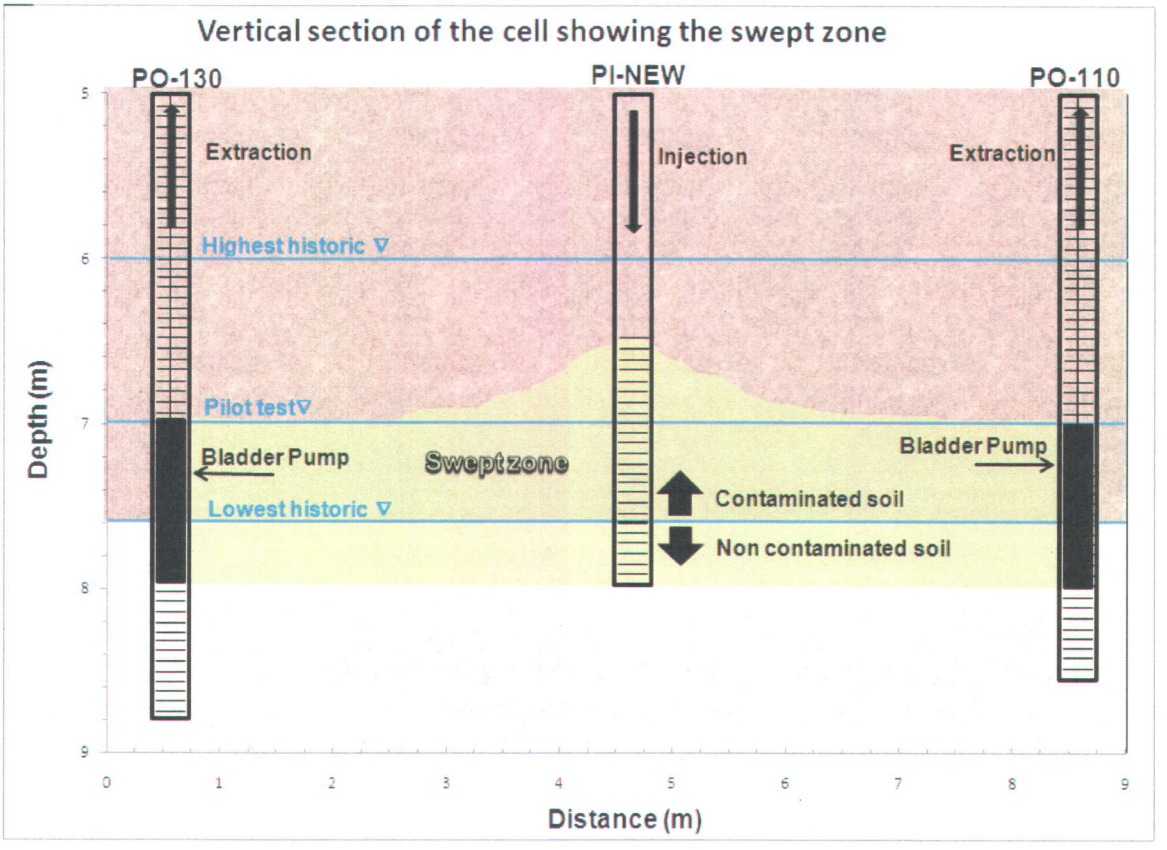

Figure 3.1. Vertical section of the cell showing the swept zone

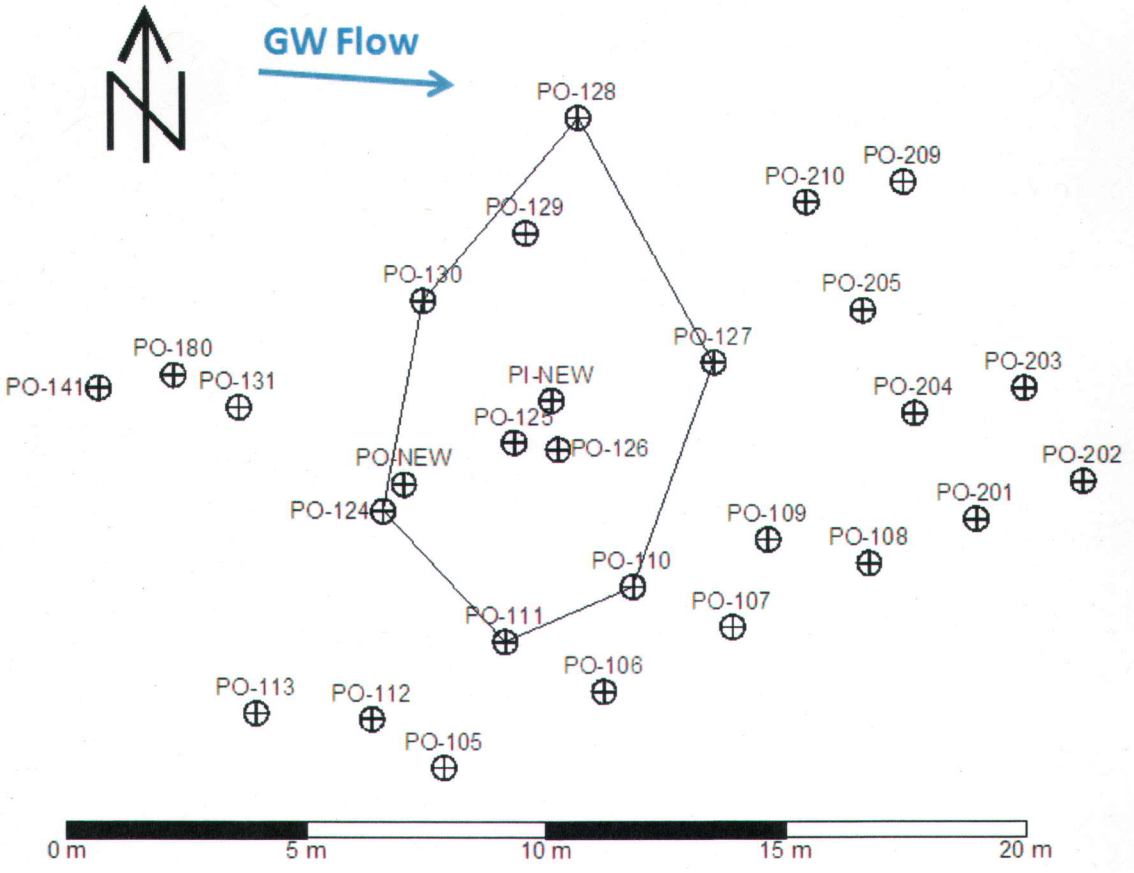

Figure 3.2. Area of the pilot test: the 7-point hexagonal pattern

Figure 3.3. 1 m^3 tote tank containing injection solutions

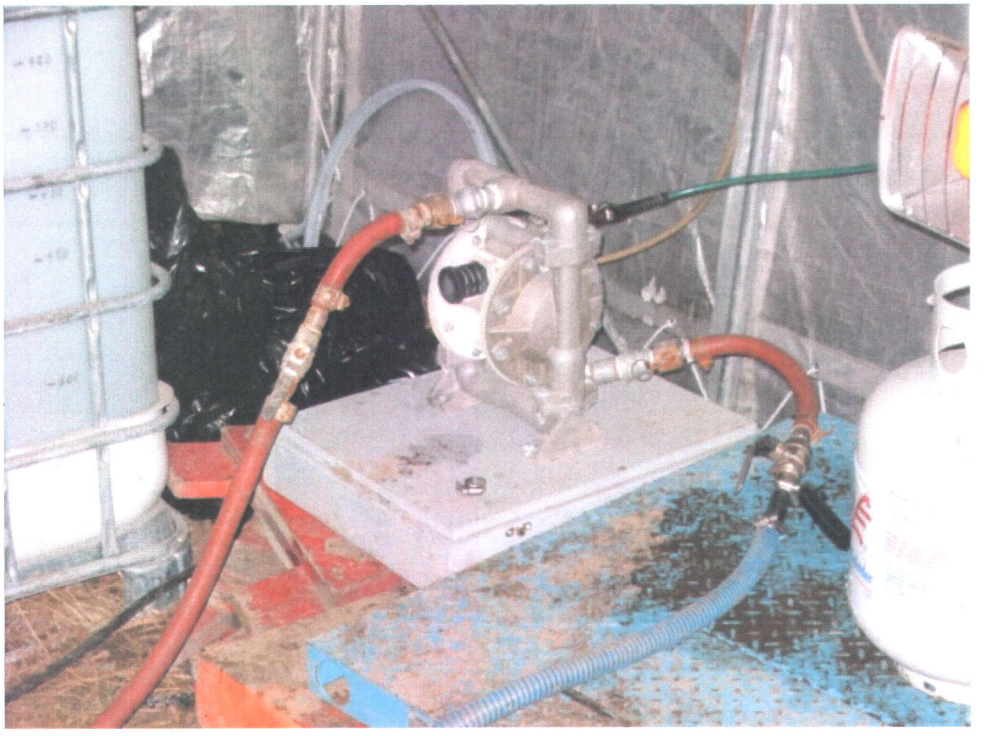

Figure 3.4. Diaphragm pump to inject solutions from the 1 m^3 tote tank to the injection well

Figure 3.5. Gate valve followed by flowmeter on the injection line

Figure 3.6. Control panels for bladder pumps

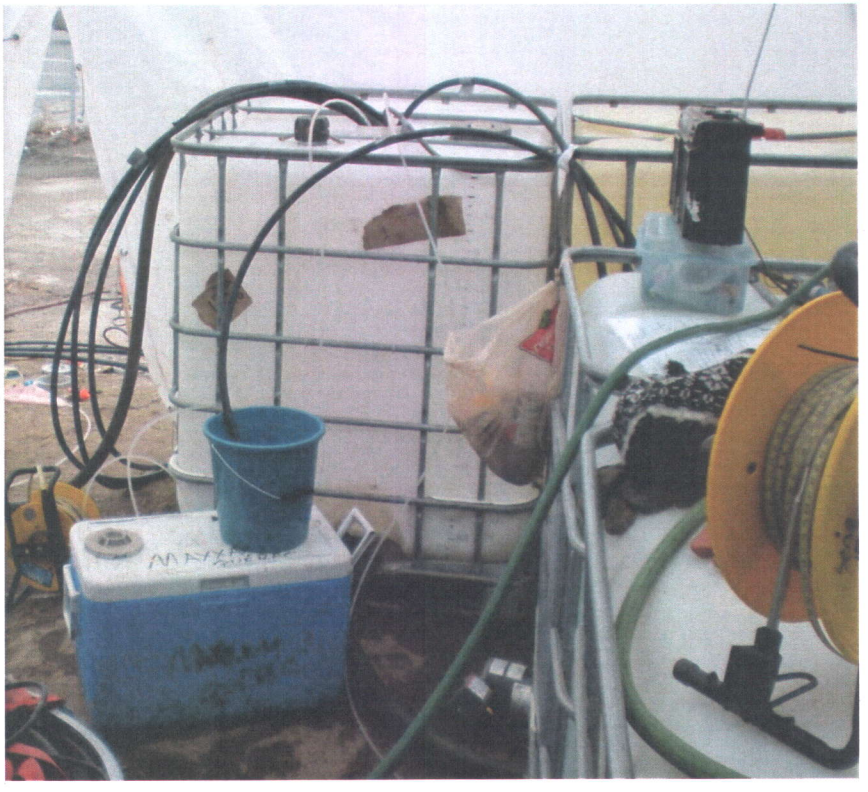

Figure 3.7. Effluent 1 m^3 tote tank

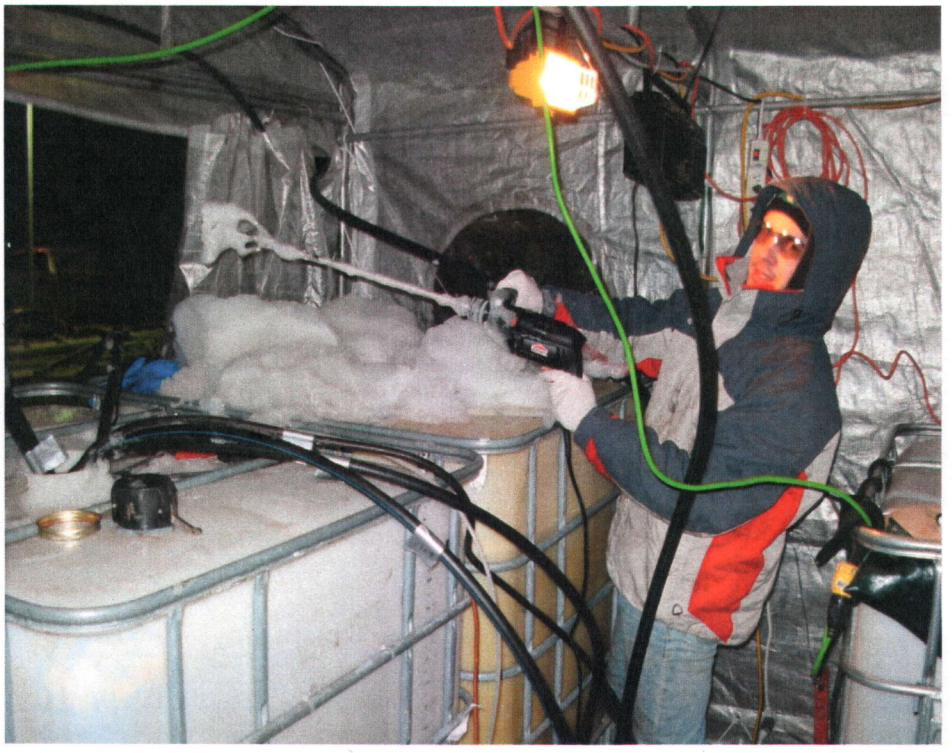

Figure 3.8. Homogenization of the effluent before sampling

- Figure 3.9. Low flow sampling: Peristaltic pump via a flexible Viton® tube connected to a ¼" Teflon® tube

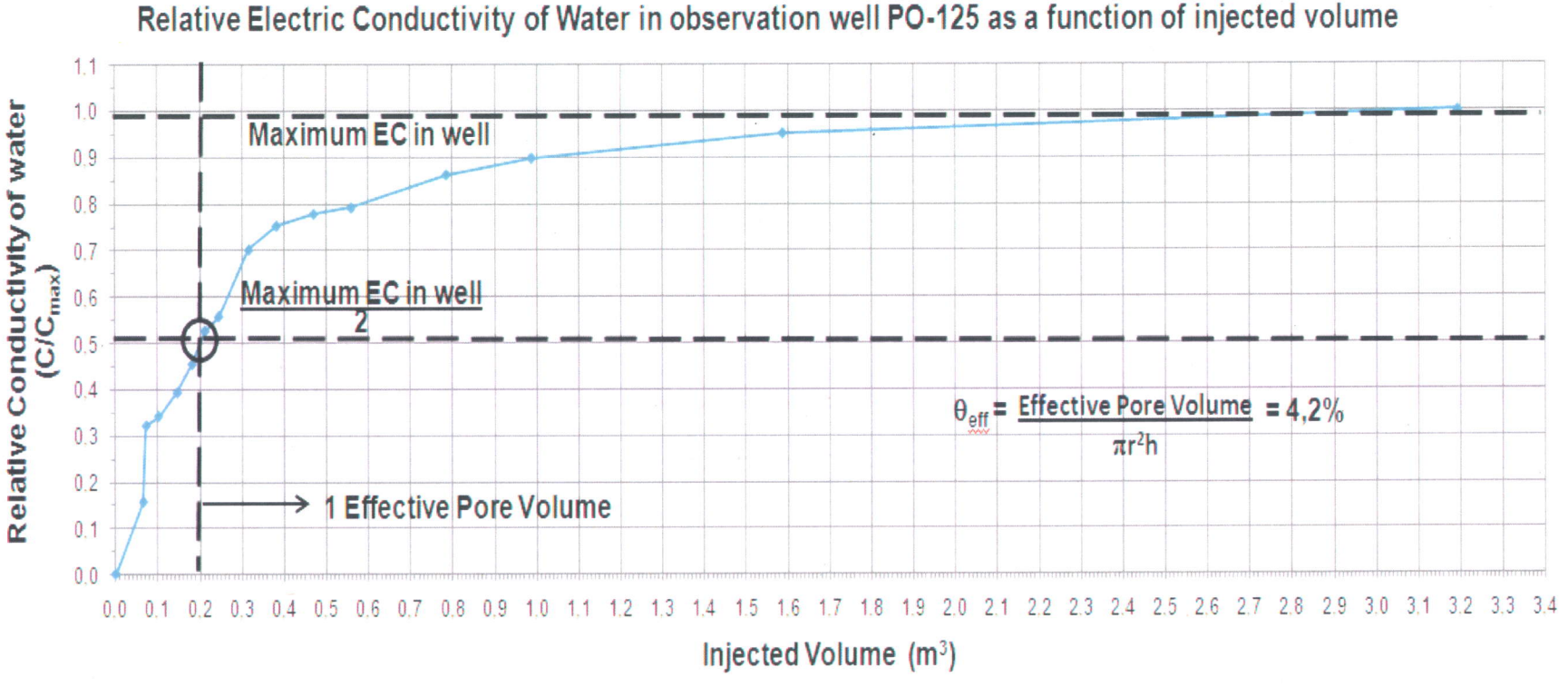

Figure 3.10. Relative electric conductivity of water in observation well PO-125 as a function of injected volume

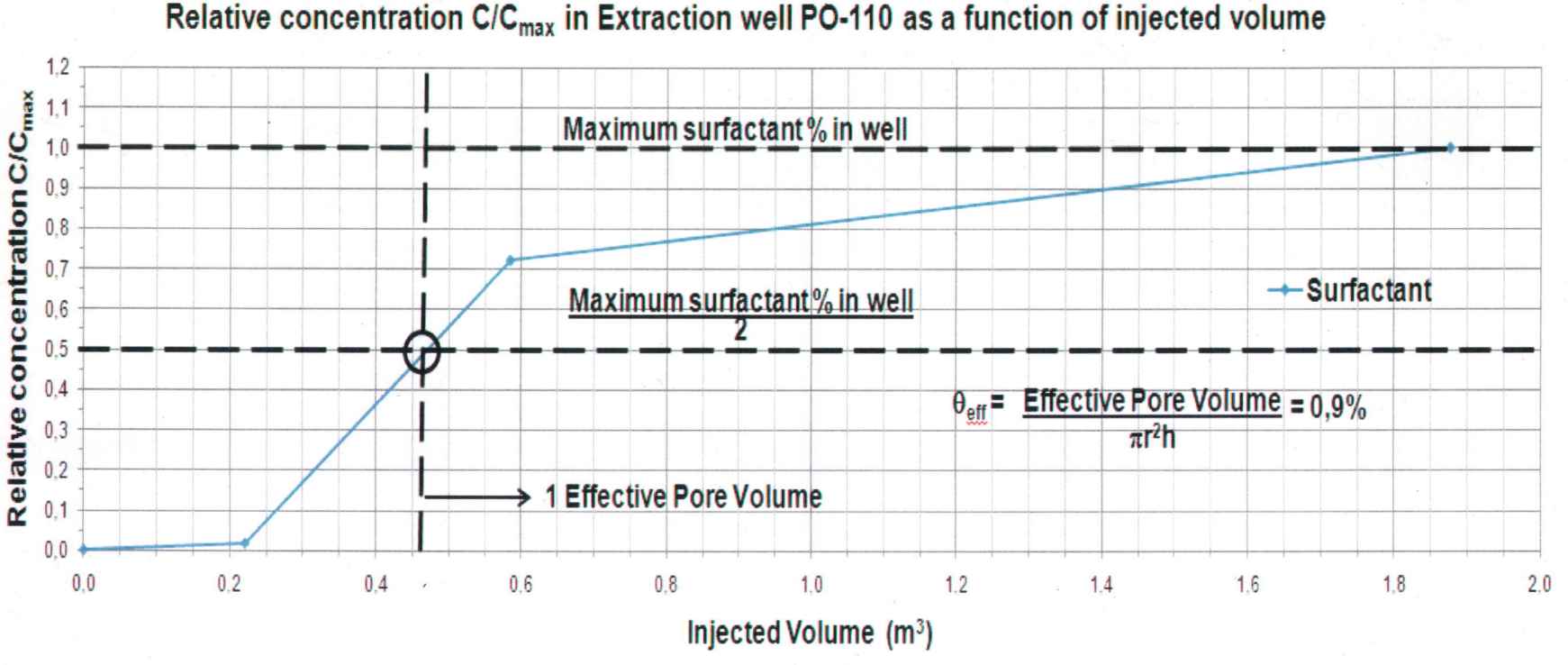

Figure 3.11. Relative surfactant concentration C/C_{max} in extraction well PO-110 as a function of injected volume

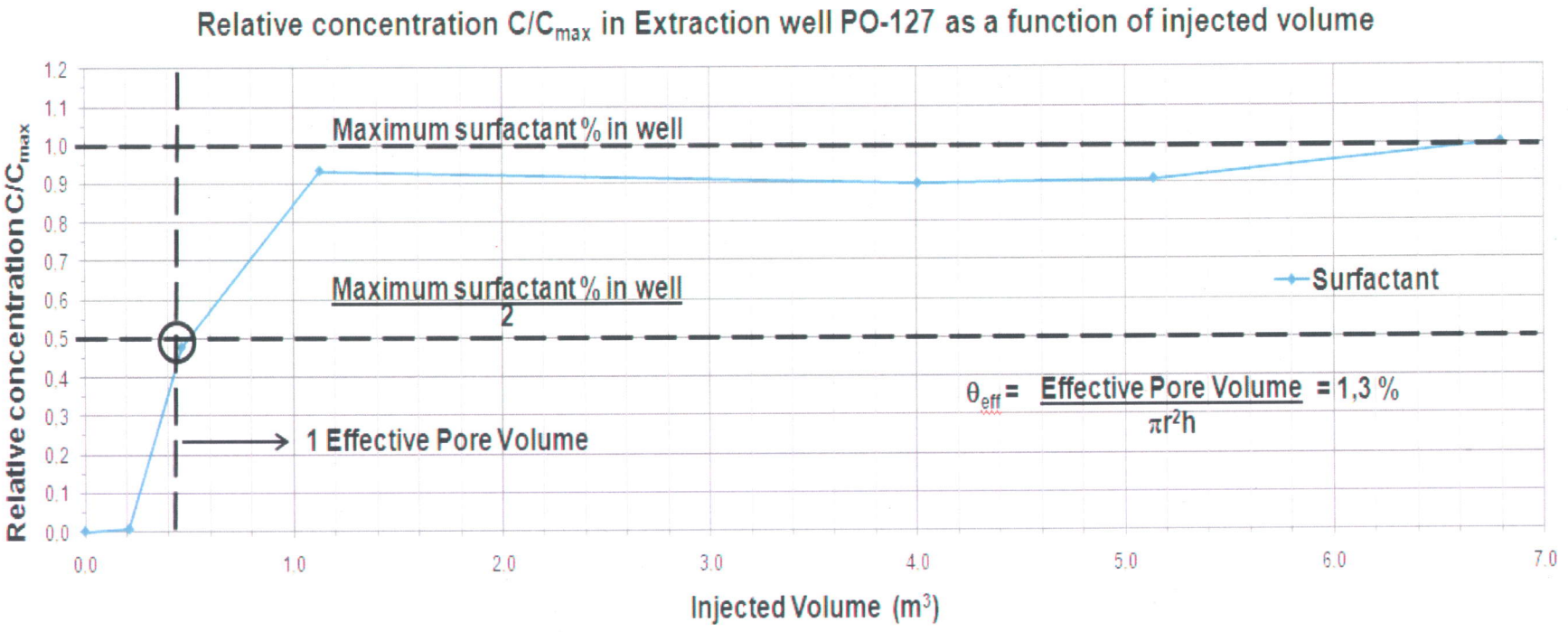

Figure 3.12. Relative surfactant concentration C/C$_{max}$ in extraction well PO-127 as a function of injected volume

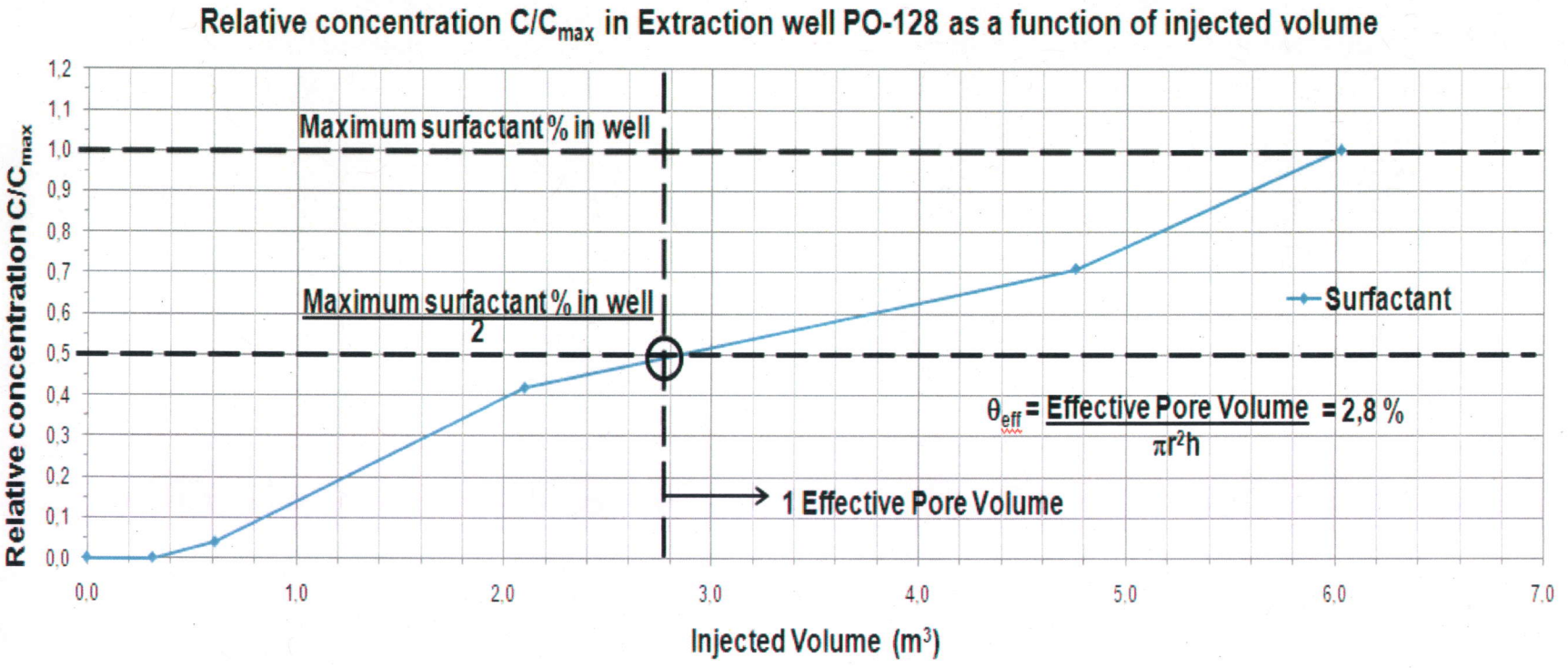

Figure 3.13. Relative surfactant concentration C/C_{max} in extraction well PO-128 as a function of injected volume

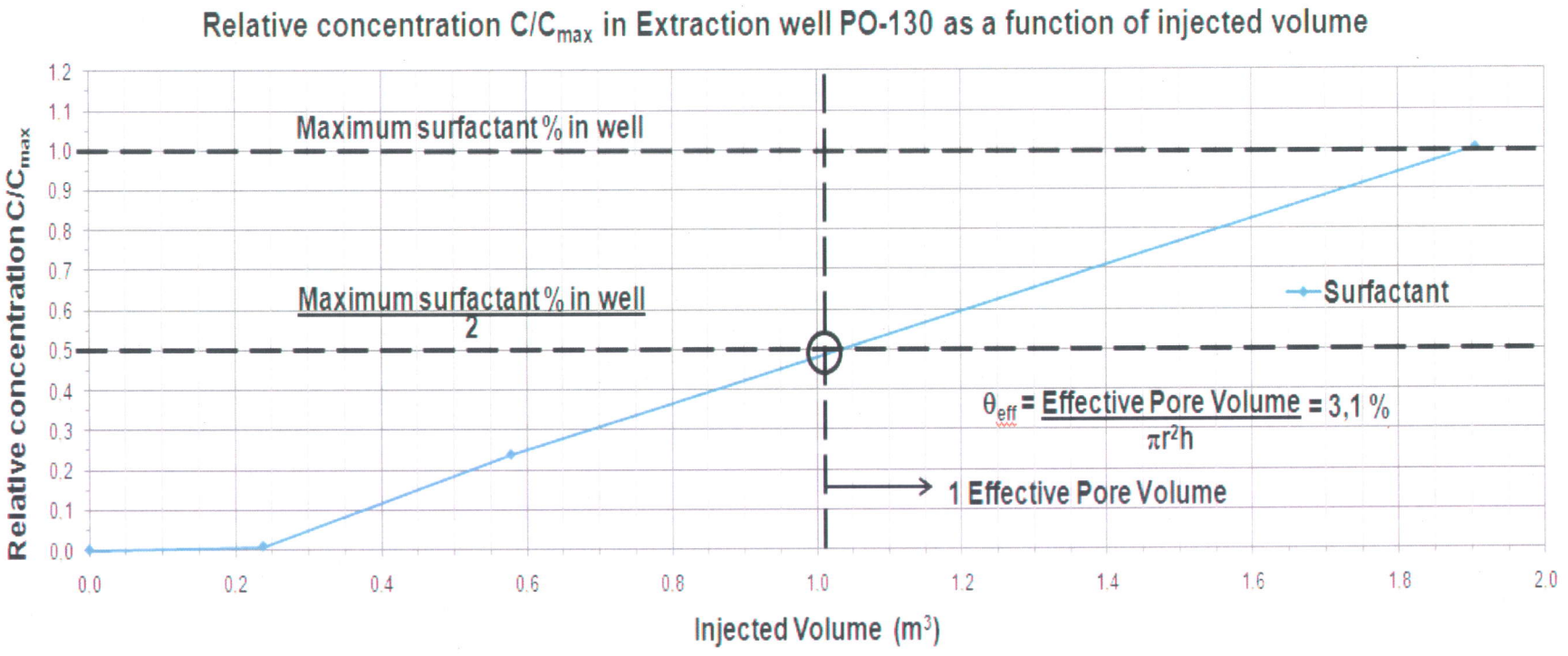

Figure 3.14. Relative surfactant concentration C/C_{max} in extraction well PO-130 as a function of injected volume

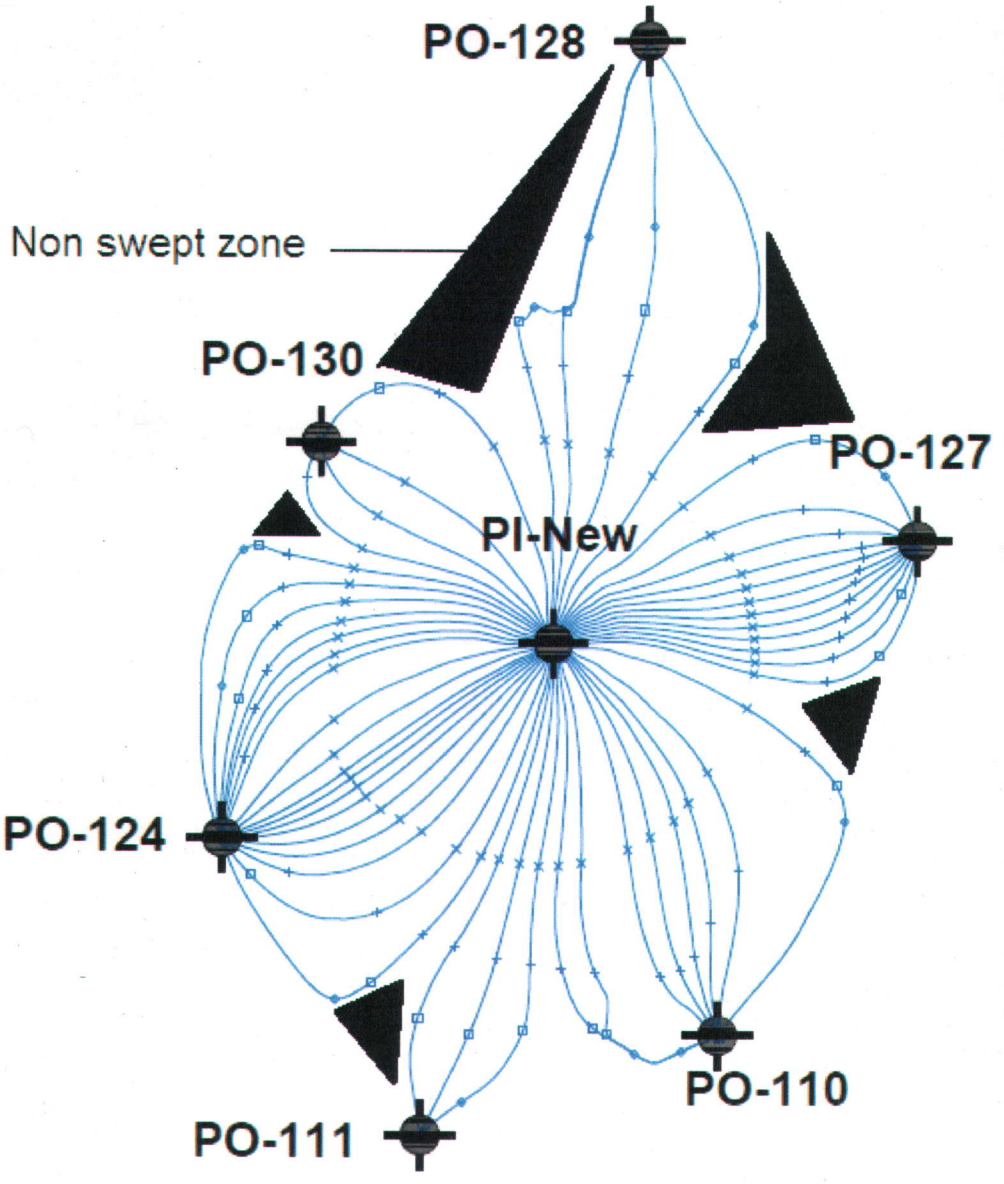

Figure 3.15. Simulated flow lines from the injector to the extractors

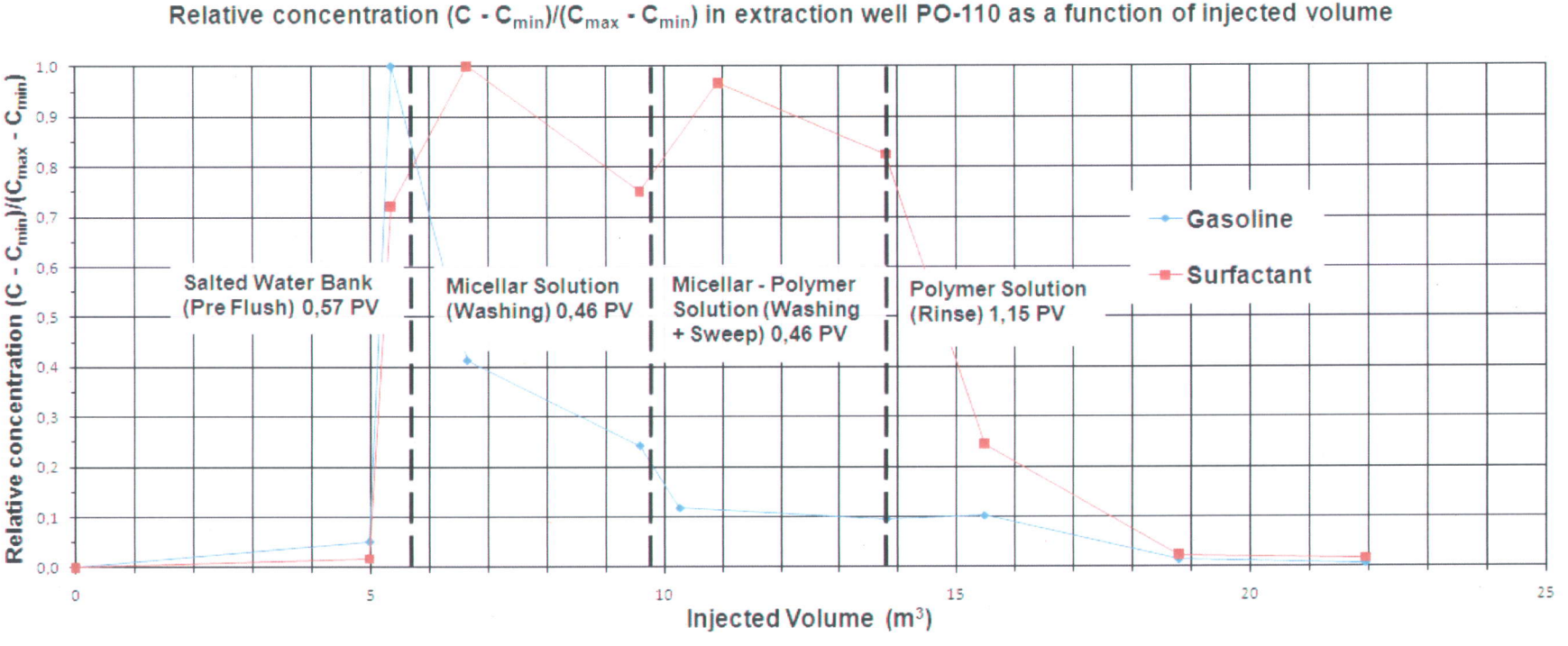

Figure 3.16. Relative gasoline and surfactant concentration in extraction well PO-110 as a function of injected volume

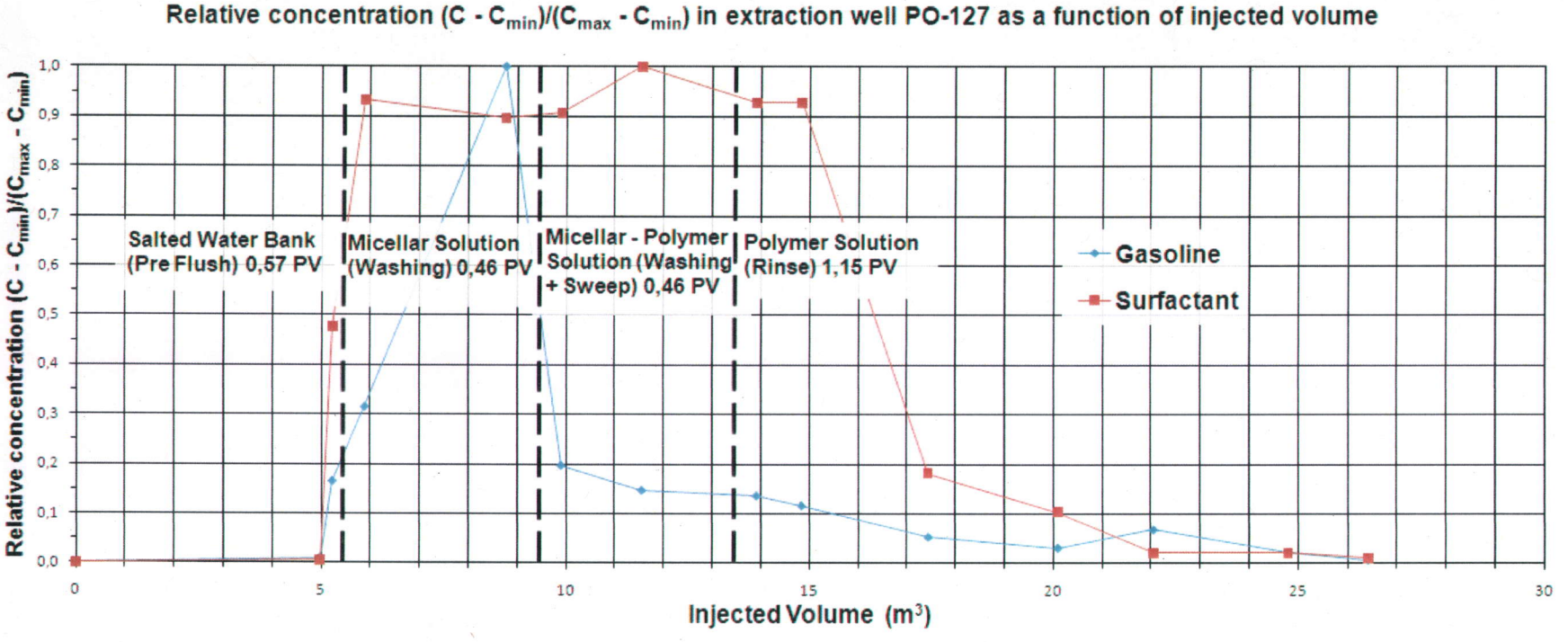

Figure 3.17. Relative gasoline and surfactant concentration in extraction well PO-127 as a function of injected volume

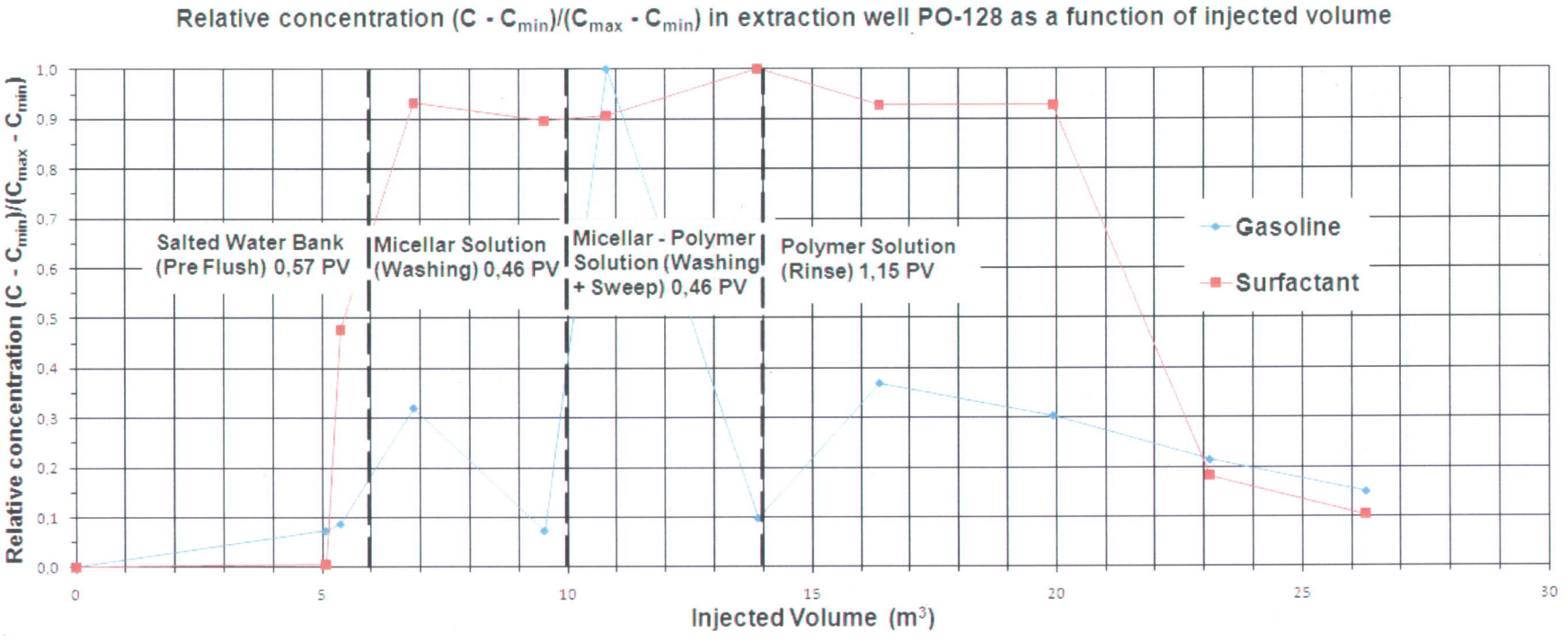

Figure 3.18. Relative gasoline and surfactant concentration in extraction well PO-128 as a function of injected volume

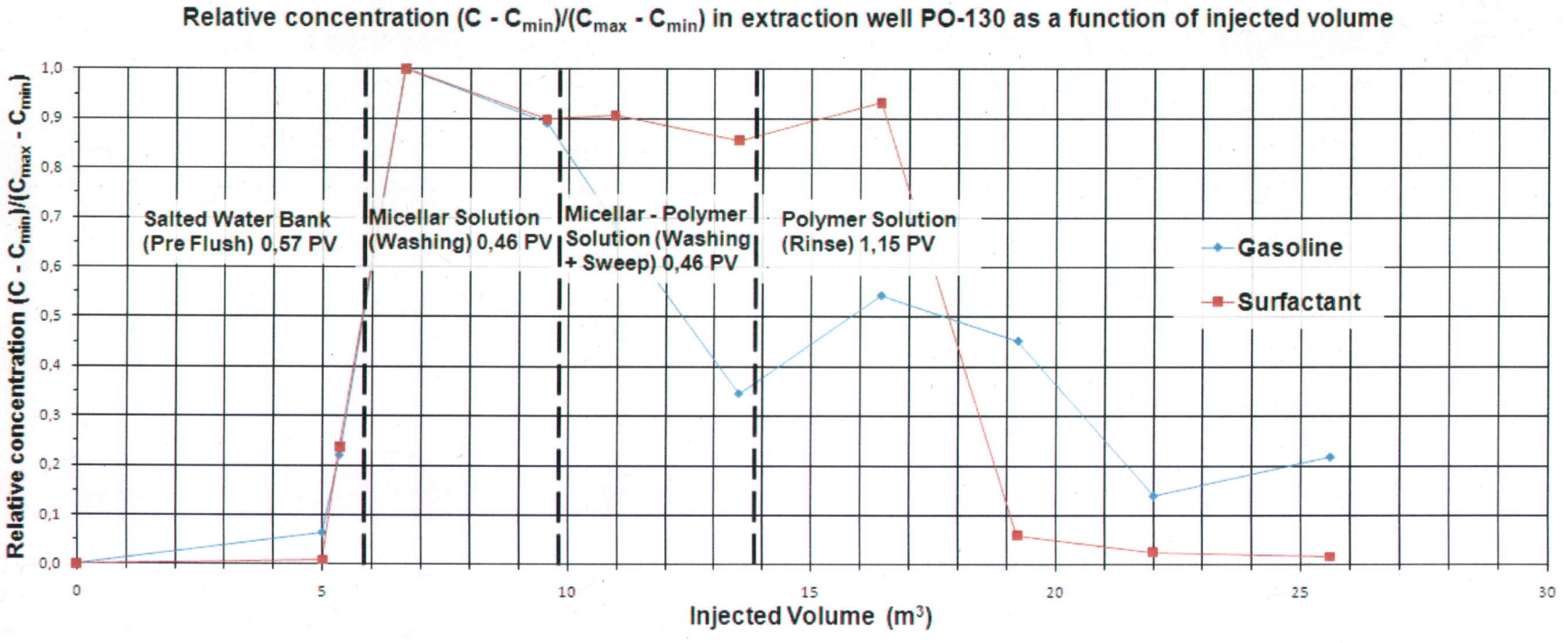

Figure 3.19. Relative gasoline and surfactant concentration in extraction well PO-130 as a function of injected volume

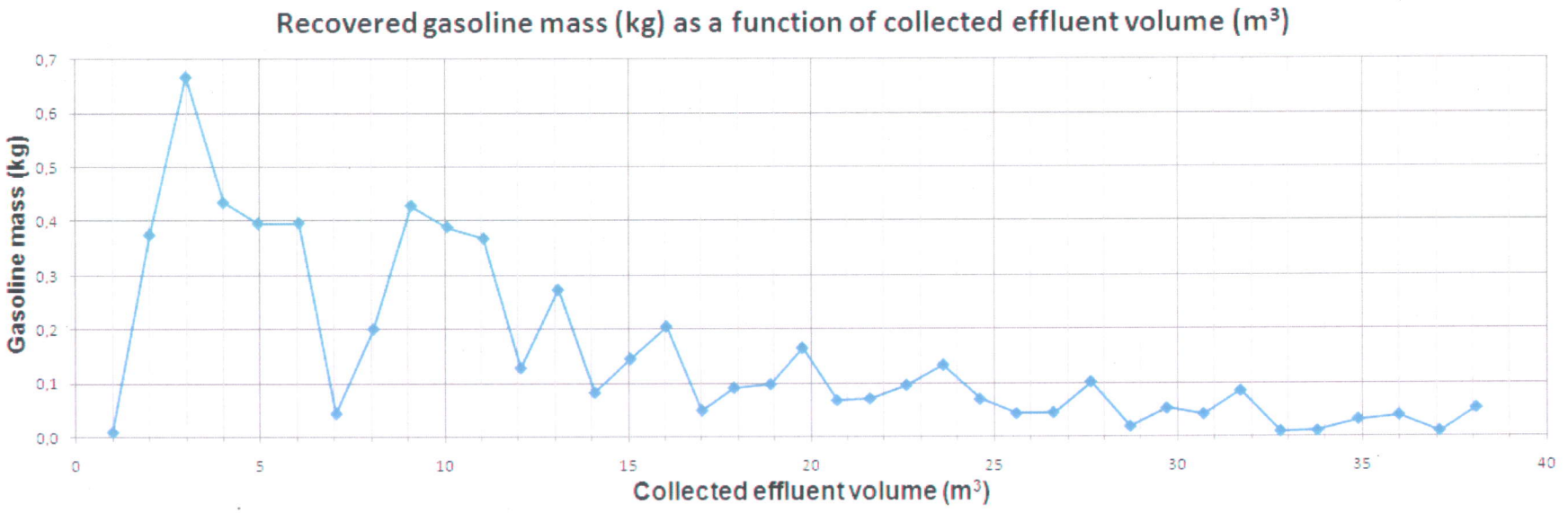

Figure 3.20. Recovered gasoline mass (kg) as a function of collected effluent volume (m^3)

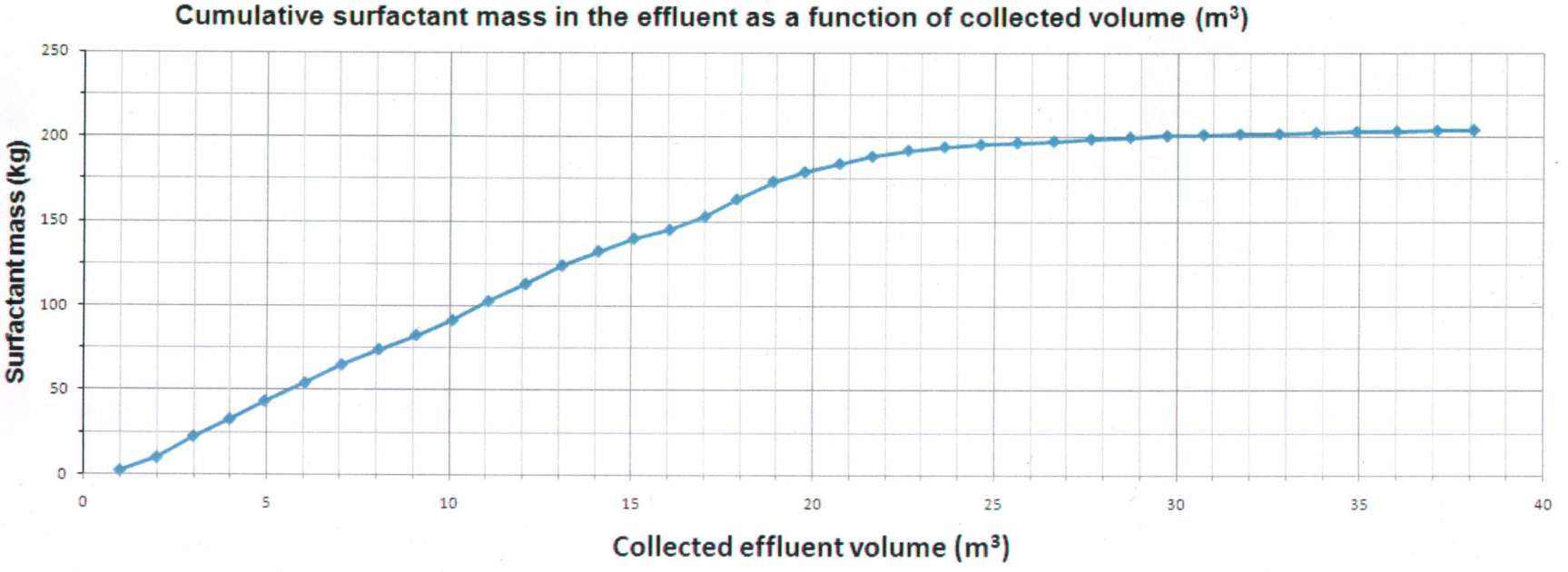

Figure 3.21. Cumulative surfactant mass (kg) in the effluent as a function of collected volume (m^3)

BIBLIOGRAPHIE

Bradner, C.F., Slotboom, R.A. 1975. Vertical immiscible displacement experiments in a non-homogeneous flow cell. *J. Can. Petroleum Technol.* 1975, Vol. 14, 1.

CCME. 2001. *Standard pancanadien relatif aux hydrocarbures pétroliers dans le sol.* s.l. : Le conseil canadien des ministres de l'environnement, 2001.

Chatzis, I. et Morrow, N.R. 1983. Magnitude and detailed structure of residual oil saturation. *SPE Journal no. 23.* 1983, pp. 311-326.

Clariant. 2002. *Determination of anionic–active matter by use of two phase volumetric.* 2002.

Delshad, M., Pope, G.A., Sepehrnoori, K. 1996. A compositional simulator for modeling surfactant enhanced aquifer remediation: 1. Formulation. *Journal of Contaminant Hydrology.* Elsevier, 1996, Vol. 23, 303-327.

Desnoyers, J.E., Qurion, F., Hétu, D., Perron, G. 1983. Tar sands extractions with microemulsions: 1 - The dissolution of light hydrocarbons by microemulsion using 2-butoxyethanol and diethylamine as cosurfactants. *The Canadian Journal of Chemical Engineering.* 1983, Vol. 61, pp. 672-679.

Dwarakanath, V., Kostarelos, K., Pope, G.A., Shotts, D., Wade, W.H. 1999. Anionic surfactant remediation of soil columns contaminated by nonaqueous phase liquids. *Journal of Contaminant Hydrology, 38.* 1999, pp. 465-488.

Falta, R.W. 1998. Using phase diagrams to predict the performance of cosolvent floods for NAPL remediation. 1998, pp. 1-9.

Farley, K.J., Falta, R.W., Brabdes, D., Milazzo, J.T., Brames, S.E. 1993. *Remediation of hydrocarbon-contaminated groundwater by alcohol flooding.* s.l. : Final Report, Submitted to Hazardous Waste Management Research Fund, 148 pages, 1993.

Fetter, C.W. 1999. *Contaminant Hydrogeology - Second Edition.* New Jersey : Prentice Hall, 1999.

Fisher. Material Safety Data Sheets. *Fisher Scientific.* [En ligne] http://iris.fishersci.ca/MSDS2.nsf/Search?OpenForm.

Fountain, J.C., Klimek, A., Beikirch, M.G., Middleton, M. 1991. The use of surfactants for in-situ extraction of organic polluants from a contaminated aquifer. *Journal of Hazardous Materials, 28.* 1991, pp. 295-311.

Fountain, J.C., Starr, R.C., Middelton, T., Beikirch, M.G., Taylor, C., Hodge, D. 1996. A controlled field test of surfactant-enhanced aquifer remediation. *Ground Water, 34 (35).* 1996, pp. 910-916.

Grenier, M., Martel, R., Robert, T, Gabriel, U., Lauzon, J-M. 2009. *Impact of surfactant solutions on conventional technologies efficiency for gasoline contaminated aquifer remediation.* Halifax : AIH, 2009. p. 8.

Grenier, M., Martel, R., Trépanier, L, Gabriel, U, Rancourt, C, Robert, T, Lauzon, J-M. 2010. *Soil Washing with a Micellar Solution: Pilot Test at a Gas Station (Laval, Québec, Canada).* Banff : Remediation Technologies Symposium, 2010. p. 12.

ITRC. 2005. *Technical and Regulatory Guidance for In Situ Chemical Oxidation for Contaminated Soil and Groundwater - Second Edition.* Washington D.C. : Interstate Technology & Regulatory Council - In Situ Chemical Oxidation Team, 2005.

Knox, R.C., Sabatini, D.A., Harwell, J.H., Brown, R.E., West, C.C. Blaha, F., Griffith, C. 1997. Surfactant remediation field demonstration using a vertical circulation well. *Ground Water, 33 (4).* 1997, pp. 948-953.

Lake, L.W. 1989. *Enhanced oil recovery.* Englewood Cliffs, New Jersey : Prentice Hall, inc. 550 pp., 1989.

Larousse. 1994. *Le Petit Larousse illustré.* Paris, France : s.n., 1994.

Larson, R.G., Scriven, L.E. et Davis, T.H. 1980. Percolation theory of two phase flow in porous media. *Chem Eng. Sci. no. 36.* 1980, pp. 55-73.

Lefebvre, R. 2006. *GEO-9602 Écoulement multiphase en milieu poreux.* Québec : Note de cours, INRS - ETE, 2006.

Lide, David R. 2004. *Handbook of chemestry and physics, 84th edition, 2003-2004.* s.l. : CRC Press, 2004.

Martel, K.-E. 1995. *Utilisation des solutions de polymères pour améliorer l'efficacité de balayage des solutions tensioactives développées pour la restauration d'aquifères contaminés aux hydrocarbures immiscibles lourds.* Québec : Thèse de maîtrise, Université Laval, 1995.

Martel, K.-E., et al. 1998. Laboratory Study of Polymer Solutions Used for Mobility Control During In Situ NAPL Recovery. *Ground Water Monitoring & Remediation.* Summer 1998, 1998, Vol. 18, 3.

Martel, R. 1996. *Développement de solutions tensioactives pour la récupération de phases liquides non aqueuses à saturation résiduelle dans les aquifères.* Québec : Thèse de doctorat, Université Laval. 310 pp., 1996.

Martel, R. et Gélinas, P.J. 1998. Aquifer washing by micellar solutions: 1 - Optimization of alcohol/surfactant/solvent solutions. *Journal of Contaminant Hydrology, Volume 29, Issue 4.* 1 March 1998, pp. 319-346.

Martel, R. et Gélinas 1996. *Surfactant solutions developped for NAPL recovery in contaminated aquifers.* 1996.

Martel, R. 2007. *Impact de solutions tensioactives sur le rendement de technologies conventionnelles pour la remédiation d'aquifères contaminés par des hydrocarbures pétroliers.* Québec : Formulaire de demande de subvention au CRSNG, 2007.

Martel, R., Gélinas, P.J., Desnoyers, J.E., Masson, A. 1993. Phase diagrams to optimize surfactant solutions for oil and DNAPL recovery in aquifers. *Ground Water.* 1993, Vol. 31, Issue 5.

Martel, R., Gélinas, P.J. *Phase diagrams to optimize surfactant solutions for oil and DNAPL recovery in aquifers.* 1996.

Martel, R., Hébert, A., Lefebvre, R., Gélinas, P., Gabriel, U. 2004. Displacement and sweep efficiencies in a DNAPL recovery test using micellar and polymer solutions injected in a five-spot pattern. *Journal of Contaminant Hydrology.* Elsevier, 2004, Vol. 75, 1-2. pp.1-29.

Martel, R., Lefebvre, R. et Gélinas, P.J. 1998. Aquifer washing by micellar solutions: 2 - DNAPL recovery mechanisms for an optimized alcohol/surfactant/solvent solution. *Journal of Contaminant Hydrology, Volume 30, Issue 1-2.* March 1998, pp. 1-31.

Miller, Ralinda R. 1996. *Bioslurping - Technology Overview Report.* Pittsburg : Ground-Water Remediation Technologies Analysis Center, 1996.

Morrow, N.R. 1979. Interplay of capillary, viscous and buoyancy forces in the mobilisation of residual oil. *J. Can. Pet. Tech.* Sept (1979), 1979, p-35-46.

Payne, F.C., Quinnan, J.A. et S.T., Potter. 2008. *Remediation Hydraulics.* Boca Raton, FL, USA : CRC Press, Taylor & Francis Group, 2008.

Pope, G.A. et Wade, W.H. 1995. Lessons from enhanced oil recovery research for surfactant-enhanced aquifer remediation. *Surfactant-Enhanced Subsurfac Remediation - Emerging Technologies.* Washington DC : American Chemical Society, 1995, pp. 142-160.

Ripple, C.D., James, R.V. et Rubin, J. 1973. Radial particle-size segregation during packing of particles into cylindrical containers. *Power Tech.* 1973, Vol. 8, pp. 165-175.

Robert, T. 2004. *Visualisation des mécanismes de récupération du TCE par des solutions micellaires et polymères dans un modèle physique 2D hétérogène.* Québec : Université du Québec, INRS-ETE, 2004.

Roote, Diane S. 1997. *In Situ Flushing - Technology Overview Report.* Pittsburg : Ground-Water Remediation Technolgies Analysis Center, 1997.

Sabatini, D.A., Knox, R.C., Harwell, J.H., Soerens, T., Chen, L., Brown, R.E., West, C.C. 1997. Design of a surfactant remediation field demonstration based on laboratory and modeling studies. *Ground Water, 35 (6).* 1997, Vol. 35, 6, pp. 954-963.

Shiau, B.J., Sabatini, D.A., Harwell, J.H., Vu, D.Q. 1996. Microemulsion of mixed chlorinated solvents using food grade (edible) surfactants. *Environmental Sc. Tech., 30.* 1996, pp. 97-103.

St-Pierre, C., Martel, R., Gabriel U., Lefebvre, R., Robert, T. et Hawari, J. 2004. TCE recovery mechanisms using micellar and alcohol solutions: pase diagrams and sand column experiments. *Journal of Contaminant Hydrology.* Elsevier, 2004, Vol. 71, 1-4. pp. 155-192.

USGS. 2009. Light Non-Aqueous Phase Liquids (LNAPLs). *Toxic Substances Hydrology Program.* [En ligne] May 2009. http://toxics.usgs.gov/definitions/lnapls.html.

VWR. *VWR International.* [En ligne] https://www.vwrcanlab.com/catalog/page.cgi?tmpl=products.

Wardlaw, N.C. et McKellar, M. 1985. Oil blob populations and mobilization of trapped oil in unconsolidated packs. *Can J. of Chem Eng v. 63.* 1985, pp. 525-532.

ANNEXE A

Article présenté à la 10e conférence conjointe SCG/AIH-CNC, Halifax, Septembre 2009

Impact of surfactant solutions on conventional technologies efficiency for gasoline contaminated aquifer remediation

Maxime Grenier
INRS - Eau, Terre et Environnement, Québec, Qc, Canada
Richard Martel, Thomas Robert, Uta Gabriel
INRS - Eau, Terre et Environnement, Québec, Qc, Canada
Jean-Marc Lauzon
TechnoRem, Laval, Qc, Canada

ABSTRACT
By coupling vacuum extraction and in situ chemical oxidation (ISCO) with soil washing, it may be possible to improve global aquifer remediation efficiency to reach environmental standards. Vacuum extraction comes to its efficiency limit when gasoline reaches residual saturation. A first surfactant solution injection allows mobilizing gasoline through a vacuum extraction (slurping) system that is used to recover gasoline as a free phase. A second surfactant solution injection before ISCO allows dissolving remaining gasoline adsorbed on soil particles or trapped into the porous media and makes gasoline available for ISCO destruction. The main goal of this research is: (1) to find promising surfactant solutions allowing mobilization of residual gasoline and dissolution of the remaining gasoline, and (2) to test their efficiency on contaminated sediments in laboratory columns, in a 4m^3 triangular sand tank and on site at the pilot test scale. This paper presents the physical and chemical properties of the studied gasoline and identifies the promising washing solutions with the help of pseudo-ternary phase diagrams. Results from phase diagrams show that surfactant and alcohol mixtures are more efficient than both ingredients used individually. The observed gasoline recovery mechanism in phase diagrams and anticipated in the porous media is mainly dissolution. These solutions should be adapted to mobilize gasoline.

RÉSUMÉ
En combinant l'extraction sous vacuum et l'oxydation chimique avec la technologie de lavage de sol aux solutions tensioactives, il serait possible d'améliorer le rendement global de la réhabilitation afin d'atteindre les critères environnementaux. L'extraction sous vacuum atteint sa limite d'efficacité lorsque l'essence atteint sa saturation résiduelle. L'injection d'une solution tensioactive permet la mobilisation de l'essence par un système d'extraction sous vide, utilisé pour récupérer l'essence en phase mobile. L'injection d'une solution tensioactive précédant l'oxydation chimique permet de solubiliser l'essence restante, adsorbée aux particules de sol ou prise dans le milieu poreux, et rend l'essence disponible pour la destruction in-situ par oxydation chimique. Le but principal de cette étude est donc d'identifier des solutions tensioactives prometteuses permettant la mobilisation de l'essence résiduelle et la solubilisation de l'essence restante, et de tester leur efficacité sur des sédiments contaminés par la suite en petites colonnes de sable, en bac de sable triangulaire de 4 m^3 et in situ à une échelle d'essai pilote. Le présent article porte sur les propriétés physico-chimiques de l'essence à l'étude et l'identification des solutions tensioactives prometteuses à l'aide de la construction de diagrammes de phases pseudo-ternaires. Les résultats obtenus en diagrammes de phases montrent qu'un mélange composé d'un tensioactif et un alcool est plus efficace que chacun pris individuellement. Le mécanisme de récupération de l'essence observé dans les diagrammes de phases et anticipé dans le milieu poreux est principalement la solubilisation. Ces solutions devront être adaptées pour mobiliser l'essence.

1 INTRODUCTION

Aquifer contamination by petroleum hydrocarbons (PH) is a plague that is spread all over the world, and particularly in industrialized countries like Canada. In Canada, PH like gasoline are the most spread contaminants and contaminated sites containing PH are counted by tens of thousands (CCME, 2001). Besides their toxicity and mobility, PH are persistent contaminants in soil because of their low water solubility and their high interfacial tensions (IFT) with water. Because of their persistence in soil, existing remediation technologies are not efficient enough to reach environmental standards for groundwater and soils quality.

According to Bradner and Slotboom, 1975, three forces act on PH behavior in the saturated zone: capillary forces, gravity forces and viscous forces. Capillary forces are defined by Young-Laplace equation: $P_c = 2\sigma\cos\theta / R$ and depend on PH-water IFT (σ), soil particles-PH-water contact angle (θ) and soil pore radius (R). Gravity forces are defined by the following equation: $F_g =$

$\Delta\rho gh$ and depend on density difference between water and gasoline ($\Delta\rho$), gravitational acceleration (g) and on gasoline droplets size (h). Viscous forces are governed by the following equation: $F_v = v\mu = k(dp/dx)$ and are a function of displacing fluid velocity (v), dynamic viscosity (μ), porous media permeability (k) and pressure variation in the displacing fluid for an horizontal flow (dp/dx). To improve gasoline recovery in aquifers, among other possibilities, capillary forces can be decreased through wettability changes and IFT decreasing.

In situ recovery technologies were developed in the last decades to improve aquifer remediation like vacuum extraction (slurping), in situ chemical oxidation (ISCO) and soil washing. These technologies, when used alone, have efficiency limits. For vacuum extraction, when gasoline comes to residual saturation, the remaining gasoline exists as a discontinuous phase which is immobile and unrecoverable. For the chemical oxidation, it is adsorbed gasoline on soil particles or trapped into pore spaces that resists to oxidation. Finally, the soil washing technology generates huge washing solutions volumes that have to be treated/disposed off and the high initial active matter cost make this technology non economic.

Washing solutions are composed of a combination of surfactant and alcohol. Surfactant is an amphiphilic molecule, i.e. having two different polarity parts, one hydrophilic and one lipophilic. Four types of surfactant exist: anionic having the hydrophilic part negatively charged, cationic having the hydrophilic part positively charged, amphoteric having both charges and non ionic having no charge. Surfactant solutions can recover gasoline by two main mechanisms: dissolution and mobilization. Dissolution happens when the active matter (surfactant and alcohol) partitions preferentially in the aqueous phase, so gasoline is "dissolved" into it. Mobilization happens when the active matter partitions preferentially in the oily phase (gasoline), this way the gasoline volume is increased and can be mobilized via an oil bank.

To overcome these limitations, a technology train is proposed. By coupling vacuum extraction and ISCO with the soil washing technology, it may be possible to improve global aquifer remediation efficiency in order to reach environmental standards. This technology train starts with vacuum extraction to recover the mobile part of the gasoline floating free phase until it comes to residual saturation. By injecting a surfactant solution to mobilize gasoline at residual saturation in an oil bank (by reconnecting isolated blobs), gasoline can be recovered by vacuum extraction. By injecting a second type of surfactant solution able to dissolve remaining adsorbed gasoline on soil particles and trapped into porous media, it makes gasoline available in the aqueous phase and can be oxidized with the ISCO technology. Finally, by injecting an acclimated bacteria population to polish the cleaning process.

To accomplish such a technology sequence, laboratory experiments and a characterization of the porous media and the contaminant (gasoline) have to be done. The plan is to characterize at first the gasoline and its relation with the porous media, after that pseudo-ternary phase diagrams will be made to identify promising surfactant solutions. The best washing solutions will be tested in small sand columns experiments, in a $4m^3$ triangular sand tank experiment and on the field with a pilot test. This paper presents the initial phase of this project: characterization of contaminant physical and chemical properties and characterization of soil grain size and mineralogy; identification of promising washing solutions with the help of pseudo-ternary phase diagrams and their dominant recovery mechanism with tie lines solutions.

2 EXPERIMENTAL METHODS

2.1 Characterization of gasoline and geological materials from the contaminated site

A composite sample of weathered gasoline was obtained from observation wells located in the zone of interest at the site. Physical and chemical properties of gasoline such as density, viscosity, water content and chemical composition were respectively measured by a DMA 35N density meter (Anton Paar, Austria), an uncalibrated viscometer size 50 (Cannon Instrument Company, USA), an Aquastar V-200 titrator for Karl Fisher titration method (EM science, USA) and a Clarus 500 GCMS (Perkin Elmer, USA). Grain size analyses were done with conventional sieves and an Analysette 22 laser particle sizer (Fritsch, Germany). For mineralogy, thin sections of coarse fraction (> 2mm) were observed with a microscope under polarized light (Zeiss, Germany). X-ray diffraction analyses were done on the fine fraction with a D5000 x-ray diffractometer (Siemens, Germany). Pending drop method was used with a FTA200 apparatus (First Ten Angstrom, USA), to measure water-gasoline interfacial tension, mineral-water-gasoline contact angle (with quartz, calcite and feldspath) and gasoline surface tension at the ambient temperature (20°C).

2.2 Phase diagrams

Phase diagrams were carried out to evaluate the efficiency of different mixtures of surfactant and alcohol for the gasoline dissolution/mobilization. Pseudo-ternary diagrams have the three following poles: water at the down left, gasoline at the down right and active matter at the center top

(Figure 1). The phase diagram shows for different concentrations of each element, if the mixture consists of only one phase, or separated in two or even three phases. The initial aqueous surfactant solution has to show only one phase before its injection in aquifers.

The boundaries of the one/multiple phase zones are determined with the cloud point method (Martel et al, 1993), consisting of adding one of the three element with a gas tight syringe to bring the resulting solution from clear (one phase) to cloudy (two or three phases). A miscibility curve is obtained by connecting all the cloud points. *MS Excel 2007* is used to compile every cloud point and to trace down the miscibility curves in diagrams. The lower the position of the curve in the diagram, the more efficient is the active matter of the solution because it dissolves the same quantity of gasoline at a lower concentration level. However, other considerations such as adsorption on soil particles, overall viscosity or density, or even cost and availability of the chemicals have to be considered also. The construction of diagrams is realized at groundwater temperature at the site, i.e. 8°C. For that, a refrigerated circulator (VWR International, USA), is used to cool down the 40 ml vial wherein the liquids are added to make the phase diagrams.

To find promising solutions, 7 alcohols and 18 surfactants were tested (Table 1). Previous studies showed that using a combination of alcohol and surfactant was more efficient than using a single component (Martel et al., 1993, Saint-Pierre et al. 2004). In order to simplify the number of possible combinations of alcohol and surfactant, all variables, i.e. alcohol, surfactant and their ratio are considered independents. The optimal ratio between the alcohol and the surfactant is first found by choosing one surfactant and one alcohol that are combined at various ratios (0.5, 1.0, 2.0, and 3.0) to make phase diagrams. When the alcohol: surfactant ratio is fixed by the lower miscibility curve, the alcohol type is changed to find the best alcohol. Seven alcohols were tested. With a fixed ratio and a fixed alcohol, 18 other curves were traced to find to best surfactant. Finally, the ultimate step is to readjust the ratio as precisely as possible with the alcohol and the surfactant selected. Also, alcohols were tested alone, to check which one is the most performing when used alone.

Table 1. Surfactants tested in phase diagrams, with their water content and hydrophilic charge type

Identification	Type	% H_2O
Surfactant A	Amphoteric	50,000
Surfactant B	Anionic	27,200
Surfactant C	Anionic	0,248
Surfactant D	Anionic	29,000
Surfactant E	Anionic	69,000
Surfactant F	Anionic	55,200
Surfactant G	Anionic	46,900
Surfactant H	Anionic	8,170
Surfactant I	Anionic	4,740
Surfactant J	Anionic	56,400
Surfactant K	Anionic	2,154
Surfactant L	Anionic	3,340
Surfactant M	-	3,510
Surfactant N	-	3,670
Surfactant O	-	11,800
Surfactant P	Non ionic	2,260
Surfactant Q	Non ionic	1,010
Surfactant R	Non ionic	0,796

A straight line (tie line) relates the compositions of the aqueous phase and the oily phase to the overall composition of all compounds in the system. Tie lines indicate the recovery mechanism involved with each solution. Experimentally, they are determined by preparing mixtures with proportions of the three poles under the miscibility curve, so the three elements in solutions get separated in two phases, an aqueous and an oily one. By preparing four mixtures under the miscibility curve with the same proportion of water and gasoline and an increasing active matter proportion, it is possible to check in which phase (aqueous or oily) the active matter partitions preferentially (Figure 1). If the aqueous phase increases proportionally with the active matter, then dissolution is the principal recovery mechanism. If the oily phase increases proportionally with the active matter, then mobilization is the principal recovery mechanism. To quantify the proportion of all components in all phases, chemical analyses are necessary. Tie lines are carried out for all seven alcohols tested alone and for every promising alcohol/surfactant solutions.

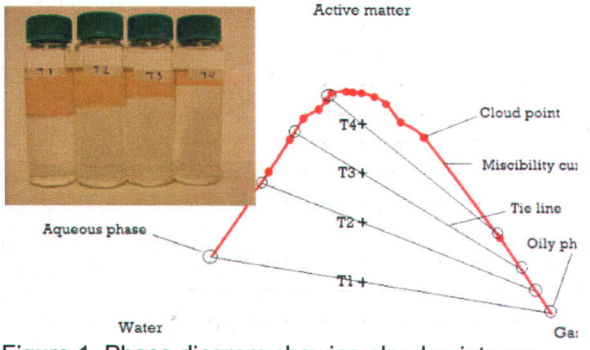

Figure 1. Phase diagram showing cloud points on the miscibility curve, model tie lines and corresponding initial mixtures for their construction (Alcohol III)

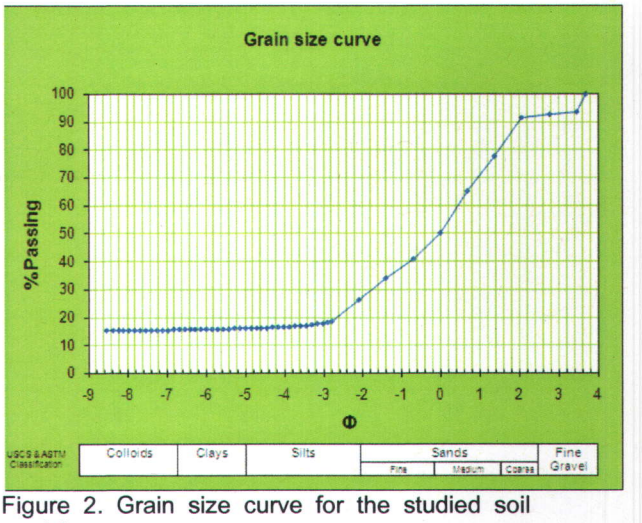

Figure 2. Grain size curve for the studied soil particles

3 RESULTS

3.1 Characterization of gasoline and geological materials

Mineralogical analyses of soil particles show that main minerals in the fine fraction (< 63 microns) by x-ray diffraction are in order of importance: quartz (51%), feldspaths (26%) (albite, orthoclase and microcline) and calcite (22%). Thin sections observation on the coarse fraction are planned to check if the same proportion of minerals is observed. Grain size of soil particles is distributed with coarse sand (33%), medium sand (19%), fine sand (18%), fine gravel (17%), coarse gravel (10%) and silt (3%) (see grain size curve on Figure 2).

The mean gasoline surface tension was evaluated from 12 measurements at 20,6 mN/m with a measured range of 17-24 mN/m. The mean interfacial tension was evaluated from 10 measurements at 28,1 mN/m with a measured range of 27-30 mN/m. Based on mineralogical analyses, three different minerals (quartz, calcite and feldspath) were chosen for the measurement of mineral-water-gasoline contact angle. On quartz, the mean contact angle was evaluated from 10 measurements at 68° with a measured range of 43-83°. With feldspath, 8 measurements were done for a mean value of 87° with a measured range of 68-128°. With calcite, the mean value was 47° with a measured range of 36-55°, evaluated from 10 measurements. Mean gasoline density is 0,788 g/cm^3 and viscosity is 689 µPa-S at 8°C. The chemical composition of the weathered gasoline is 36% xylene, 28% toluene, 16% 1,2,4 trimethylbenzene, 10% ethylbenzene and 10% compounds of the methyl ethylbenzene family. Table 2 summarizes all physical and chemical properties of gasoline and geological materials.

Table 2. Physical and chemical properties of gasoline and geological materials

Properties	Values
Gasoline	
Surface tension - 20°C (mN/m)	20,6
IFT with water - 20°C(mN/m)	28,1
Contact angle - 20°C (°)	
Quartz	68,4
Feldspath	86,7
Calcite	46,6
Density - 8°C (g/cm3)	0,788
Viscosity - 8°C (µPa-S)	689
Chemical composition (%)	
Xylene	36
Toluene	28
1,2,4 Trimethylbenzene	16
Ethylbenzene	10
Methyl ethylbenzene family	10
Geological materials	
Minerals (%)	
Quartz	51
Feldspath	26
Calcite	22
Grain size distribution (%)	
Fine gravel	17
Coarse sand	34
Medium sand	22
Fine sand	25
Silt	2

3.2 Phase diagrams

Used alone, alcohols IV and V seem to be the best ones (Figure 3). Alcohol V and Surfactant L (75% pure) have been selected for determination of the optimal alcohol/surfactant mass ratio. Results show that the best alcohol/surfactant mass ratio was 1.0 (Figure 4), confirming previous experiments for gasoline (Martel et al, 1993). From seven tested alcohols, Alcohol II showed the lowest miscibility curve in the water-rich zone with the Surfactant B (Figure 5). Therefore, Alcohol II was selected to evaluate the efficiency of 18 surfactants at a fixed mass ratio of 1.0 (Figure 6). Four surfactants (Surfactants L, M, N, O) were not compatible with Alcohol II and further tests will be carried out especially for these surfactants. From the 14 remaining, five were selected based on the low position of their miscibility curve in the water-rich zone (Figure 7). Surfactant R seems to be the most promising at this point. Further diagrams will be done to optimize the ratio with these five most promising alcohol/surfactant solutions. These optimized solutions will then be used for sand columns experiments.

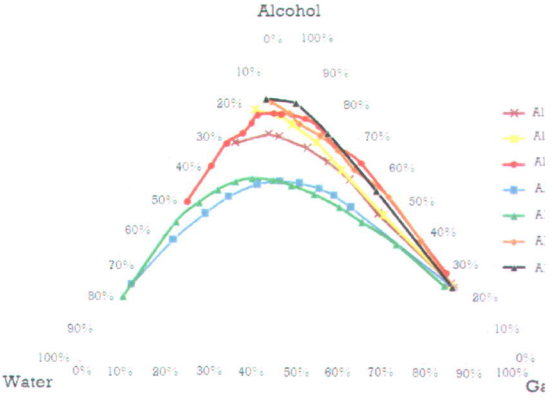

Figure 3. Phase diagram with miscibility curves for alcohols alone

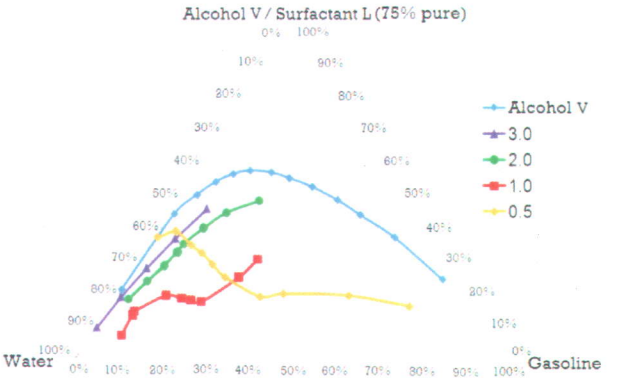

Figure 4. Phase diagrams with miscibility curves for different Alcohol V / Surfactant L (75% pure) ratios

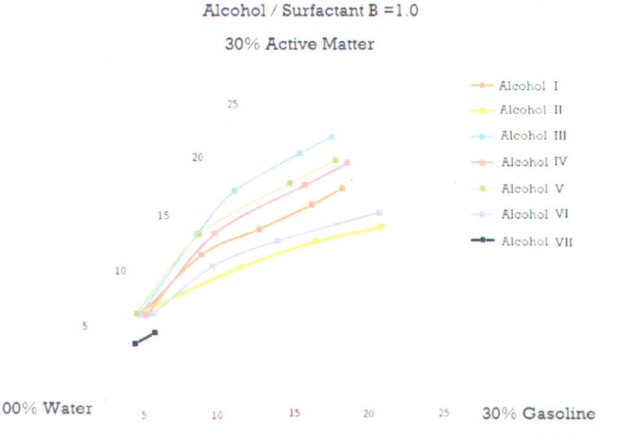

Figure 5. Phase diagram with miscibility curves for different alcohols at a ratio of 1.0

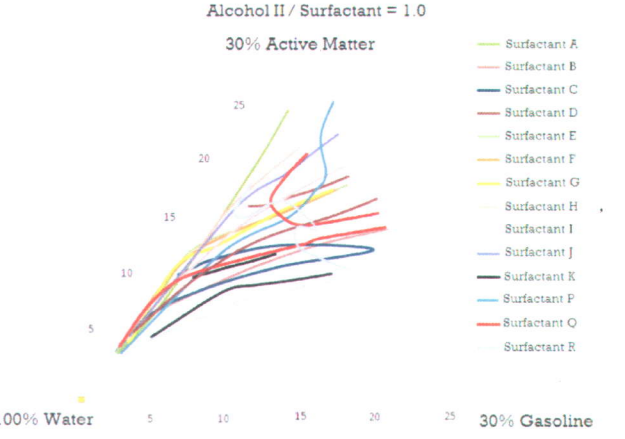

Figure 6. Phase diagram with miscibility curves for all surfactants at a ratio of 1.0

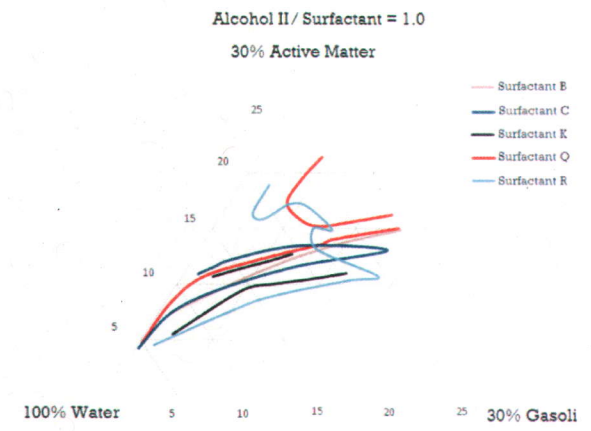

Figure 7. Phase diagram with miscibility curves for best surfactants at a ratio of 1

3.3 Prediction of the dominant recovery mechanism through tie lines

Tie lines have been prepared for alcohols alone and for Alcohol/Surfactant B = 1.0 solutions. Chemical analyses will be carried out with these solutions to identify the main recovery mechanism. Visual interpretation on apparent volumes of the corresponding initial mixture for tie lines construction allows the prediction of the dominant recovery mechanism in a qualitative way. For alcohols, mobilization is the dominant recovery mechanism for 5 of 7 alcohols (alcohols I, II, IV, VI and VII) and dissolution is the main mechanism for alcohols III and V (Figure 8). For Alcohol/Surfactant B = 1.0 solutions, dissolution becomes the dominant recovery mechanism for all alcohol types (Figure 9). Because the Alcohol/Surfactant B solutions are prepared in the water-rich zone, the oily phase is less present in the corresponding initial mixtures for tie lines construction. Figure 9 is a zoom on the oily phase section to see the recovery mechanism. However, because of a shortage of solution, some Alcohol/Surfactant B solutions are represented by only three tie lines points instead of four. Alcohol VII is not shown because of its incompatibility with Surfactant B (see Figure 5). On Figures 8 and 9, the aqueous phase is clear and the oily phase is yellowish.

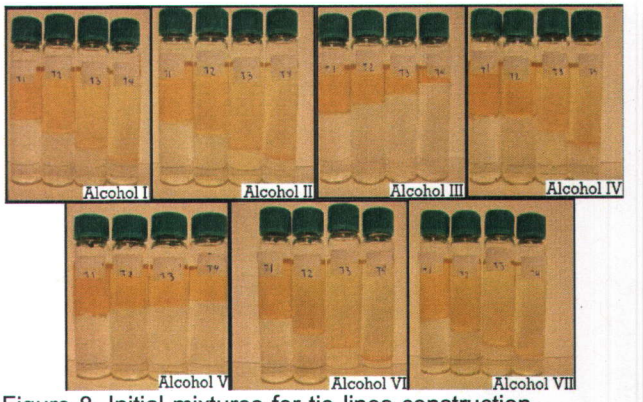

Figure 8. Initial mixtures for tie lines construction for alcohols types

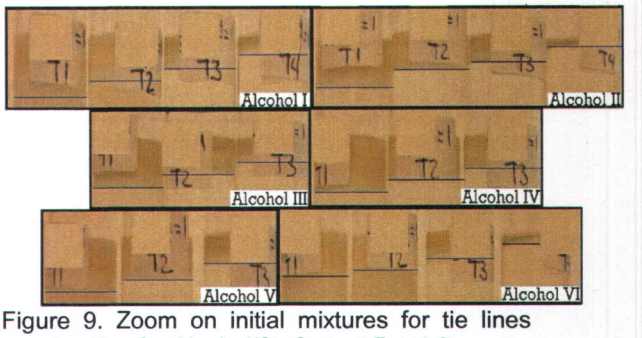

Figure 9. Zoom on initial mixtures for tie lines construction for Alcohol/Surfactant B = 1.0

4 DISCUSSION

4.1 Phase diagrams

Phase diagrams on Figures 3 and 5 show that the performance of an alcohol used alone is not a good indicator to predict its performance when used in combination with a surfactant. Indeed, when used alone, alcohols IV and V are the most promising, while they are poorly performing with the Surfactant B compared to other alcohols. Phase diagram on Figure 4 show that adding surfactant to an alcohol solution increases its dissolution power until it reaches an alcohol/surfactant critical ratio, which is 1.0 in the present study. Phase diagram on Figure 7 reveals that the combination of alcohol and anionic surfactant is as good as a combination of alcohol and non ionic surfactant. Effectively, for five surfactants retained for further tests, three are anionic and 2 are non ionic, which means that both types of surfactant have similar behavior when used with an alcohol.

4.2 Tie lines solutions

Tie lines prepared for alcohols and for Alcohol/Surfactant B on Figures 8 and 9 reveal that the dissolution power of the surfactant, at an

alcohol/surfactant ratio of 1.0, can change the dominant recovery mechanism from mobilization to dissolution (alcohols I, II, IV, VI). By increasing the alcohol/surfactant ratio at values greater than 1.0, it could be possible to change gradually the dominant recovery mechanism from dissolution to mobilization. This way, only one surfactant could be used for the technology train and the recovery mechanism could switch from mobilization (for bioslurping) to dissolution (for chemical oxidation) by changing the alcohol/surfactant ratio.

4.3 Future work

Further tests will include column experiments with on-site soil, followed by adsorption tests and compatibility tests with oxidants. A larger scale test (4 m^3 sand tank) will also be conducted prior to implement the technology train on-site. During all these tests, a numerical model will be used to better understand and to predict the phase behavior (UTCHEM) (Delshad et al, 1996).

5 CONCLUSION

This paper was about characterization of physical and chemical properties of gasoline and soil from the studied site. Identification of promising washing solutions with pseudo-ternary phase diagrams and their dominant recovery mechanism with tie lines solutions was carried out. The most performing alcohol used with a surfactant at an optimal alcohol/surfactant ratio of 1.0 is Alcohol II and most promising surfactants are surfactants B, C, K, Q and R. These 5 combinations give the lowest miscibility curves in the water-rich zone. Tie lines show that the recovery mechanism can be changed by changing surfactant, alcohol or alcohol/surfactant ratio. This way, only one surfactant could be used for the technology train with a recovery mechanism that can switch from mobilization (for bioslurping) to dissolution (for chemical oxidation) by changing the alcohol/surfactant ratio.

ACKNOWLEDGMENTS

This project is funded through grants from the Natural Sciences and Engineering Research Council of Canada (NSERC) CRD program with TechnoRem as the industrial partner. Special thanks to Richard Levesque for his help in laboratory experiments.

References

Bradner, C.F., Slotboom, R.A. 1975. Vertical immiscible displacement experiments in a non-homogeneous flow cell. *J. Can. Petroleum Technol.* 1975, Vol. 14, 1.

CCME. 2001. *Standard pancanadien relatif aux hydrocarbures pétroliers dans le sol.* s.l. : Le conseil canadien des ministres de l'environnement, 2001.

Delshad, M., Pope, G.A., Sepehrnoori, K. 1996. A compositional simulator for modeling surfactant enhanced aquifer remediation: 1. Formulation. *Journal of Contaminant Hydrology.* Elsevier, 1996, Vol. 23, 303-327.

Lake, L.W. 1989. *Enhanced oil recovery.* Englewood Cliffs, New Jersey : Prentice Hall, inc. 550 pp., 1989.

Lefebvre, R. 2006. *GEO-9602 Écoulement multiphase en milieu poreux.* Québec : Note de cours, INRS - ETE, 2006.

Lide, David R. 2004. *Handbook of chemestry and physics, 84th edition, 2003-2004.* s.l. : CRC Press, 2004.

Martel, R. 1996. *Développement de solutions tensioactives pour la récupération de phases liquides non aqueuses à saturation résiduelle dans les aquifères.* Québec : Thèse de doctorat, Université Laval. 310 pp., 1996.

Martel, R. 2007. *Impact de solutions tensioactives sur le rendement de technologies conventionnelles pour la remédiation d'aquifères contaminés par des hydrocarbures pétroliers.* Québec : Formulaire de demande de subvention au CRSNG, 2007.

Martel, R., Gélinas, P.J., Desnoyers, J.E., Masson, A. **1993.** *Phase diagrams to optimize surfactant solutions for oil and DNAPL recovery in aquifers.* Québec : Université Laval, 1993.

Martel, R., Hébert, A., Lefebvre, R., Gélinas, P., Gabriel, U. 2004. Displacement and sweep efficiencies in a DNAPL recovery test using micellar and polymer solutions injected in a five-spot pattern. *Journal of Contaminant Hydrology.* Elsevier, 2004, Vol. 75, 1-2. pp.1-29.

Morrow, N.R. 1979. Interplay of capillary, viscous and buoyancy forces in the mobilisation of residual oil. *J. Can. Pet. Tech.* Sept (1979), 1979, p-35-46.

St-Pierre, C., Martel, R., Gabriel U., Lefebvre, R., Robert, T. et Hawari, J. 2004. TCE recovery mechanisms using micellar and alcohol solutions: pase diagrams and sand column experiments. *Journal of Contaminant Hydrology.* Elsevier, 2004, Vol. 71, 1-4. pp. 155-192.

ANNEXE B

Résumé présenté à la 9e conférence RemTech, Banff, Octobre 2010

Soil Washing with a Micellar Solution: Field Test at a Gas Station (Laval, Québec, Canada)

Maxime Grenier
INRS - Eau, Terre et Environnement, Québec, Qc, Canada
Richard Martel, Uta Gabriel, Luc Trépanier, Clarisse D.-Rancourt, Thomas Robert
INRS - Eau, Terre et Environnement, Québec, Qc, Canada
Jean-Marc Lauzon
TechnoRem, Laval, Qc, Canada

ABSTRACT

Soil washing with a micellar solution as an *in situ* aquifer remediation technology, allows recovering petroleum hydrocarbons at residual saturation. A field test at pilot scale took place at a decommissioned gas station (Laval, Quebec, Canada) where a gasoline contamination occured. The soil washing was launched after a preliminary step of vacuum extraction to remove most of the floating phase and to bring gasoline at residual saturation. The micellar solution was injected into the aquifer through an injection well located in the middle of a 7-spot pattern (6 pumping wells set with a hexagonal pattern). The micellar solution solubilised the remaining gasoline adsorbed on soil particles or trapped into the porous media. The polymer-micellar solution swept 40 m^3 of contaminated aquifer. The optimal micellar solution for this site specific contaminant and geological materials was previously optimised in the lab through phase diagrams and small sand column tests (110 cm^3). Hydrogeological modelling was also performed to optimise the injection/pumping ratio. The main goal of this field test is to evaluate the efficiency of soil washing in a heterogeneous medium following a vacuum extraction step at the pilot scale. This paper presents lab and field methodology and results.

Maxime Grenier is a M.Sc. student at Institut National de la Recherche Scientifique in Quebec City, under the supervision of Professor Richard Martel.

RÉSUMÉ

Comme technique de restauration *in situ* d'aquifère, le lavage de sol avec une solution micellaire permet de récupérer des hydrocarbures pétroliers à saturation résiduelle. L'essai de terrain s'est déroulé sur une station service désaffectée (Laval, Québec, Canada), où le contaminant majeur était l'essence. Le lavage de sol a été précédé d'une étape d'extraction sous vacuum permettant de récupérer la plus grande partie de la phase flottante afin d'amener l'essence à saturation résiduelle. La solution micellaire a été injectée dans l'aquifère à partir d'un puits d'injection situé au centre d'un patron à 7 points (6 puits de pompage formant un patron hexagonal). La solution micellaire solubilise l'essence restante adsorbée sur les particules de sol ou trappée dans le milieu poreux. La solution micellaire comprenant aussi un polymère a balayée 40 m^3 d'aquifère contaminé. Cette solution a été optimisée en laboratoire en fonction du contaminant et du type de

matériaux géologiques retrouvés sur le site par des diagrammes de phases et des essais en petites colonnes de sol (110 cm^3). Une modélisation hydrogéologique a aussi été effectuée pour optimiser le ratio injection/pompage. Le but principal de cet essai de terrain est d'évaluer le rendement du lavage de sol suite à une étape d'extraction sous vacuum dans un milieu hétérogène à une échelle pilote. Ce papier présente la méthodologie et les résultats obtenus en laboratoire et sur le terrain.

Maxime Grenier est étudiant à la maîtrise en Sciences de la Terre à l'institut National de la Recherche Scientifique à Québec, sous la supervision du professeur Richard Martel.

ANNEXE C

Diagrammes de phases supplémentaires

Effet de la salinité de l'eau sur la solution n-BuOH / SAS = 1,0

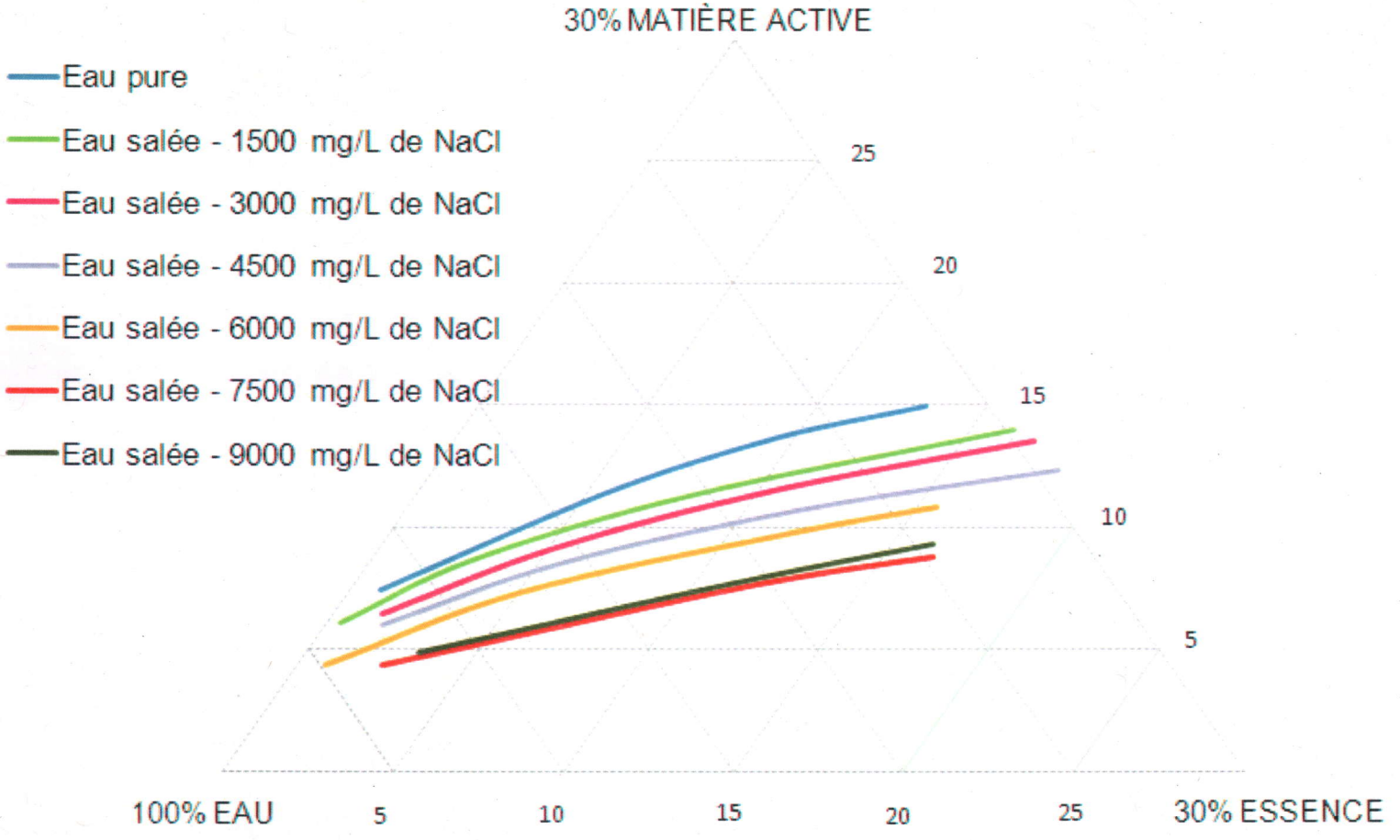

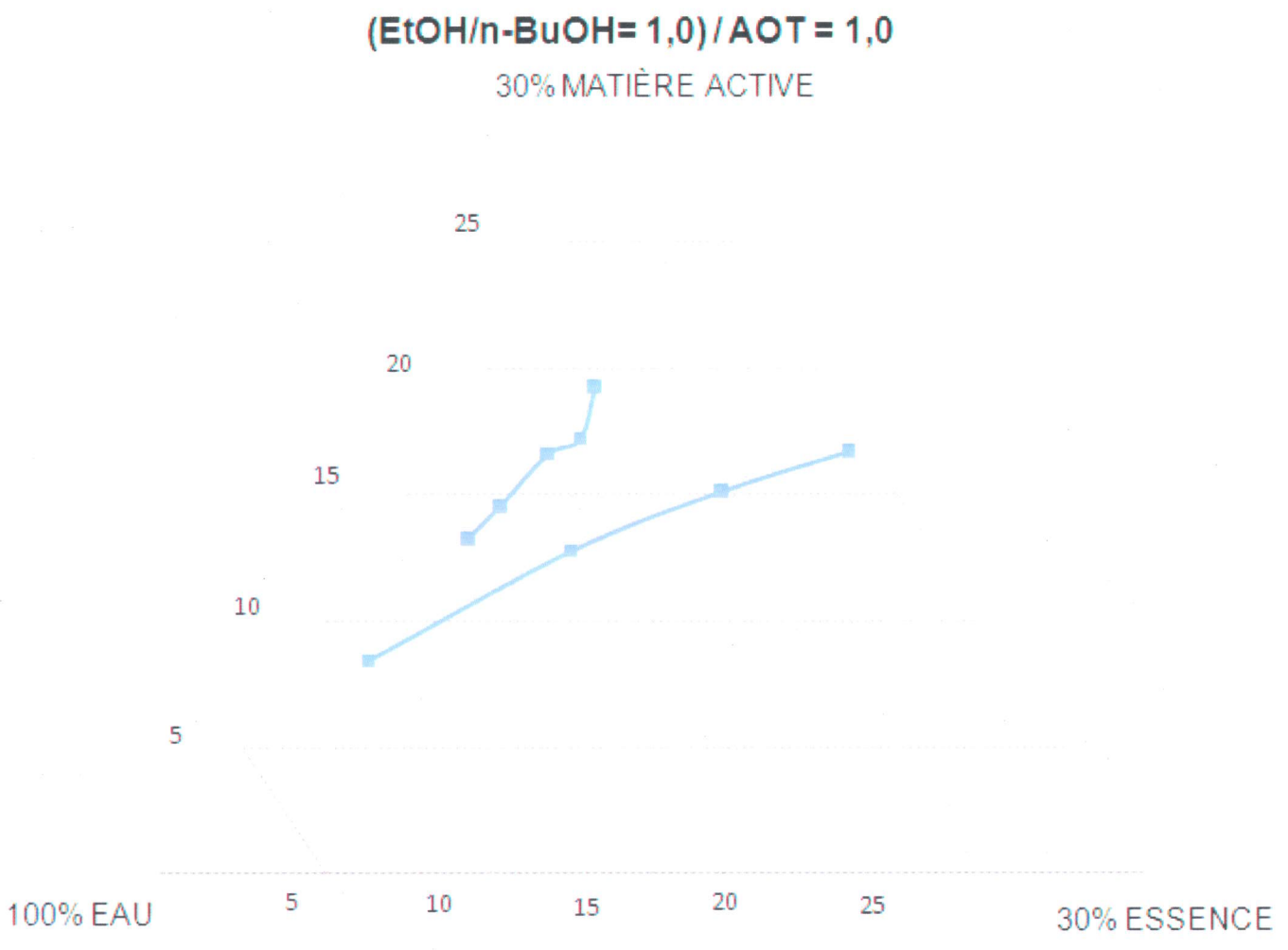
(EtOH/n-BuOH= 1,0) / AOT = 1,0
30% MATIÈRE ACTIVE
25
20
15
10
5
5
10
15
20
25
100% EAU
30% ESSENCE

n-AmOH / LRO = 1,0

30% MATIÈRE ACTIVE

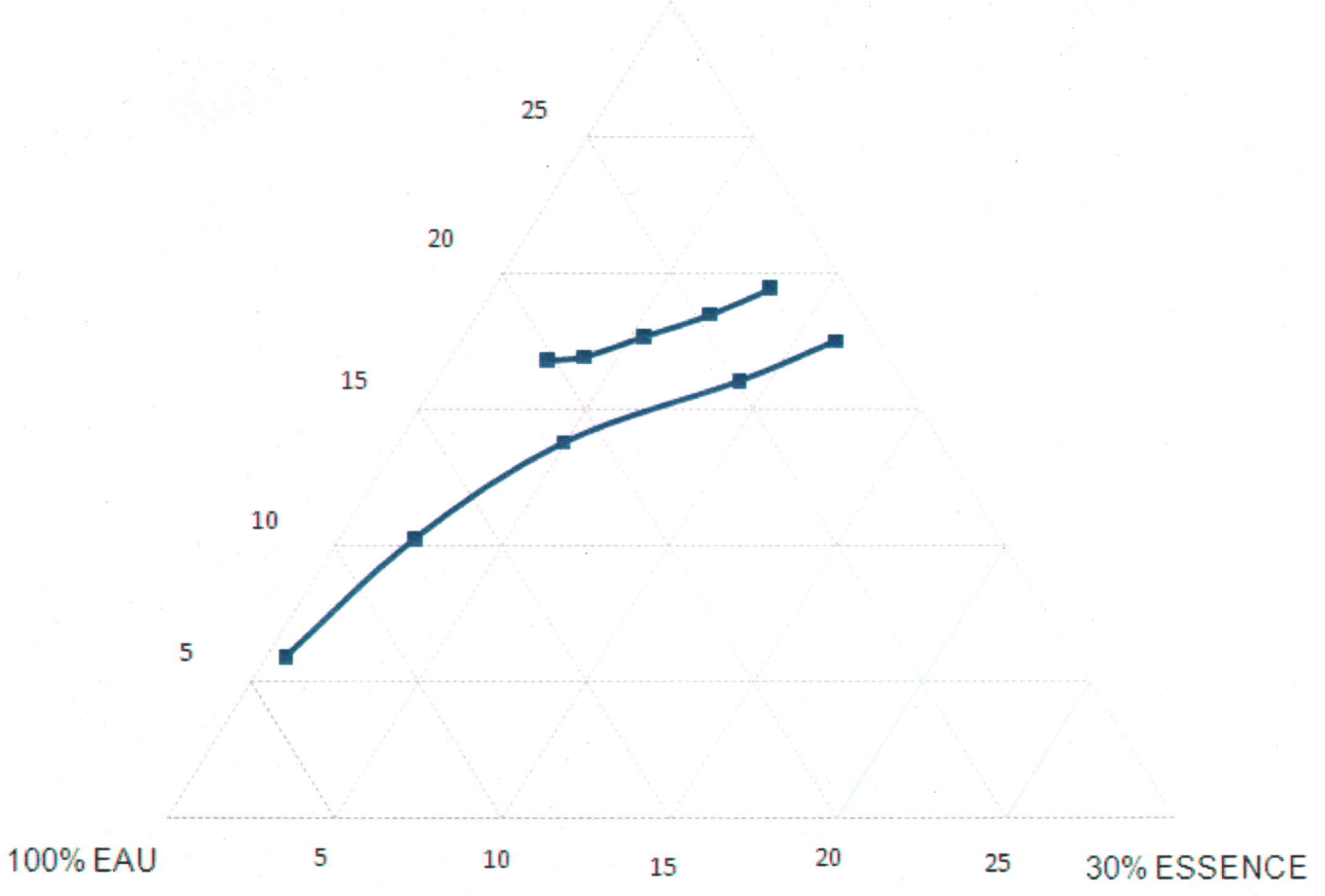

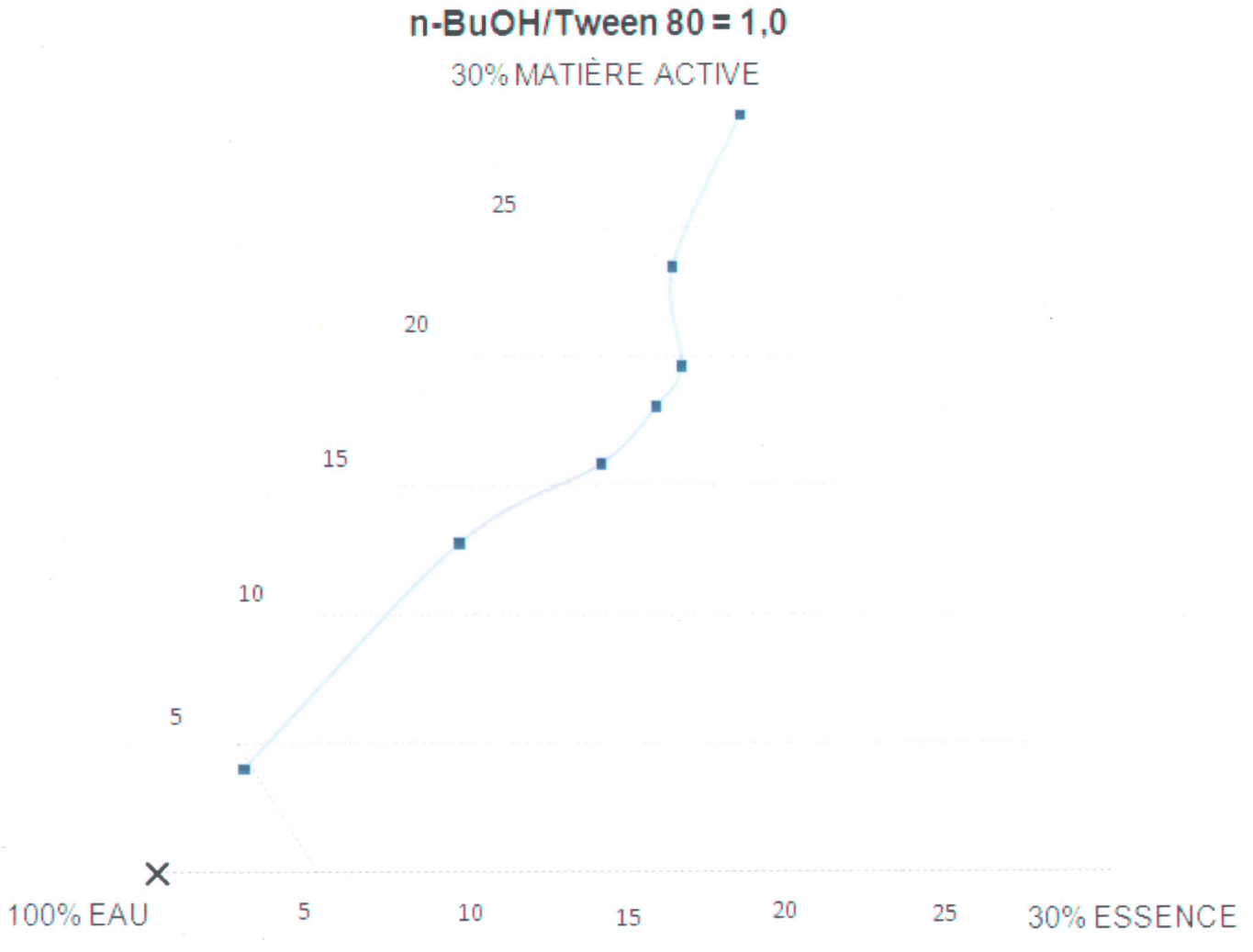
n-BuOH/Tween 80 = 1,0
30% MATIÈRE ACTIVE
25
20
15
10
5
100% EAU
5
10
15
20
25
30% ESSENCE

n-BuOH/Hostapur OS = 1,0

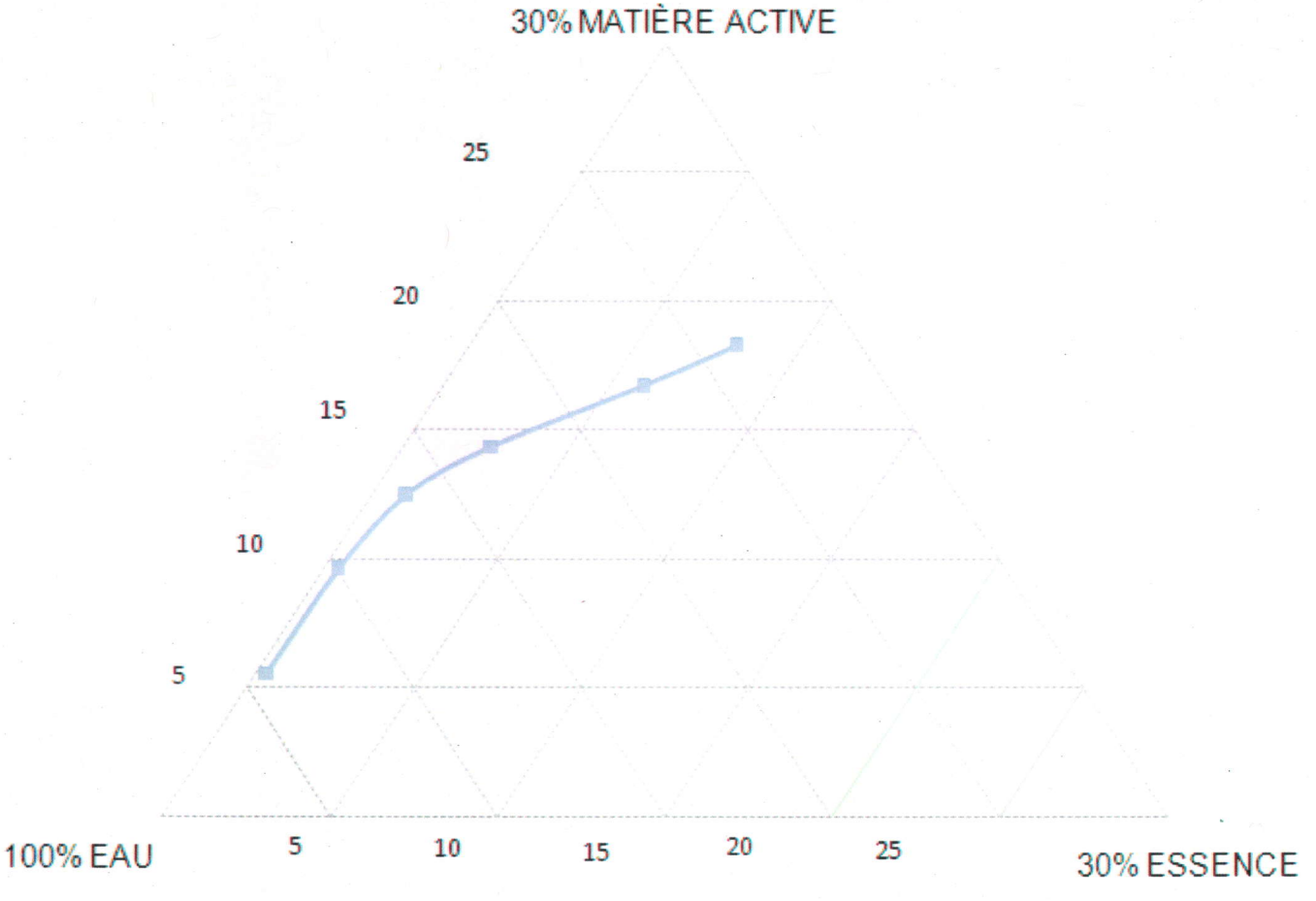

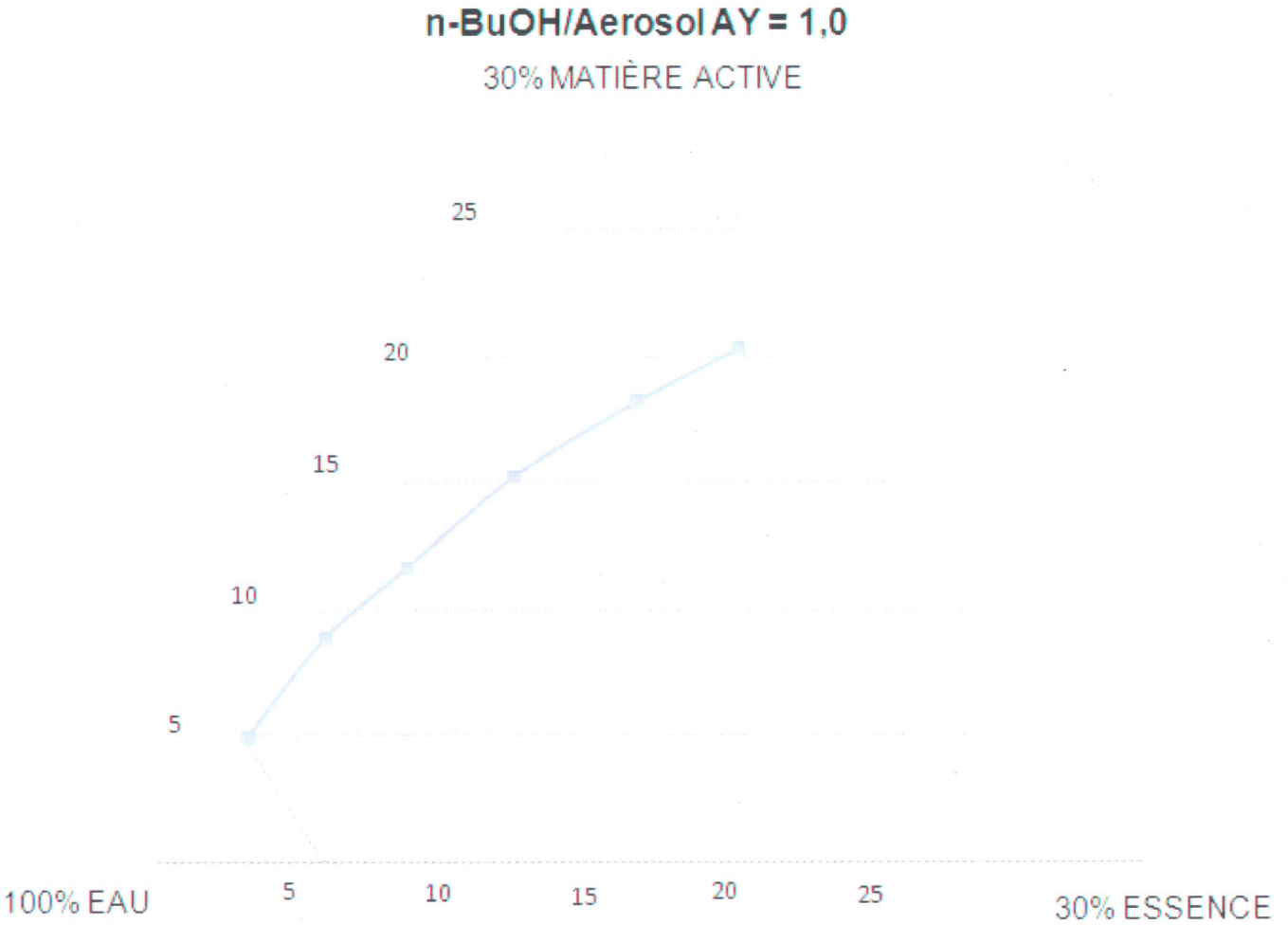
n-BuOH/Aerosol AY = 1,0
30% MATIÈRE ACTIVE
25
20
15
10
5
100% EAU
5
10
15
20
25
30% ESSENCE

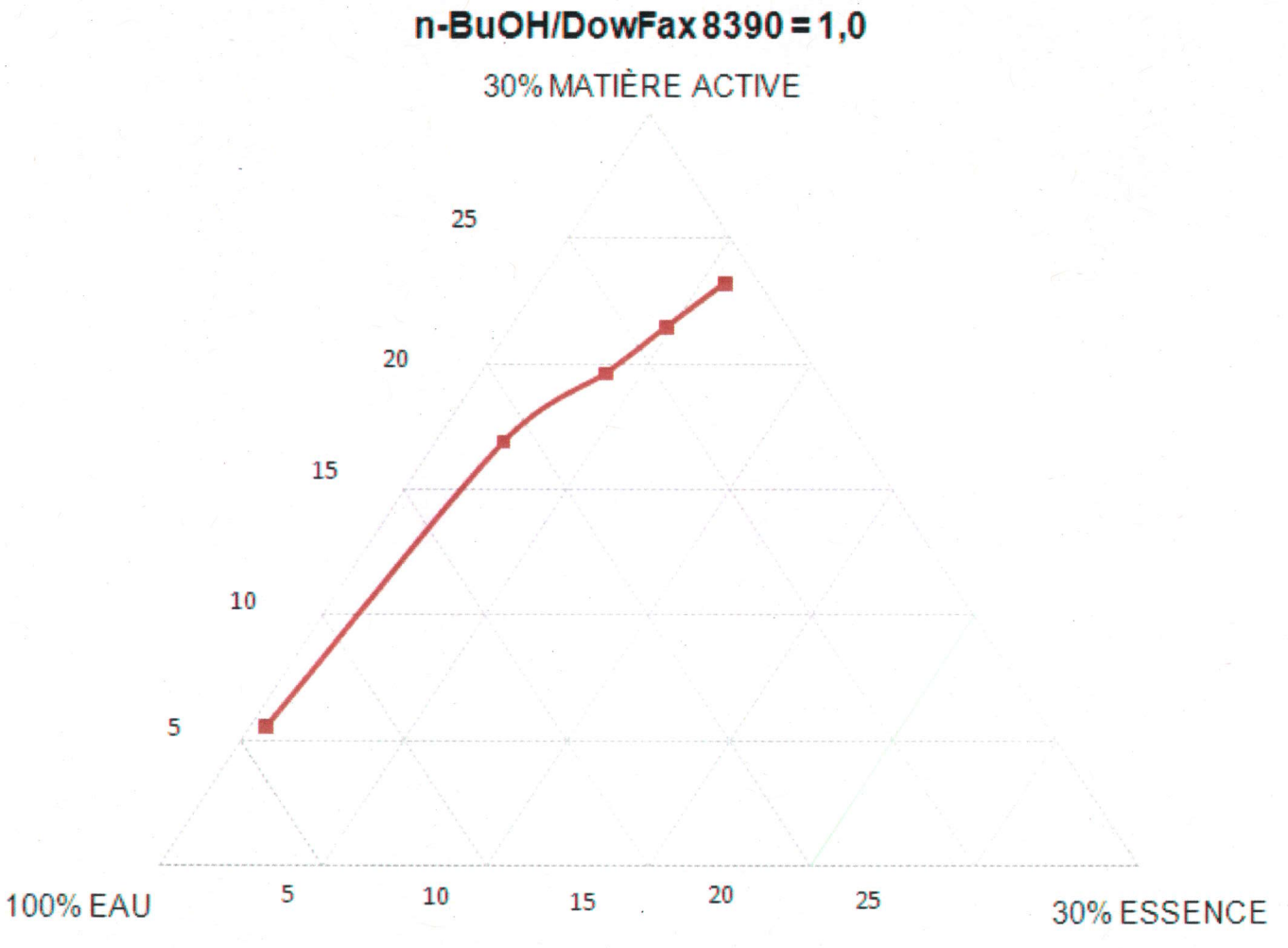
n-BuOH/DowFax 8390 = 1,0
30% MATIÈRE ACTIVE
25
20
15
10
5
100% EAU
5
10
15
20
25
30% ESSENCE

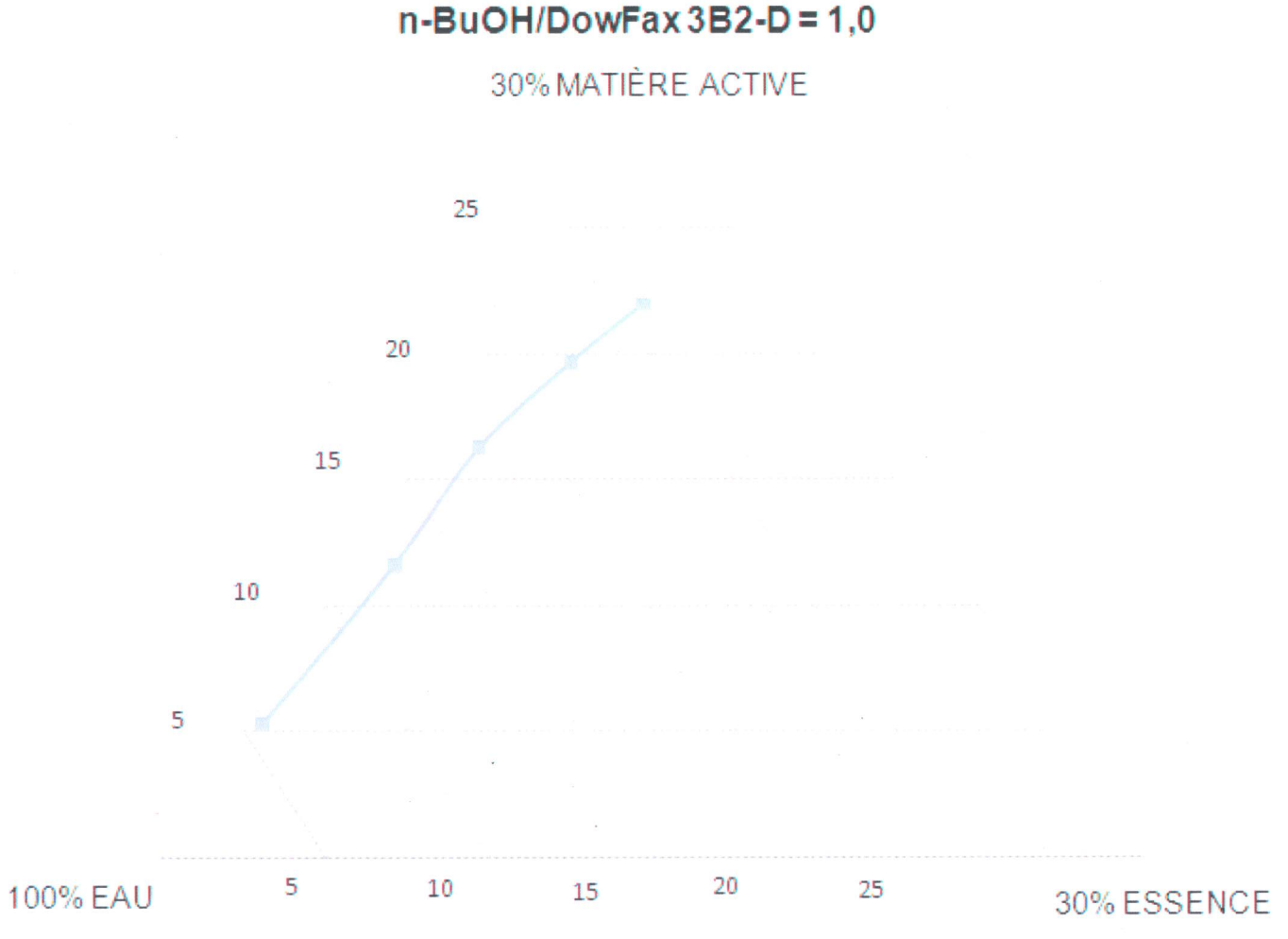
n-BuOH/DowFax 3B2-D = 1,0
30% MATIÈRE ACTIVE
25
20
15
10
5
100% EAU
5
10
15
20
25
30% ESSENCE

n-BuOH/Hostapal BV = 1,0

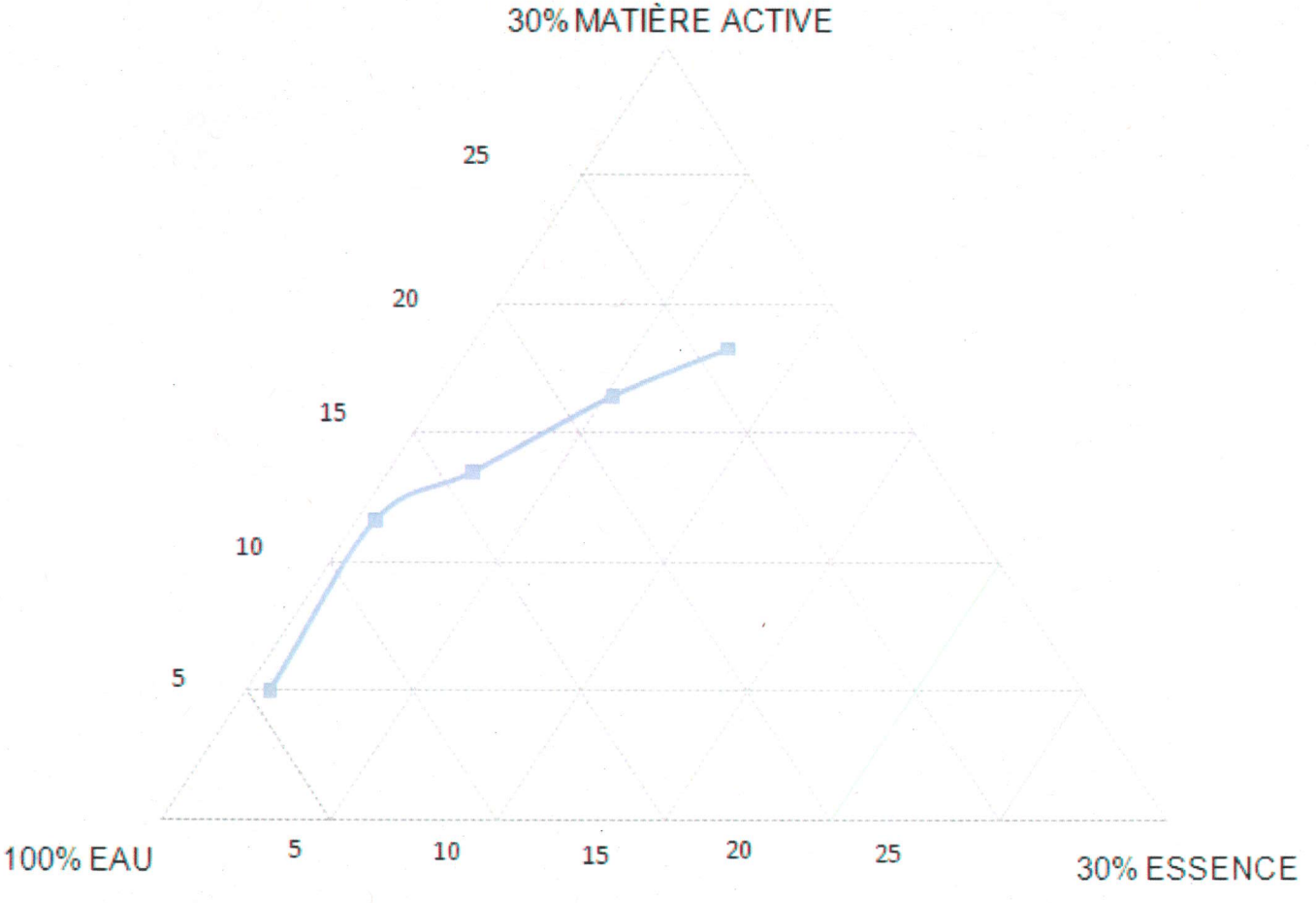

(n-BuOH/n-AmOH = 1,0)/Arkopal N090 = 1,0

30% MATIÈRE ACTIVE

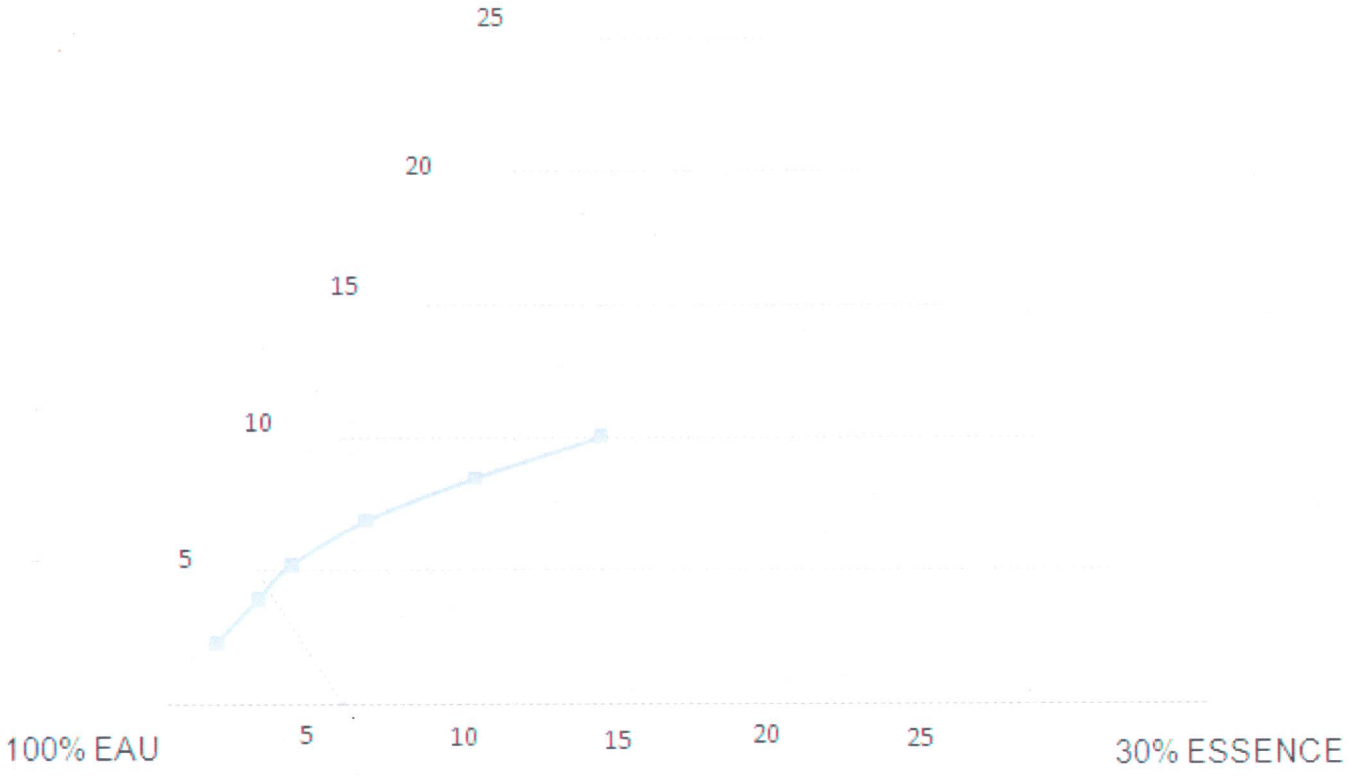

(n-BuOH/n-AmOH = 3,0)/Nansa HS90 = 1,0

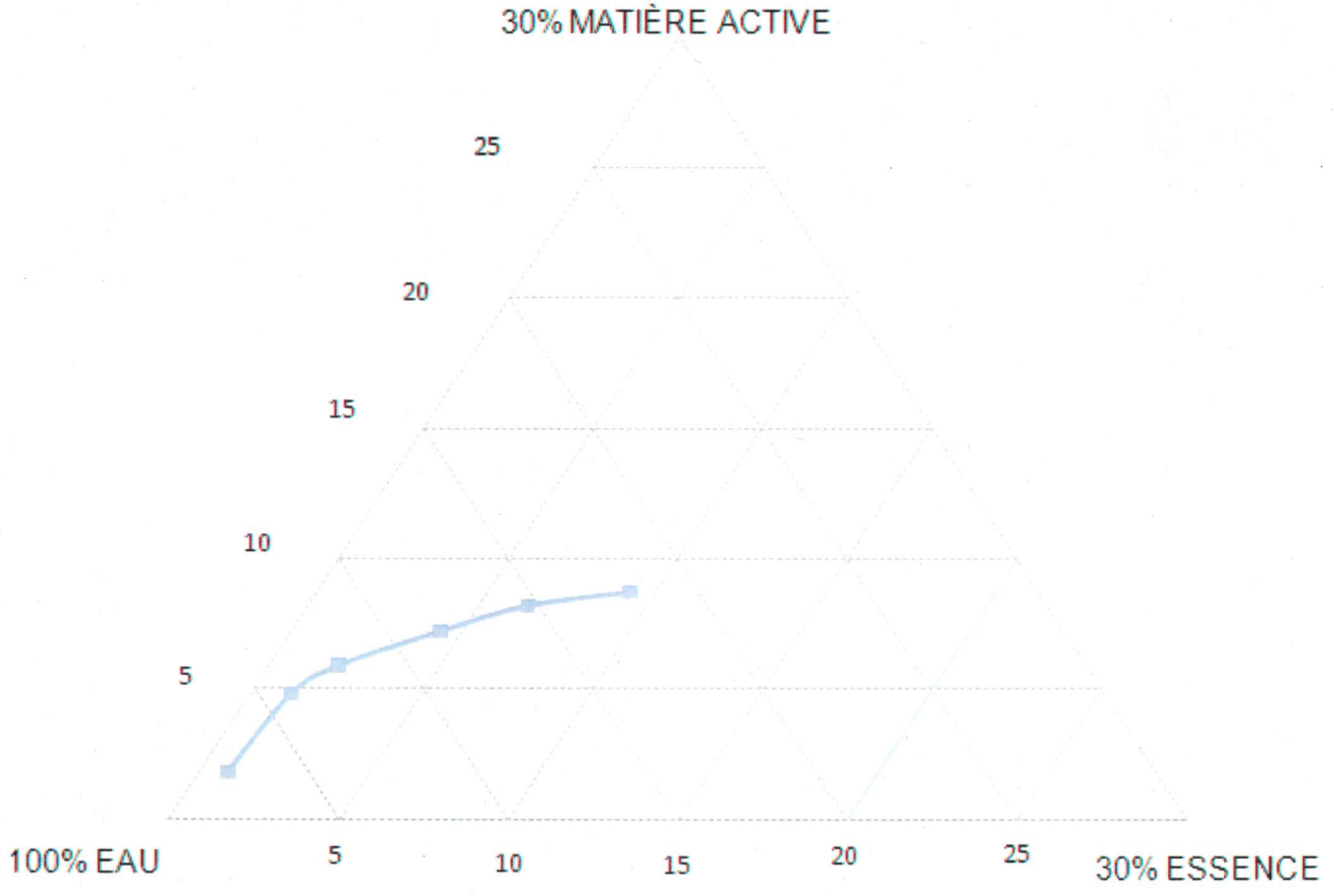

(n-BuOH/n-AmOH= 1,0)/PE-2597 = 1,0

30% MATIÈRE ACTIVE

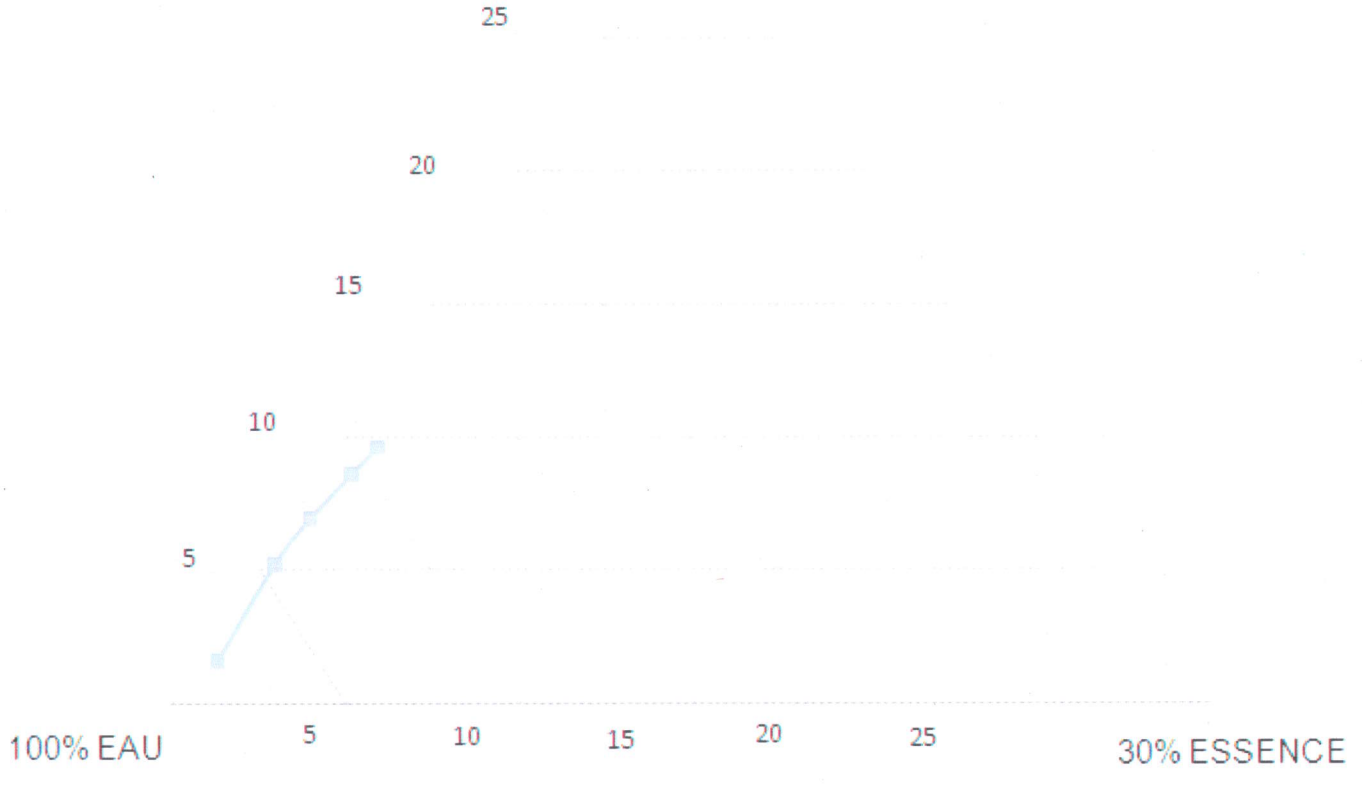

(n-BOH/n-AmOH = 1,0)/Triton GR7M = 1,0

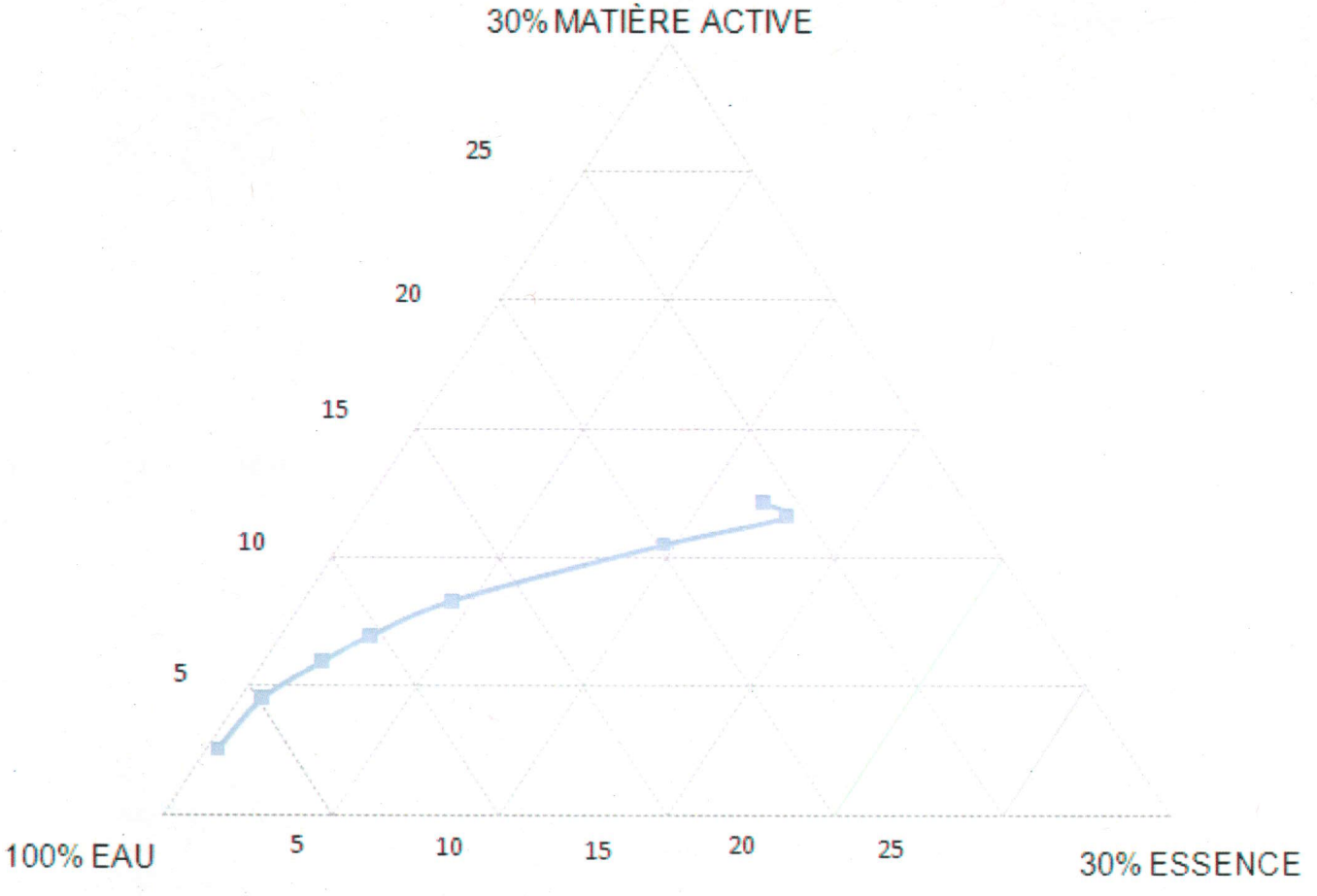

n-BuOH/PE-2597 = 1,0

30% MATIÈRE ACTIVE

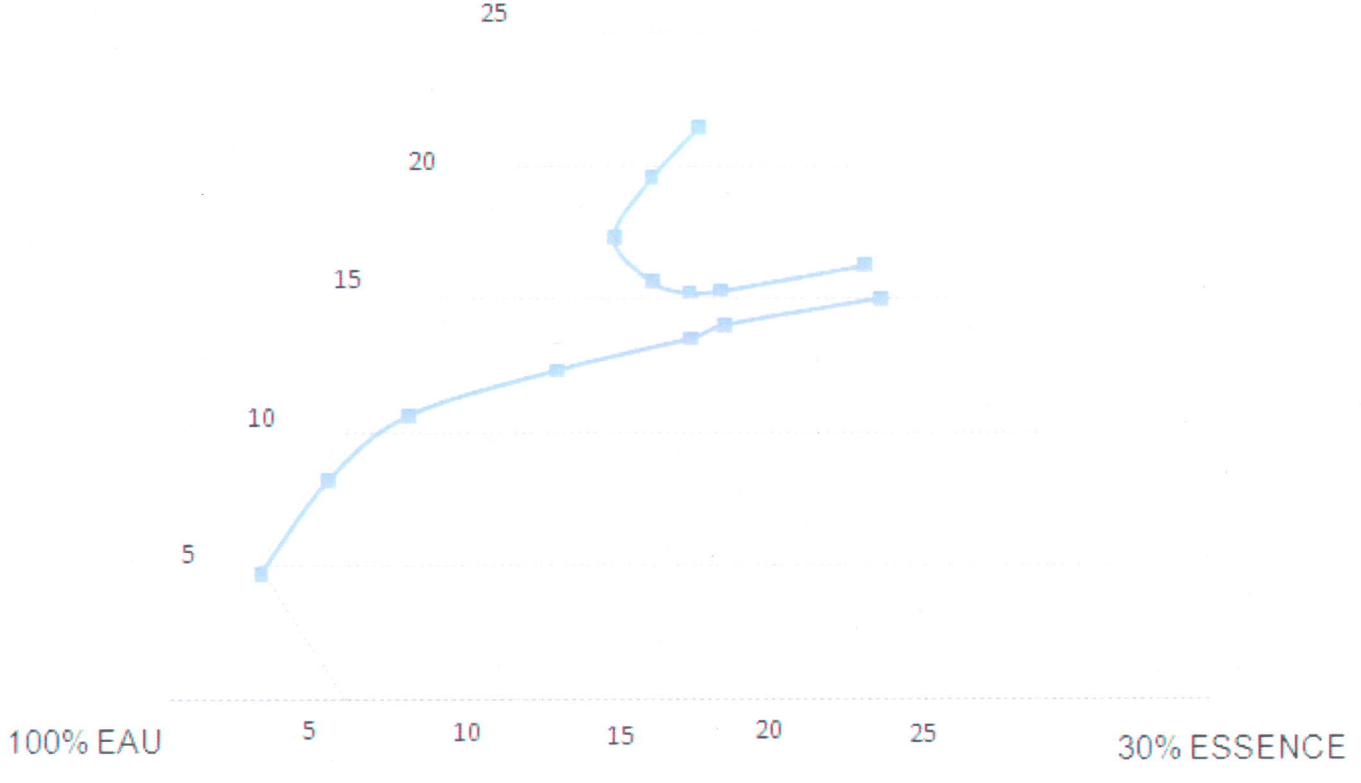

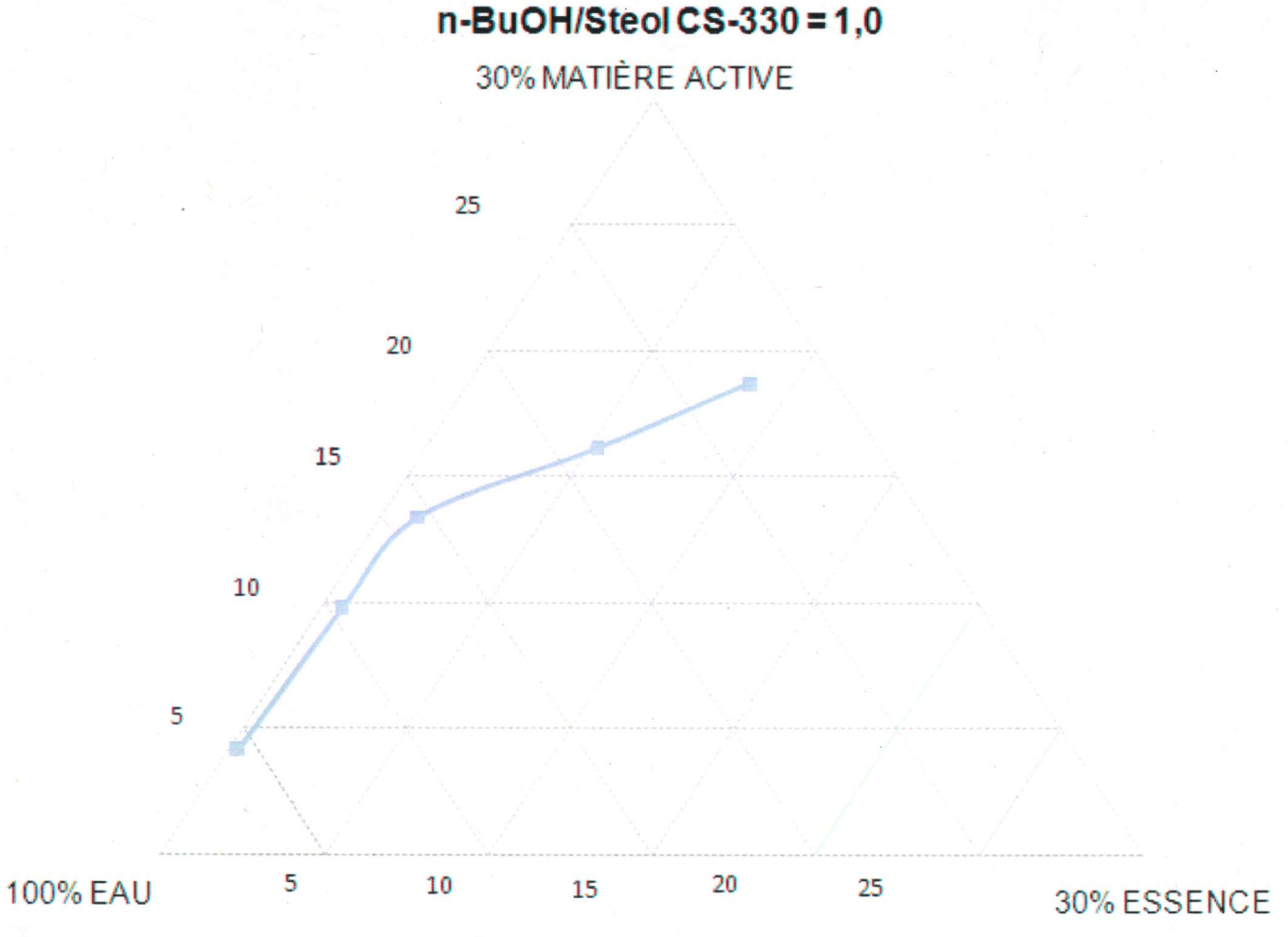
n-BuOH/Steol CS-330 = 1,0
30% MATIÈRE ACTIVE
25
20
15
10
5
100% EAU
5
10
15
20
25
30% ESSENCE

n-BuOH/Triton GR7M = 1,0

30% MATIÈRE ACTIVE

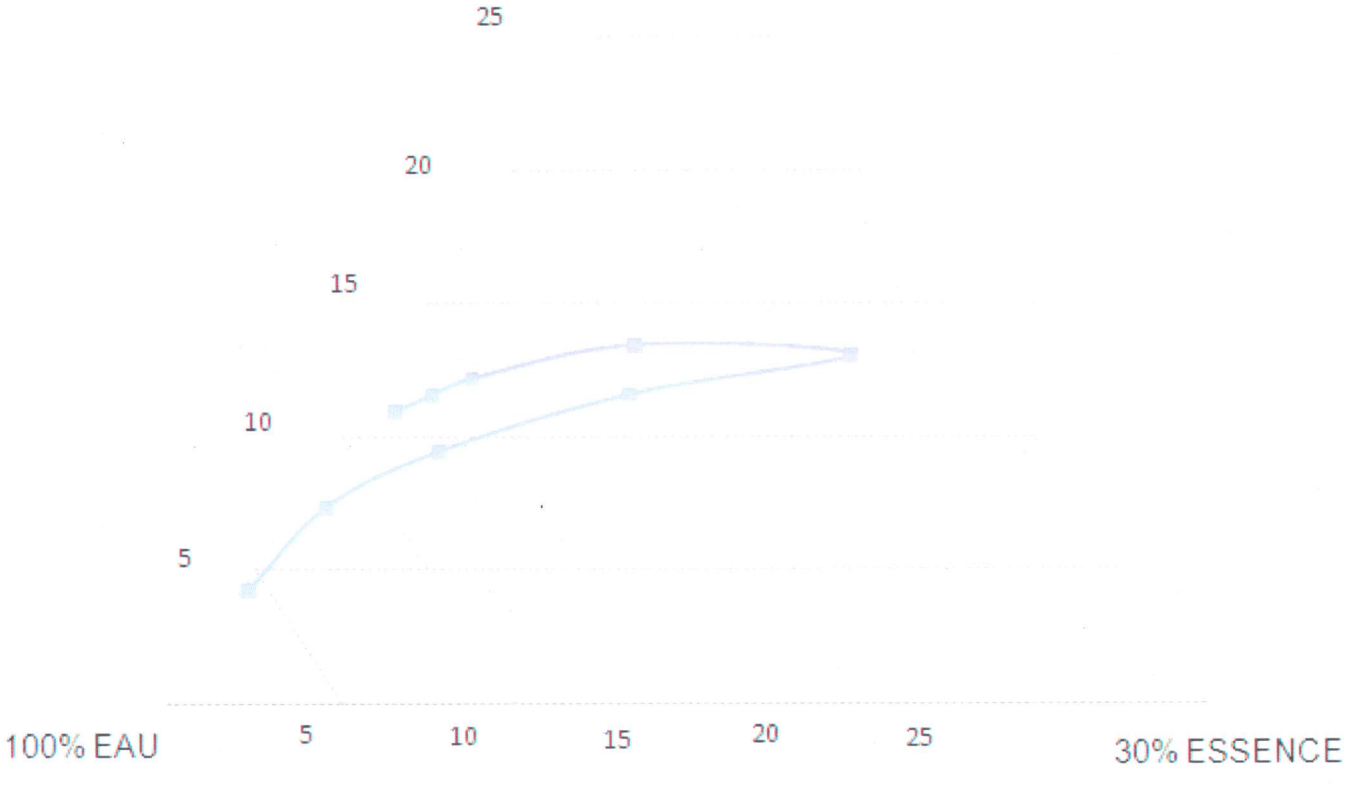

ANNEXE D

Cédérom de données